Simulación Numérica por Ordenador en Astrofísica

J.M$^{\underline{a}}$. Ibáñez, J.M$^{\underline{a}}$. Martí, J.A. Font, J.A. Miralles y P. Cerdá-Durán
Departamento de Astronomía y Astrofísica
Universidad de Valencia
46100-Burjassot, España

VNIVERSITAT DE VALÈNCIA

1 Introducción

Simulación Numérica en Astrofísica:

La conexión "teoría–observación"

As in other fields of science, numerical simulations has emerged as **the third scientific methodology** alongside **observation** and **analytic theory**

A key goal of simulations is the rationalization of the various morphological classes of an astrophysical object (jets, e.g.) in terms of a few underlying parameters.

Numerical simulations opens a unique "spectral window" on our theoretical understanding of astrophysical phenomena. Most numerical simulations are designed to elucidate complex dynamical behavior contained within a theoretical model rather than to reproduce an observation, although the latter is certainly an end goal.

Alan Bridle remarked that the Oxford English dictionary defines simulation as "...an attempt to deceive". While it is true that a poorly executed or interpreted numerical simulation may have that effect, this is also true of a poorly executed observation or analytical derivation. Bridle goes on to suggest that we use the word model instead of simulation to avoid this connotation. Within the computational science community, no such semantic difficulties exist, and furthermore, to simulate and to model have very different meanings.

In astronomy, a model is a mathematical description of some object of interest. Models are generally either kinematic or dynamic when describing macroscopic systems (e.g., jets).

The following steps show how numerical models of **jets** have matured over time; although these are representative of other areas in **computational astrophysics**:

First $\Longrightarrow$ One starts by simulating a **simple dynamical model**. One uses simple physics (ideal gas) and the minimum number of spatial dimensions required to capture the essential physics. At this stage, one generally discovers gross flow structures and the sensitivity of these structures to *initial parameters*.

Second $\Longrightarrow$ To generalize the dynamical model by **adding more physics and/or more spatial dimensions**. At this stage, with sufficient numerical resolution two qualitative barriers are breached, one observational (the 3D models of jets begin to exhibit complex asymmetric morphologies reminiscent of actual sources) and one theoretical (the models can exhibit the full range of dynamical behavior: flow structures, modes of instability...).

Third $\Longrightarrow$ Construction of a **predictive astrophysical model** adding, e.g., an emission model (or turbulence) so that numerical models can be compared with observations. One needs to worry about physical processes occurring on unresolved scales in the simulation and incorporate mathematical models into the system of equations to deal with them. Once a predictive model is constructed, one can begin testing the model against observations –in an iterative process – and attempt to reproduce generic features of an entire class of objects (morphology, spectra, polarization,...).

Fourth $\Longrightarrow$ In the final stage the predictive model is applied to a specific source. The outputs at this stage are synthetic maps, spectra and other observables convolved with telescope response functions so that meaningful comparisons with observations can be made. This is the stage at which science in the pure sense can be done. A hypothesis can be falsified or further refined. Predictions can be made which can be tested by subsequent observations.

The above classification is an obvious oversimplification, because it ignores the fact that observations steadily improve. What was once a predictive model when only crude observations existed becomes downgraded as observations improve.

Referencias:

– M. Norman, in "Astrophysical Jets", ed. by D. Burgarella, M. Livio and C.P. O'Dea, page 211, Cambridge University Press (1993) . – M. Norman, in "Energy Transport in Radio Galaxies and Quasars, ed. by P.E. Hardee, A. H. Bridle, and J.A. Zensus, Astron. Soc. Pac. Conf. Ser., vol. 100. page 405 (1996).

2 Dinámica de fluidos

2.1 Dinámica de fluidos: Introducción

$\Longrightarrow$ Un **fluido simple** (a diferencia de un sólido) es un material en el que las *posiciones relativas de sus elementos cambian mucho* al aplicar una fuerza, aunque ésta sea pequeña en magnitud.

Rango interacción molecular (que no forman un enlace químico): $d_0 \approx 3 - -4 \times 10^{-8} cm$.

En sustancias compuestas por moléculas simples, la *distancia intermolecular promedio, en la fase gaseosa,* es del orden de $10 d_0$.

$\Longrightarrow$ La **dinámica de fluidos** $\Longrightarrow$ Evolución de *magnitudes macroscópicas*, i.e., magnitudes promediadas en elementos de volumen de tamaño $l \gg d_0$.

Supondremos que el comportamiento macroscópico del fluido es el mismo que si éste fuera **perfectamente continuo** $\Longrightarrow$ *Las magnitudes que caracterizan el fluido* serán funciones de $(\vec{r}, t)$

$\Longrightarrow$ Descripción **euleriana**: Cómo varian las propiedades del fluido, con el paso del tiempo, en un *punto fijo del espacio.*

$\Longrightarrow$ Descripción **lagrangiana**: Cómo varian las propiedades de una *partícula del fluido* en su movimiento.

$\Longrightarrow$ **Líneas de corriente**: $\vec{r} = \vec{r}(\lambda)$

$\Longrightarrow$ Curvas integrales del campo de velocidades:

$$\frac{d\vec{r}}{d\lambda} = \vec{v}\,(\vec{r}(\lambda), t) \quad \Longleftrightarrow \quad \frac{d\,x}{v_x(\vec{r}, t)} = \frac{d\,y}{v_y(\vec{r}, t)} = \frac{d\,z}{v_z(\vec{r}, t)} \ (= d\lambda)$$

$\Longrightarrow$ **Flujo estacionario** $\Longrightarrow$ *El campo de velocidades no depende del tiempo*

$\Longrightarrow$ Las líneas de corriente son las mismas en todo instante.

$\Longrightarrow$ Las líneas de corriente coinciden con las trayectorias de las partículas de fluido.

2.2 Ecuaciones de la Dinámica de Fluidos Perfectos

- **Ecuación de Continuidad :**

$$\frac{\partial\rho}{\partial t} + \vec{\nabla}.(\rho\vec{v}) = 0 \iff -\frac{\partial}{\partial t}\int\int\int_V \rho dV = \int\int_\Sigma \rho\vec{v}d\vec{\Sigma} \tag{1}$$

$\Longrightarrow$ *Conservación de la masa*

$\Longrightarrow$ *Flujo incompresible* $\iff \vec{\nabla}.\vec{v} = 0 \iff d\rho/dt = 0$

- **Ecuación de Euler:**

$$\frac{d\vec{v}}{dt} = -\frac{1}{\rho}\vec{\nabla}p \iff \int\int\int_V \rho\frac{d\vec{v}}{dt}dV = -\int\int\int_V \vec{\nabla}pdV = -\int\int_\Sigma pd\vec{\Sigma} \tag{2}$$

$\Longrightarrow -\vec{\nabla}p\ dV$ *es la fuerza que ejerce el fluido que rodea cada elemento de volumen sobre dicho elemento de volumen*

$\Longrightarrow -\int\int_\Sigma pd\vec{\Sigma}$ *es la fuerza total que ejerce el fluido sobre el volumen* V

$\Longrightarrow$ *Ecuación del movimiento* (de un elemento de volumen del fluido)

$$\frac{d}{dt} = \frac{\partial}{\partial t} + \vec{v}.\vec{\nabla} \Longrightarrow \frac{\partial\vec{v}}{\partial t} + (\vec{v}.\vec{\nabla})\vec{v} = -\frac{1}{\rho}\vec{\nabla}p + \vec{g} \tag{3}$$

$\Longrightarrow$ siendo $\vec{g} = (1/\rho)\vec{f}$ un campo de fuerzas (por unidad de masa) exterior.

$\Longrightarrow$ *Campo gravitatorio*: $\vec{g} = -\vec{\nabla}\Phi$ con Φ solución de la ecuación de Poisson.

Ecuación de continuidad $\Longrightarrow \dfrac{\partial\rho\vec{v}}{\partial t} = -\rho(\vec{v}.\vec{\nabla})\vec{v} - \vec{v}\left(\vec{\nabla}.(\rho\vec{v})\right) - \vec{\nabla}p + \vec{f}$

i) Multiplicando escalarmente por un vector fijo $\vec{e}$, ii) integrando en el volumen V, y iii) aplicando el teorema de la divergencia:

$$\frac{\partial}{\partial t}\vec{e}\int\int\int_V \rho\vec{v}\,dV = -\int\int_\sum (p\vec{e} + \rho\vec{v}(\vec{v}.\vec{e})).d\vec{\Sigma} + \int\int\int_V \vec{e}.\vec{f}dV \tag{4}$$

La cantidad $p\vec{e} + \rho\vec{v}(\vec{v}.\vec{e})$ es el **flujo**, a través de la frontera, $\sum = \partial V$, **de la componente de la densidad de momento en la dirección** $\vec{e}$

- **Ecuación de la energía:**

Sean $\left(\frac{1}{2}\rho\vec{v}^2 + \rho\epsilon\right)dV$ las contribuciones a la energia cinética e interna de un elemento de volumen del fluido (ϵ = energia interna específica).

$$\frac{d}{dt}\int\int\int_V \left(\frac{1}{2}\rho\vec{v}^2 + \rho\epsilon\right)\, dV = -\int\int_{\sum} (p\vec{v})\,.d\vec{\Sigma} + \int\int\int_V \vec{f}.\vec{v}dV \quad (5)$$

i) Desarrollando la derivada total, ii) aplicando el teorema de la divergencia en la integral de supericie, y iii) agrupando términos bajo la divergencia $\Longrightarrow$ La igualdad anterior debe verificarse para todo volumen:

$$\frac{\partial}{\partial t}\left(\frac{1}{2}\rho\vec{v}^2 + \rho\epsilon\right) + \vec{\nabla}.\left[\left(\frac{1}{2}\rho\vec{v}^2 + \rho\epsilon + p\right)\vec{v}\right] = \rho\vec{g}.\vec{v} \quad (6)$$

La cantidad $\left(\frac{1}{2}\rho\vec{v}^2 + \rho\epsilon + p\right).\vec{v}$ es el **flujo de energía** a través de la frontera.

- **Las ecuaciones de la dinámica de fluidos ideales como un sistema hiperbólico de leyes de conservación:**

$$\boxed{\frac{\partial \mathbf{u}}{\partial t} + \frac{\partial \mathbf{f}^i(\mathbf{u})}{\partial x^i} = \mathbf{s}(\mathbf{u})}$$

$$\begin{aligned}
\mathbf{u} &= \left(\rho, \rho v^j, e\right)\\
\mathbf{f}^i(\mathbf{u}) &= \left(\rho v^i, \rho v^i v^j + p\delta^{ij}, (e+p)v^i\right)\\
\mathbf{s}(\mathbf{u}) &= \left(0, -\rho\frac{\partial\Phi}{\partial x^j} + Q^j_M, -\rho v^i\frac{\partial\Phi}{\partial x^i} + Q_E + v^i Q^i_M,\right)
\end{aligned}$$

donde $\mathbf{u}$ es el *vector de variables conservadas*, $\mathbf{f}^i(\mathbf{u})$ son los *flujos* en cada dirección i, $\mathbf{s}(\mathbf{u})$ son las *fuentes*, y Q^i_M, Q_E son los términos fuentes en las ecuaciones, respectivamente, de la densidad de momento y de energía, debidos al acoplamiento materia-radiación (en el supuesto de considerar fenómenos de transporte). Una *ecuación de estado* $p = p(\rho, \epsilon)$ cierra el sistema.

Flujo **isoentrópico**: $\Longrightarrow$ *La entropía se conserva en espacio y tiempo*

$\Longrightarrow \quad \dfrac{Ds}{Dt} = 0 \;\; , \;\; \dfrac{D}{Dt} \equiv \dfrac{\partial}{\partial t} + \vec{v}.\vec{\nabla}$

Flujo **adiabático**: $\vec{v}.\vec{\nabla} s = 0 \Longrightarrow$ *La entropía se conserva a lo largo de las trayectorias* $\Longleftarrow$ Ecuación de la energía (fluido perfecto) y estacionario

Fluido **perfecto, estacionario**, en un campo de fuerzas externo **conservativo**, $\vec{g}$

$\Longrightarrow \; \vec{g} = -\vec{\nabla}\Phi$

$\Longrightarrow \; h = \epsilon + \dfrac{p}{\rho}$ es la *entalpía específica*

$$\textbf{Teorema de Bernouilli:} \quad \mathcal{B} \;\equiv\; \frac{1}{2}\vec{v}^2 + \Phi + h \;=\; cte.$$

$\Longrightarrow \; \mathcal{B}$ *es constante a lo largo de las trayectorias*

$\Longrightarrow$ *Flujo isoentrópico*: $\vec{\nabla}\; \mathcal{B} = \vec{v} \times \vec{\omega} \;\; , \;\; \vec{\omega} = \vec{\nabla} \times \vec{v}$

$\Longrightarrow \; \mathcal{B}$ constante a lo largo de las trayectorias

$\Longrightarrow \; \mathcal{B}$ constante a lo largo de las líneas de vorticidad

$\Longrightarrow \; \mathcal{B}$ constante en espacio (*si el flujo es* **irrotacional**)

Flujo **incompresible**: $\Longrightarrow \quad \dfrac{D\rho}{Dt} = 0 \;\; , \;\; \Longleftrightarrow \;\; \vec{\nabla}.\vec{v} = 0$

$\Longrightarrow$ Si $\rho(t = 0, \vec{r}) = cte \quad \rightarrow \quad \rho(t, \vec{r}) = cte \;\forall t \;,\; \forall \vec{r}$

$\Longrightarrow \; \dfrac{D\vec{\omega}}{Dt} = (\vec{\omega}.\vec{\nabla})\vec{v} \;\; \Longrightarrow$

El flujo de un fluido perfecto incompresible e irrotacional permanece irrotacional $\rightarrow$ Flujo **potencial**

Flujo Potencial:

$$\vec{v} = \vec{\nabla}\phi$$

$$\Delta\phi = 0$$

- **Equilibrio Hidrostático**

$\vec{v} = 0$ & **estacionario** $\Longrightarrow$

$$-\frac{1}{\rho}\vec{\nabla}p + \vec{g} = 0 \tag{7}$$

$\Longrightarrow$ *Campo gravitatorio*: $\vec{g} = -\vec{\nabla}\Phi$, con Φ solución de la ecuación de Poisson: $\Delta\Phi = 4\pi G\rho$

$$\Updownarrow$$

Aplicando el operador *divergencia* a ambos lados de (7)

Ecuación de Equilibrio Hidrostático:

$$\vec{\nabla}.\left(\frac{1}{\rho}\vec{\nabla}p\right) = -4\pi G\rho$$

$\Longrightarrow$ **Simetría esférica** (coordenadas esféricas):

$$\boxed{\frac{1}{r^2}\frac{d}{dr}\left(\frac{r^2}{\rho}\frac{dp}{dr}\right) = -4\pi G\rho}$$

$\Longrightarrow$ Integrando una vez (en la variable r) y dado que:

$$m(r) = \int_0^r 4\pi r^2 \rho dr \Longleftrightarrow \frac{dm}{dr} = 4\pi r^2 \rho \tag{8}$$

$$\boxed{\begin{gathered} \frac{dp}{dr} = -G\,\frac{m(r)\,\rho(r)}{r^2} \\ \frac{dm}{dr} = 4\pi r^2 \rho \\ p = p(\rho) \end{gathered}}$$

$\Longrightarrow$ **Condiciones de contorno**:

A) *Centro* : $m(0) = 0$, $p(0) = p_c$ $\Longrightarrow$ *Superficie*: $p(R) = p_{sup}$

B) *Mixtas* : $m(0) = 0, m_{sup} = M$ $\Longrightarrow$ *Variable independiente* $r \rightarrow m$

$$\frac{dp}{dm} = -G\,\frac{m}{4\pi r(m)^4} \tag{9}$$

$$\frac{dr}{dm} = \frac{1}{4\pi r(m)^2 \rho(m)} \tag{10}$$

$\Longrightarrow$ **Versión relativista (TOV)**:

$$\frac{dp}{dr} = -G\,\frac{m(r)\,\rho(r)}{r^2}[h]\left[1 + \frac{4\pi r^3 p}{m}\right]\left[1 - \frac{2m}{r}\right]^{-1} \tag{11}$$

$\Longrightarrow$ **Energía Gravitacional**:

$$\boxed{\Omega = -G\int_0^M \frac{m(r)}{r}\,dm}$$

- **Teorema del Virial**

  Ecuación de Euler (descripción lagrangiana):

$$\frac{d\vec{v}}{dt} = -\frac{1}{\rho}\vec{\nabla}p + \vec{g} \implies \frac{d^2\vec{r}}{dt^2} = -\frac{1}{\rho}\vec{\nabla}p + \vec{g} \tag{12}$$

Aplicamos el operador: $\int \vec{r} dm$

$$\begin{aligned}
\implies \quad & \vec{r}.\frac{d^2\vec{r}}{dt^2} = \frac{d}{dt}(\vec{r}.\frac{d\vec{r}}{dt}) - \frac{d\vec{r}}{dt}.\frac{d\vec{r}}{dt} = \frac{d^2}{dt^2}(\frac{r^2}{2}) - \vec{v}.\vec{v} \\
\implies \quad & \int dm \left(\vec{r}.\frac{d^2\vec{r}}{dt^2}\right) = \frac{1}{2}\frac{d^2 I}{dt^2} - 2T \\
\implies \quad & \int dm \left(\vec{r}.\frac{\vec{\nabla}p}{\rho}\right) = \int dV \left(\vec{\nabla}.(p\vec{r}) - p\vec{\nabla}.\vec{r}\right) = \\
& = \int_{\sum} p\vec{r}.d\vec{\Sigma} - 3\int pdV
\end{aligned}$$

$$\boxed{\frac{1}{2}\frac{d^2 I}{dt^2} = 2T + 3\int pdV - \int_{\sum} p\vec{r}.d\vec{\Sigma} + \int \vec{r}.\vec{g}dm}$$

$$\vec{g} = -\vec{\nabla}\Phi \implies \int \vec{r}.\vec{g}dm = \Omega \tag{13}$$

i) Estático, ii) $p_{sup} = 0 \implies$

$$\boxed{3(\gamma - 1)U + \Omega = 0}$$

- **Colapso gravitatorio**

  I. Polvo: p = 0 $\Longrightarrow$

$$\frac{d^2r}{dt^2} = -\frac{G\,m(r)}{r^2} \tag{14}$$

$\Longrightarrow \quad t = 0,\ r = r_0,\ v = 0,\ \rho = \rho_0$ (constante en r) $\;\rightarrow$

$\rightarrow \;\; m(r_0) \;=\; (4/3)\pi r_0^3 \rho_0$ (constante en t)

Dado que:

$$\begin{aligned}
& \frac{d^2r}{dt^2} = \frac{dv}{dr}\frac{dr}{dt} = \frac{1}{2}\frac{dv^2}{dr} \\
\Longrightarrow \quad & \frac{1}{2}\frac{dv^2}{dr} = -\frac{G\,m}{r^2} \;\rightarrow\; \frac{v^2}{2} = G\,m\left(\frac{1}{r} - \frac{1}{r_0}\right) \;\rightarrow \\
\rightarrow \quad & \left(\frac{2Gm}{r_0}\right)^{1/2} dt \;=\; \left(\frac{r_0}{r} - 1\right)^{-1/2} dr \;\rightarrow \\
\rightarrow \quad & \left(\frac{2Gm}{r_0}\right)^{1/2} t \;=\; (r_0 - r)^{1/2} r^{1/2} \; + r_0 arcsen\left(\frac{r_0 - r}{r_0}\right)^{1/2} \;\rightarrow \\
\rightarrow \quad & \left(\frac{8\pi G\rho_0}{3}\right)^{1/2} t \;=\; (1 - x)^{1/2} x^{1/2} \; + arcsen(1 - x)^{1/2} \,\mathrm{siendo x} \equiv \mathrm{r/r_0}
\end{aligned}$$

Tiempo característico hidrodinámico, $\tau_\rho \Longrightarrow$ Haciendo $x = 0$ en la expresión anterior:

$$\boxed{\tau_\rho \;=\; \left(\frac{3\pi}{32G\rho_0}\right)^{1/2}}$$

Para el Sol, haciendo $\rho_0 \approx <\rho>_\odot \quad \rightarrow \;\; \tau_\rho \;\approx\; 1 hora$

II. Colapso homólogo de polítropos: $p = k\rho^\gamma$

$$\Longrightarrow \quad \frac{d^2r}{dt^2} = -\frac{G\,m(r)}{r^2} - \frac{1}{\rho}\frac{\partial\, p}{\partial\, r}$$

$$\Longrightarrow \quad t=0,\ r=r_0,\ \frac{d^2r}{dt^2}=0,\ \rho(r=r_0, t=0),=\rho_0 \rightarrow$$

$$\rightarrow \quad p(t=0) \ = k\rho_0^\gamma \equiv p_0$$

$\Longrightarrow$ *Homólogo*: $\rho(t) = \rho_0(r_0/r)^3 \Longrightarrow \quad p = p_0(r_0/r)^{3\gamma}$

$$\frac{1}{\rho}\frac{\partial\, p}{\partial\, r} = \left(-\frac{3\gamma p_0 r_0}{\rho_0}\right)\left(\frac{r_0}{r}\right)^{3\gamma-4}\left(\frac{1}{r^2}\right) \tag{15}$$

En $t=0$ es: $\left(\dfrac{1}{\rho}\dfrac{\partial\, p}{\partial\, r}\right)_{t=0} = -\dfrac{3\gamma p_0}{\rho_0 r_0}$

En $t=0$ es: $\dfrac{d^2r}{dt^2} = 0 \quad \rightarrow \quad \left(\dfrac{1}{\rho}\dfrac{\partial\, p}{\partial\, r}\right)_{t=0} = -\dfrac{Gm}{r_0}$

De las dos anteriores expresiones $\Longrightarrow \quad G\ m = \dfrac{3\gamma p_0 r_0}{\rho_0}$

$\rightarrow \quad m(r_0)$ es constante en t

Sustituyendo en (15) y sacando factor común el término $-\dfrac{Gm}{r}$

$$\boxed{\frac{d^2r}{dt^2} = -\frac{Gm}{r}\left(1 - \left(\frac{r_0}{r}\right)^{3\gamma-4}\right)}$$

$\Longrightarrow$ **Valor crítico** de $\gamma : \gamma_c = 4/3$

III. Masa de Jeans:

$$\frac{\partial \rho}{\partial t} + \vec{\nabla}.\left(\rho \vec{v}\right) = 0 \tag{16}$$

$$\frac{\partial \vec{v}}{\partial t} + (\vec{v}.\vec{\nabla})\vec{v} = -\frac{1}{\rho}\vec{\nabla}p - \vec{\nabla}\Phi \tag{17}$$

$$\Delta\Phi = 4\pi G\rho \tag{18}$$

$\Longrightarrow$ **Linealizando:** $\mathcal{Q} = \mathcal{Q}_0 + \lambda \mathcal{Q}_1$ (para: $\mathcal{Q} = \rho, p, \vec{v}, \Phi$)

$\Longrightarrow$ Suponiendo: $\rho_0 = cte.$, $\vec{v}_0 = 0$

$\Longrightarrow$ Eliminando $\vec{v}$ y Φ

$$\boxed{\left(\Delta - \frac{1}{c_s^2}\frac{\partial^2}{\partial t^2} + \frac{4\pi G\rho_0}{c_s^2}\right)\rho_1 = 0}$$

$\Longrightarrow$ $c_s^2 = p_1/\rho_1$ es el cuadrado de la **velocidad local del sonido** ($c_s^2 \sim T$, para gas ideal).

$\Longrightarrow$ Ensayando una solución tipo *ondas planas*:

$$\rho_1 = Aexp\{i(\vec{k}\vec{r} - \omega t)\} \tag{19}$$

se obtiene la **relación de dispersión**: $\omega^2 = k^2 c_s^2 - 4\pi G\rho_0$

$\Longrightarrow$ **Valor crítico:** $\omega^2 = 0 \rightarrow$

$$\rightarrow \qquad k_J^2 = \frac{4\pi G\rho_0}{c_s^2}$$

$$\rightarrow \qquad l_J = \frac{2\pi}{k_J}$$

$$\rightarrow \qquad M_J \sim \rho_0 l_J^3 \sim \rho_0^{-1/2} T^{3/2} \text{ (gas ideal).}$$

$\Longrightarrow$ **Inestabilidad** (perturbaciones crecen exponencialmente en el tiempo)

$$\boxed{M > M_J}$$

$\Longrightarrow$ **Estimaciones:** $l_J \approx 8 \times 10^7 \rho^{-1/2} T^{1/2} cm.$ (gas ideal).

$\rightarrow$ Componente *caliente y tenue*: $l_J \approx 3 \times 10^3 pc$

$\rightarrow$ Componente *fría y densa*: $l_J \approx 10pc$

Nebulosas Oscuras (Medio Interestalar)

Propiedades	Glóbulos		Nubes	
	Pequeños	Grandes	Intermedias	Grandes
$M/M_\odot$	≥ 0.1	3	800	1.8 $\times 10^4$
R (pc)	0.03	0.25	4	20
n (H/cm^3)	$\geq 4 \times 10^4$	1.6 $\times 10^3$	100	20

2.3 Fluidos Viscosos

$\Longrightarrow$ Admitimos la existencia de **gradientes de velocidad**.

$$d\vec{F} = -\mathcal{P} d\vec{\Sigma}$$

$\Longrightarrow$ $\mathcal{P}$ es un tensor (*tensor de presiones*), función de la *presión termodinámica* y del *gradiente de velocidades.*

$\Longrightarrow$ En coordenadas cartesianas, $\mathcal{P}_{ij}$ es la *i-componente de la fuerza sobre la unidad de superficie orientada en la j-dirección.*

$\Longrightarrow$ En general:

$$\mathcal{P} = p\mathcal{I} - \mathcal{S} \tag{20}$$

$\mathcal{I}$ es la matriz unidad, y $\mathcal{S}$ es el **tensor de tensiones**:

$$\mathcal{S}_{ij} = 2\mu\left(\mathcal{D}_i j - \frac{1}{3}\mathcal{D}_{kk}\delta_{ij}\right) + \xi\mathcal{D}_{kk}\delta_{ij}$$

$\Longrightarrow$ μ: *primer coeficiente de viscosidad* (**shear viscosity**)
$\Longrightarrow$ ξ: *segundo coeficiente de viscosidad* (**bulk viscosity**)
$\Longrightarrow$ $\mathcal{D}_{ij} = \dfrac{\partial v_i}{\partial x^j}$ (**tensor de deformaciones**).
$\Longrightarrow$ $\mathcal{D}_{kk} = Tr(\mathcal{D}) \equiv \Theta$ (**Expansión**).
$\Longrightarrow$ $\mathcal{D} - \frac{1}{3}\Theta\mathcal{I}$ (**tensor de distorsiones**).
$\Longrightarrow$ (traza nula: *deformación sin cambio de volumen*)

Ecuación de Euler extendida: $\dfrac{D\vec{v}}{Dt} = \vec{g} - \dfrac{1}{\rho}\vec{\nabla}.\mathcal{P}$

Ecuación de Navier-Stokes:

$$\frac{D\vec{v}}{Dt} = \vec{g} - \frac{1}{\rho}\vec{\nabla}p + \frac{\mu}{\rho}\Delta\vec{v} + \left(\frac{\xi + \frac{1}{3}\mu}{\rho}\right)\vec{\nabla}(\vec{\nabla}.\vec{v})$$

$\Longrightarrow$ Fluido **incompresible** :

$$\frac{D\vec{v}}{Dt} = \vec{g} - \frac{1}{\rho}\vec{\nabla}p + \nu\Delta\vec{v} \tag{21}$$

$\Longrightarrow$ $\nu = \mu/\rho$ es el **coeficiente de viscosidad cinemática**

$\Longrightarrow$ $\mathcal{R} \equiv \dfrac{LV}{\nu}$ es el **número de Reynolds**

$\Longrightarrow$ L, V: longitud y velocidad características

$\Longrightarrow$ $\mathcal{R} \gg 1 \quad \rightarrow$ *efectos de viscosidad despreciables*

$\Longrightarrow$ *Aplicando el operador rotacional* a N-S: **Difusión de la vorticidad**

$$\frac{D\vec{\omega}}{Dt} = (\vec{\omega}.\vec{\nabla})\vec{v} + \nu\Delta\vec{\omega} \tag{22}$$

Ecuación de la energía extendida:

$$\frac{D\left(\frac{1}{2}\vec{v}^2 + \epsilon\right)}{Dt} = \vec{g}.\vec{v} - \frac{1}{\rho}\vec{\nabla}.(\mathcal{P}.\vec{v}) \tag{23}$$

Disipación de energía $\rightarrow$ Despejando $\dfrac{D\epsilon}{Dt}$, e introduciendo el tensor de tensiones:

$$\frac{D\epsilon}{Dt} = -\frac{p}{\rho}(\vec{\nabla}.\vec{v}) + \frac{1}{\rho}Tr\left((\mathcal{S}.\vec{\nabla})\vec{v}\right) \tag{24}$$

$\Longrightarrow$ El primer término a la derecha $\rightarrow$ **expansión adiabática**

$\Longrightarrow$ El segundo término a la derecha $\rightarrow$ $\dfrac{1}{\rho}\left(\mathcal{S}_{ij}\dfrac{\partial v_j}{\partial x^i}\right)$

es un *ritmo de generación de energía –calor– por* **efectos de viscosidad**.

$\Longrightarrow$ Si hubiese *flujo de calor*, $\vec{Q} \rightarrow \quad -\dfrac{1}{\rho}\vec{\nabla}.\vec{Q}$

2.4 Flujo Compresible Unidimensional

2.4.1 Teoría lineal de perturbaciones

$\Longrightarrow$ *Perturbaciones adiabáticas* $(\delta\rho, \delta p)$ *en un fluido perfecto, homogéneo y en reposo*

$$\boxed{\left(\Delta - \frac{1}{c_s^2}\frac{\partial^2}{\partial t^2}\right)\delta\rho = 0}$$

$\Longrightarrow$ *A primer orden*: $\delta p = \left(\frac{\partial p}{\partial \rho}\right)_s \delta\rho$

$\Longrightarrow$ $c_s^2 \equiv \left(\frac{\partial p}{\partial \rho}\right)_s$

$\Longrightarrow$ $c_s^2 = \frac{\gamma p}{\rho} \sim T$, *para gas ideal*

$\Longrightarrow$ δp satisface la misma **ecuación de ondas**.

$\Longrightarrow$ Estado inicial: *irrotacional e isoentrópico* (en un fluido perfecto) $\rightarrow$ **el estado perturbado es irrotacional** $\rightarrow$ $\vec{v} = \vec{\nabla}\phi$ $\rightarrow$ ϕ y cada componente de $\vec{v}$ satisfacen la misma **ecuación de ondas**.

$\Longrightarrow$ *Flujo unidimensional*, en coordenadas esféricas (*ondas esféricas*):

$$\frac{1}{r^2}\frac{\partial}{\partial r}\left(r^2\frac{\partial A}{\partial r}\right) - \frac{1}{c_s^2}\frac{\partial^2 A}{\partial t^2} = 0 \tag{25}$$

$$A = \delta\rho, \delta p, v_i, \phi \tag{26}$$

$\Longrightarrow$ Solución general: *superposición de ondas esféricas convergentes y divergentes*:

$$A = \frac{1}{r}\left[f_1(r - c_s t) + f_2(r + c_s t)\right] \tag{27}$$

2.4.2 Invariantes de Riemann

$\Longrightarrow$ *Flujo adiabático, unidimensional*: $\rho = \rho(t,x)$, $p = p(t,x)$, $\vec{v} = v(t,x)\vec{i}$

$$\frac{\partial \rho}{\partial t} + \frac{\partial \rho v}{\partial x} = 0 \tag{28}$$

$$\frac{\partial v}{\partial t} + v\frac{\partial v}{\partial x} = -\frac{1}{\rho}\frac{\partial p}{\partial x} \tag{29}$$

$$\frac{\partial s}{\partial t} + v\frac{\partial s}{\partial x} = 0 \tag{30}$$

$\Longrightarrow$ *Ecuación de estado:* $\rho = \rho(s,p) \;\rightarrow\; c_s^{-2} = \left(\frac{\partial \rho}{\partial p}\right)_s$

$\Longrightarrow$ *Variables primitivas:* $\mathbf{U} = (p, v, s)$

$$\mathcal{A}^t \mathbf{U}_t + \mathcal{A}^x \mathbf{U}_x = 0 \tag{31}$$

$\Longrightarrow$ (31) es un **sistema cuasilineal** (subíndices: variable respecto de la cual se calcula la derivada parcial), donde las matrices $\mathcal{A}^t$ y $\mathcal{A}^x$ dependen de $\mathbf{U}$:

$$\mathcal{A}^t = \begin{pmatrix} 1 & 0 & 0 \\ 0 & \rho & 0 \\ 0 & 0 & 1 \end{pmatrix} \;,\; \mathcal{A}^x = \begin{pmatrix} v & \rho\, c_s^2 & 0 \\ 1/\rho & v & 0 \\ 0 & 0 & v \end{pmatrix}$$

Sea la *combinación lineal* de las dos primeras ecuaciones en (31):
$\lambda_1(p_t + v p_x + \rho c_s^2 v_x) + \lambda_2(p_x + \rho v_t + \rho v v_x) = 0 \;\rightarrow$
$\rightarrow \;\; p_t + (v+\zeta)p_x + \zeta\rho v_t + (\rho c_s^2 v_x + \zeta\rho v)v_x = 0$
$\rightarrow \;\; (\zeta \equiv \lambda_2/\lambda_1)$

Imponemos la condición de que las funciones *presión y velocidad* aparezcan derivadas **a lo largo de la misma dirección** (la correspondiente a una cierta curva $\mathcal{C}$):

$$\frac{v+\zeta}{1} = \frac{\rho c_s^2 + \zeta\rho v}{\zeta\rho} \Longrightarrow \zeta = \pm c_s$$

$$\rightarrow \qquad p_t + (v \pm c_s)p_x + \rho c_s\,(v_t + (v\pm c_s)v_x) = 0 \tag{32}$$

$\Longrightarrow$ **Operadores:** $D_\pm \equiv \frac{\partial}{\partial t} + (v \pm c_s)\frac{\partial}{\partial x} \;,\; D_0 \equiv \frac{\partial}{\partial t} + v\frac{\partial}{\partial x} \;,$

$$\boxed{\begin{aligned} D_\pm p \pm \rho c_s D_\pm v &= 0 \\ D_0 s &= 0 \end{aligned}}$$

Las ecuaciones en (31) se han reescrito, en (2.4.2) y (2.4.2), de modo que las derivadas $D_\pm, D_0$ son **direccionales** según las *curvas integrales* ($\mathcal{C}_\pm$, $\mathcal{C}_0$, respectivamente) de las ecuaciones diferenciales:

$$\boxed{\begin{aligned} \mathcal{C}_\pm : \ \frac{dx}{dt} &= v \pm c_s \\ \mathcal{C}_0 : \ \frac{dx}{dt} &= v \end{aligned}}$$

$\Longrightarrow$ Los campos de curvas $\mathcal{C}_\pm, \mathcal{C}_0$ son las **características** del sistema.
$\Longrightarrow$ Las ecuaciones en (2.4.2) y (2.4.2) son *ecuaciones diferenciales ordinarias sobre cada una de las curvas características* $\rightarrow$ **método de las características**
$\Longrightarrow$ *En un diagrama espacio–tiempo* $\rightarrow$ **dominio de dependencia** , **rango de influencia**
$\Longrightarrow$ *Flujo isoentrópico* $\rightarrow$ La (2.4.2) es **redundante** $\rightarrow$ $\rho = \rho(p)$ $\rightarrow$
$\rightarrow$ $c_s = c_s(p)$. En este caso, los **invariantes de Riemann**:

$$\boxed{J_\pm = v \pm \int \frac{dp}{\rho c_s}}$$

son **constantes a lo largo de** $\mathcal{C}_\pm$: $D_\pm J_\pm = 0$
$\Longrightarrow$ *Gas ideal isoentrópico:* $p = (\gamma - 1)\rho\epsilon$, $d\epsilon = -pd(1/\rho)$

$$J_\pm = v \pm \frac{2c_s}{\gamma - 1} \tag{33}$$

2.4.3 Ondas Simples

$\Longrightarrow$ **Estado Constante:** *Región del plano x-t donde los valores de todas las magnitudes que definen el fluido son constantes.*

$\Longrightarrow$ *Flujo isoentrópico* $\rightarrow$ **velocidad y presión constantes**

$\Longrightarrow$ *Flujo isoentrópico* $\rightarrow$ **Las características son rectas**

$\Longrightarrow$ **La frontera** de un estado constante (en el plano $x - t$) son *características*

$\Longrightarrow$ **Onda Simple**: *Región del plano x-t donde uno de los invariantes de Riemann* (J_+, J_-) *es constante.*

$\Longrightarrow$ *En una onda simple tal que* $J_+(J_-)$ *sea constante, las características* $\mathcal{C}_-(\mathcal{C}_+)$ son **líneas rectas**.

$\Longrightarrow$ *Las regiones adyacentes a los estados constantes son ondas simples.*

$\Longrightarrow$ *Las partículas del fluido que atraviesan una onda simple,* $J_-(J_+)$*, lo hacen de derecha a izquierda (de izquierda a derecha); en consecuencia, ven viajar la onda simple,* $J_-(J_+)$ *de izquierda a derecha (de derecha a izquierda)*

$\Longrightarrow$ De la definición de J_- en (2.4.2) $\rightarrow$ $dv - \dfrac{dp}{\rho c_s} = 0$ $\rightarrow$ *Las ondas simples* J_- verifican: $\dfrac{d(v + c_s)}{dv} > 0$

$\Longrightarrow$ De la definición de J_+ en (2.4.2) $\rightarrow$ $dv + \dfrac{dp}{\rho c_s} = 0$ $\rightarrow$ *Las ondas simples* J_+ verifican: $\dfrac{d(v - c_s)}{dv} > 0$

$\Longrightarrow$ **Onda de Rarefacción**: *Onda simple en la que la presión (densidad) disminuye al atravesarla.*

$\Longrightarrow$ *Si la onda simple,* $J_-(J_+)$ *es de rarefacción* $\rightarrow$ v y $v + c_s$ **disminuyen** (v y $v - c_s$ **aumentan)** *a lo largo de las trayectorias de las partículas del fluido.*

$\Longrightarrow$ **Onda de Compresión**: *Onda simple en la que la presión (densidad) aumenta al atravesarla.*

$\Longrightarrow$ *Si la onda simple,* $J_-(J_+)$ *es de compresión* $\rightarrow$ v y $v + c_s$ **aumentan** (v y $v - c_s$ **disminuyen)** *a lo largo de las trayectorias de las partículas del fluido.*

$\Longrightarrow$ **Onda Simple Centrada**: *La familia de características que son líneas rectas confluyen todas en un punto.*

$\Longrightarrow$ *Sea* J_- *una onda simple de rarefacción centrada.*

$\Longrightarrow$ **Obtengamos la solución para toda la región**

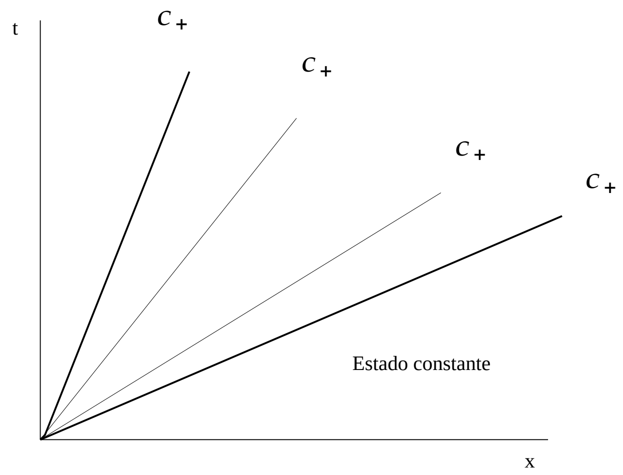

Figure 1: J_- es una rarefacción centrada, en el origen, y adyacente a un estado constante

1. *Estado constante:* $v_0, p_0, \rho_0, c_{s_0}$. *Gas ideal.*
2. De la definición de J_- en (2.4.2) $\Longrightarrow$ $v - \dfrac{2c_s}{\gamma - 1} = v_0 - \dfrac{2c_{s_0}}{\gamma - 1}$
3. *Las características* $\mathcal{C}_+$ *son rectas* $\Longrightarrow$ $\dfrac{dx}{dt} = v + c_s \;\rightarrow\; x = (v + c_s)t$
4. *Introduciendo la variable:* $\xi \equiv \dfrac{x}{t}$, de las dos últimas ecuaciones se obtienen v y c_s (y, por tanto, p) en función de ξ:

$$\boxed{\begin{aligned} v &= \frac{1}{\gamma - 1}\left[2\xi + (\gamma - 1)v_0 - 2c_{s_0}\right] \\ c_s &= \frac{\gamma - 1}{\gamma + 1}\left[\xi - v_0\right] + \frac{2c_{s_0}}{\gamma + 1} \end{aligned}}$$

La solución para el flujo es la misma en todos los puntos (x,t) tales que $\xi = cte.$ $\Longrightarrow$ **Flujo autosemejante**.

2.4.4 Ondas de Choque

$\Longrightarrow$ *En el estado definido por la* **onda simple J_- de compresión** *los valores de la presión y la velocidad* **permanecen constantes a lo largo de las características** $\mathcal{C}_+$ $\rightarrow$ En los puntos en que **las características se cruzan la solución es discontinua** $\rightarrow$ **CHOQUE**

$\Longrightarrow$ *Flujo unidimensional, ecuaciones en forma conservativa*:

$$\frac{\partial \rho}{\partial t} + \frac{\partial \rho v}{\partial x} = 0 \tag{34}$$

$$\frac{\partial \rho v}{\partial t} + \frac{\partial (\rho v^2 + p)}{\partial x} = 0 \tag{35}$$

$$\frac{\partial \rho(\frac{1}{2}v^2 + \epsilon)}{\partial t} + \frac{\partial (\frac{1}{2}\rho v^2 + \rho h) v}{\partial x} = 0 \tag{36}$$

Sistema de leyes de conservación:

$$\frac{\partial \mathbf{U}}{\partial t} + \frac{\partial \mathbf{F}(\mathbf{U})}{\partial x} = 0$$

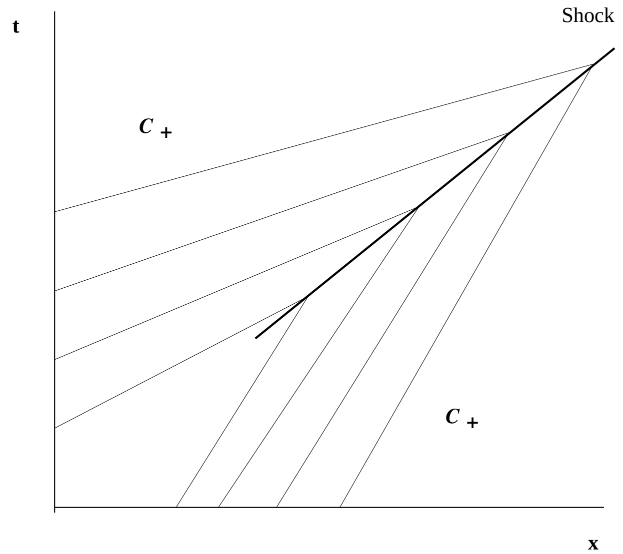

Figure 2: Onda simple J_- de compresión y onda de choque

$\Longrightarrow$ *Si el campo vectorial* $\mathbf{F}(\mathbf{U})$ *se anula en el infinito*:

$$\frac{d}{dt}\int_{-\infty}^{+\infty}\mathbf{U}dx \;=\; \int_{-\infty}^{+\infty}\frac{\partial\mathbf{U}}{\partial t}dx \;=\; -\int_{-\infty}^{+\infty}\frac{\partial\mathbf{F}}{\partial x}dx \;=\; -\;[\mathbf{F}]_{-\infty}^{+\infty} \;=\; 0 \quad (37)$$

$\Longrightarrow$ *Sea* $x=\zeta(t)$ *la trayectoria de la discontinuidad*:

$$\frac{d}{dt}\int_{-\infty}^{+\infty}\mathbf{U}dx \;=\; \frac{d}{dt}\int_{-\infty}^{\zeta(t)}\mathbf{U}dx + \frac{d}{dt}\int_{\zeta(t)}^{+\infty}\mathbf{U}dx \;= \quad (38)$$

$$= \int_{-\infty}^{\zeta(t)}\frac{\partial\mathbf{U}}{\partial t}dx + \frac{d\zeta}{dt}\mathbf{U}(\zeta_-) + \int_{\zeta(t)}^{+\infty}\frac{\partial\mathbf{U}}{\partial t}dx - \frac{d\zeta}{dt}\mathbf{U}(\zeta_+) \;= \quad (39)$$

$$= -\int_{-\infty}^{\zeta(t)}\frac{\partial\mathbf{F}}{\partial x}dx - \int_{\zeta(t)}^{+\infty}\frac{\partial\mathbf{F}}{\partial x}dx + \frac{d\zeta}{dt}\left(\mathbf{U}(\zeta_-) - \mathbf{U}(\zeta_+)\right) \;= \quad (40)$$

$$= -\mathbf{F}_- + \mathbf{F}_+ + \frac{d\zeta}{dt}(\mathbf{U}_- - \mathbf{U}_+) \quad (41)$$

Condiciones de salto:

$$\frac{d}{dt}\int_{-\infty}^{+\infty}\mathbf{U}dx \;=\; 0 \Longrightarrow [\mathbf{F}] \;=\; v_s[\mathbf{U}]$$

$\Longrightarrow$ $[X]\equiv X_+ - X_-$ es el **salto a través de la discontinuidad**

$\Longrightarrow$ $v_s \equiv \dfrac{d\zeta}{dt}$ es la **velocidad de propagación de la discontinuidad**

Relaciones de Rankine-Hugoniot:

$$[\rho v] \;=\; v_s[\rho]$$

$$[\rho v^2 + p] \;=\; v_s[\rho v]$$

$$[\rho v(\frac{1}{2}v^2 + h)] \;=\; v_s[\rho(\frac{1}{2}v^2 + \epsilon)]$$

$\Longrightarrow$ *Sistema de referencia* **ligado a la discontinuidad** $\rightarrow$ $u = v - v_s$ es la *velocidad relativa del fluido*

$$\boxed{\begin{aligned} [\rho u] &= 0 \Longrightarrow \rho_1 u_1 = \rho_2 u_2 \equiv j \\ [\rho u^2 + p] &= 0 \Longrightarrow \rho_1 u_1^2 + p_1 = \rho_2 u_2^2 + p_2 \\ [\rho u(\frac{1}{2}u^2 + h)] &= 0 \Longrightarrow [\frac{1}{2}u^2 + h] = 0 \Longrightarrow \frac{1}{2}u_1^2 + h_1 = \frac{1}{2}u_2^2 + h_2 \end{aligned}}$$

$\Longrightarrow$ El estado con subíndice 1(2) es el *delantero (trasero)* o *prechoque (postchoque).*

$\Longrightarrow$ *La cantidad* j es el **flujo de masa** *a través de la discontinuidad.*

$\Longrightarrow$ *Las relaciones de salto no determinan completamente el sistema* (**condición de entropía**).

$\Longrightarrow$ *Definiendo* $\tau \equiv 1/\rho$ (**volumen específico**), las condiciones de salto se pueden reescribir:

$$\boxed{\begin{gathered} u_1 = j\tau_1 \quad , \quad u_2 = j\tau_2 \\ j^2 = \frac{p_2 - p_1}{\tau_1 - \tau_2} \\ h_1 - h_2 = \frac{1}{2}(p_1 - p_2)(\tau_1 + \tau_2) \Longrightarrow \epsilon_2 - \epsilon_1 = \frac{1}{2}(p_1 + p_2)(\tau_1 - \tau_2) \end{gathered}}$$

$\Longrightarrow$ La (2.4.4) es *definida positiva* $\rightarrow$ A través de la onda de choque, *en principio son válidas* las dos combinaciones de relaciones siguientes: a) $p_2 > p_1$, $\tau_1 > \tau_2$, b) $p_2 < p_1$, $\tau_1 < \tau_2$ $\rightarrow$ La *condición de entropía selecciona* la **a)** $\rightarrow$ De (2.4.4) $\epsilon_2 - \epsilon_1 > 0$.

$\Longrightarrow$ La (2.4.4) es la **adiabática de Hugoniot**.

$\Longrightarrow$ La adiabática de Hugoniot (2.4.4) relaciona las variables termodinámicas a ambos lados de la onda de choque. Junto con la *ecuación de estado* ($p = p(\rho, \epsilon)$), y *fijado el estado* 1, la (2.4.4) admite una representación en el plano $\tau - p$: *lugar geométrico de todos los estados 2 que pueden ser conectados con el 1 a través de una onda de choque , la cual tiene al estado 1 como prechoque.*

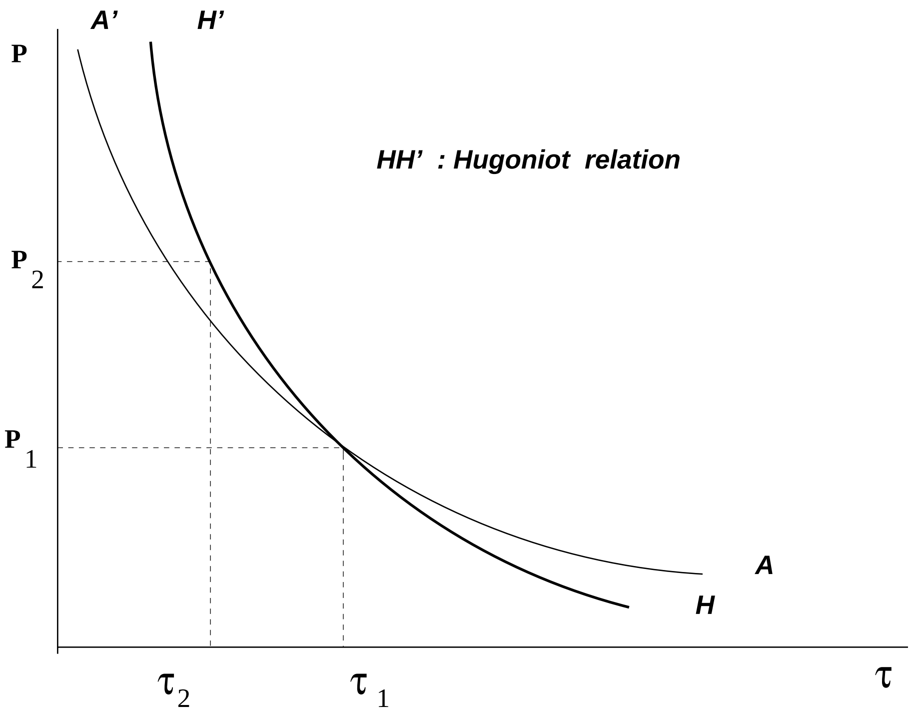

Figure 3: Diagrama $\tau - p$ donde se han representado la adiabática de Hugoniot (H) y la adiabática (A) que pasa por el estado $\tau_1 - p_1$

Algunas consecuencias de las condiciones de salto (2.4.4),(2.4.4) y (2.4.4):

$\Longrightarrow \quad \frac{dp_H}{d\tau} \mid_{\tau_1} = \frac{dp_A}{d\tau} \mid_{\tau_1}$

$\Longrightarrow \quad p_H > p_A \; \forall \tau < \tau_1$

$\Longrightarrow$ En la adiabática de Hugoniot, sean los estados (τ_1, p_1) y (τ_2, p_2):

$\mid \frac{p_2 - p_1}{\tau_2 - \tau_1} \mid > \mid \frac{dp_A}{d\tau}(\tau_1) \mid \; \rightarrow$ De (2.4.4): $j^2 \; > \; \frac{c_{s_1}^2}{\tau_1^2} \; \rightarrow$

$\rightarrow$ De (2.4.4): $\mid u_1 \mid > c_{s_1} \; \rightarrow$ *El estado prechoque, en el s.d.r. de la onda de choque, es* **supersónico**.

$\Longrightarrow$ De las (2.4.4) y (2.4.4): $u_1 - u_2 \; = \; \sqrt{(p_2 - p_1)(\tau_1 - \tau_2)}$

Discontinuidad de contacto: *No hay flujo de masa*

Condiciones de salto :

$$[v] \; = \; 0 \; , \; [p] \; = \; 0 \; , \; [\rho] \; arbitrario$$

2.4.5 Figuras

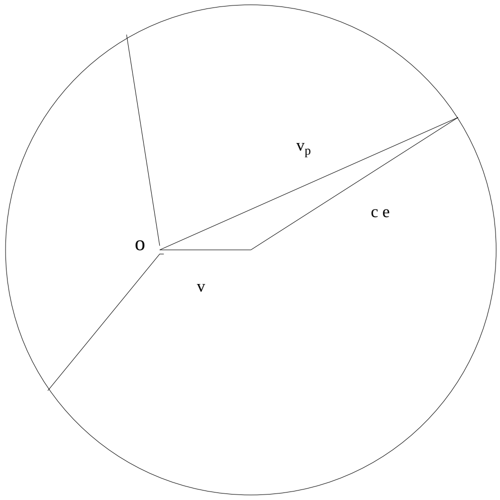

Figure 4: Caso *subsónico*: La perturbación se propaga, respecto del sistema de referencia laboratorio, con una velocidad $\vec{v}_p$ $(\vec{v}_p = \vec{v} + c\ \vec{e})$. Dicha perturbación se puede propagar en todas direcciones y, eventualmente, alcanzará cualquier punto de la región que contiene el gas.

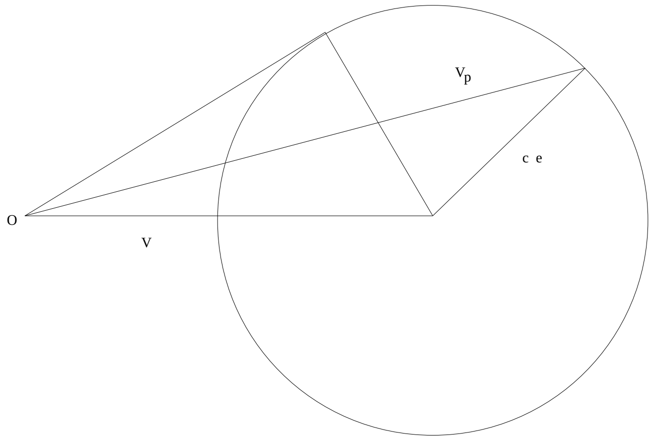

Figure 5: Caso *supersónico*: La perturbación se propaga, respecto del sistema de referencia laboratorio, con una velocidad $\vec{v}_p$ $(\vec{v}_p = \vec{v} + c\ \vec{e})$. Dicha perturbación se propaga dentro de un cono de semiapertura α: $\sin\alpha = c/v$.

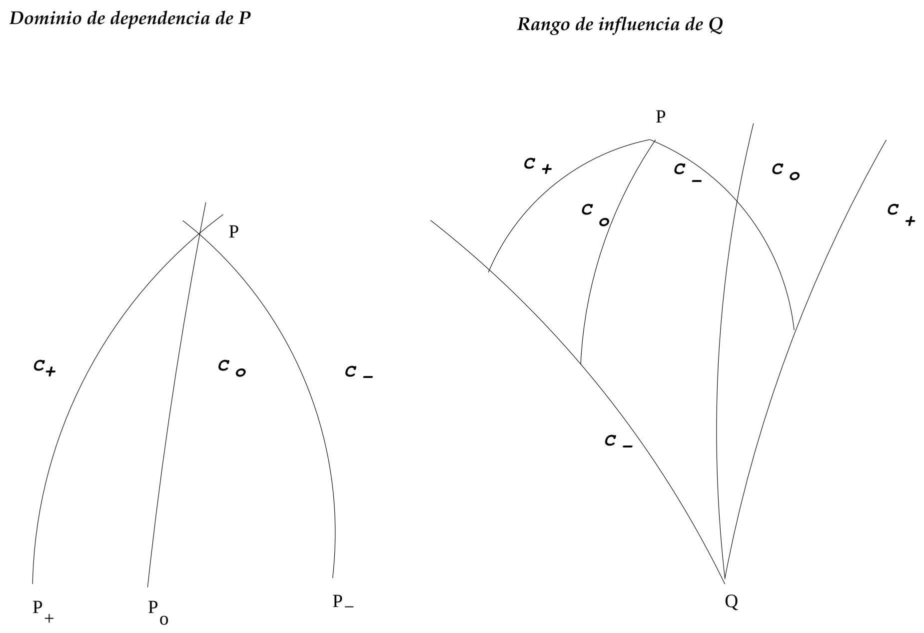

Figure 6: Dominio de dependencia de P (izquierda) y rango de influencia de Q (derecha)

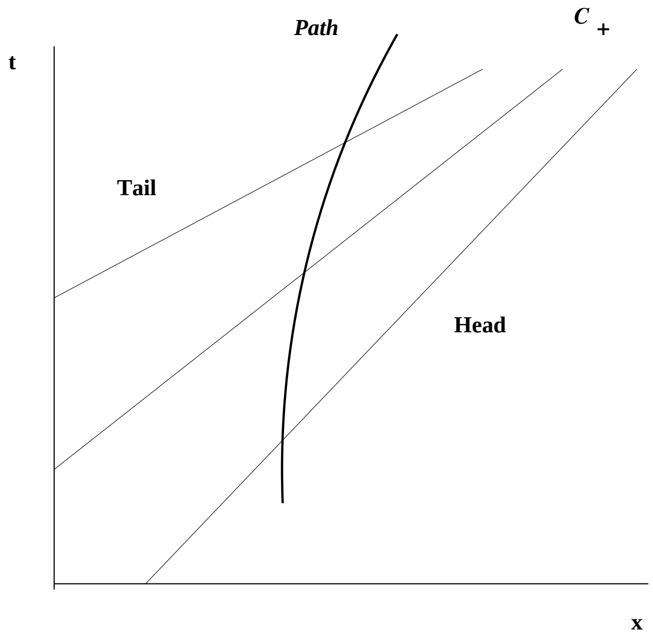

Figure 7: J_- de compresión: $v, v + c_s$ aumentan. (Forward-facing compression wave)

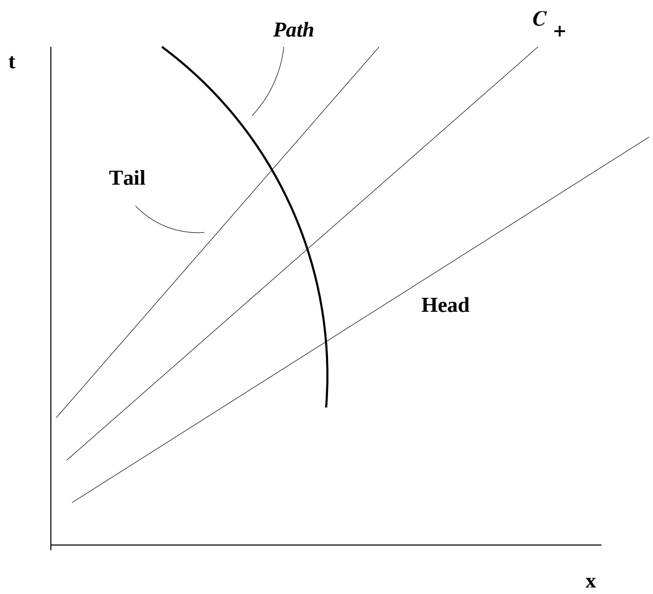

Figure 8: J_- de rarefacción: $v, v+c_s$ disminuyen. (Forward-facing expansion wave)

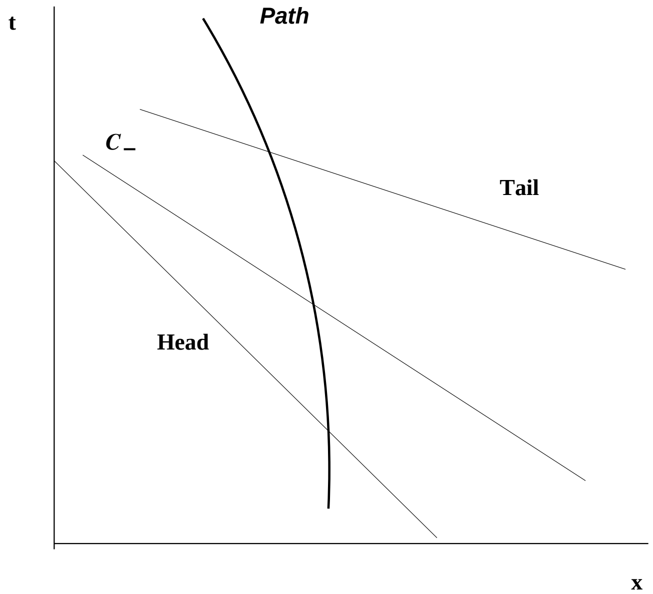

Figure 9: J_+ de compresión: $v, v - c_s$ disminuyen. (Backward-facing compression wave)

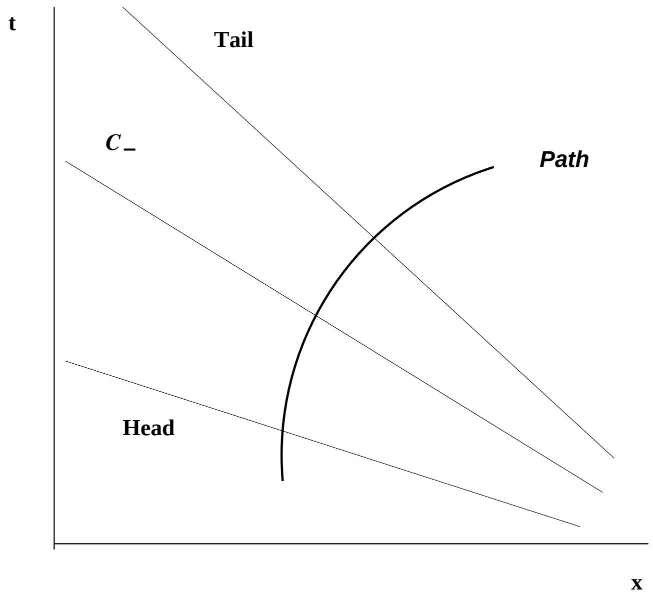

Figure 10: J_+ de rarefacción: $v, v - c_s$ aumentan. (Backward-facing expansion wave)

2.5 Relativistic Hydrodynamics

2.5.1 Equations of Relativistic Hydrodynamics in Conservation Form

The evolution of a relativistic fluid is described by a system of equations which are the expression of *local conservation laws*: the local conservation of *baryon number density*

$$\nabla_\mu J^\mu = 0 \tag{42}$$

and the local conservation of *energy-momentum*

$$\nabla_\mu T^{\mu\nu} = 0 \tag{43}$$

the current J^μ and the energy-momentum tensor $T^{\mu\nu}$ being

$$J^\mu = \rho u^\mu \tag{44}$$

$$T_{\mu\nu} = \rho h u_\mu u_\nu + p g_{\mu\nu} \tag{45}$$

(Greek and Latin indices run, respectively, from 0 to 3 and from 1 to 3. Units are used in which the speed of light is equal to one).

In the above equations ρ is the rest-mass density, p is the pressure and h is the specific enthalpy, defined by $h = 1 + \varepsilon + p/\rho$, where ε is the specific internal energy, u^μ is the four-velocity of the fluid and $g_{\mu\nu}$ defines the metric of a general space-time $\mathcal{M}$ where the fluid evolves, ∇_μ stands for the covariant derivative.

In Minkowski space-time, $\mathcal{M}$, the above system of equations, (42) and (43), can be written in a more compact way as:

$$\frac{\partial \mathbf{F}^\mu(\mathbf{w})}{\partial x^\mu} = 0 \tag{46}$$

being the five-vector of unknowns

$$\mathbf{w} = (\rho, v^i, \varepsilon) \tag{47}$$

where the components of the three-velocity, v^i, are defined according to

$$v^i = \frac{u^i}{u^0}$$

and the Lorentz factor, defined by $W \equiv u^0$, satisfies the familiar relation $W = (1 - \mathrm{v}^2)^{-1/2}$, where $\mathrm{v}^2 = \delta_{ij} v^i v^j$.

The quantities $\mathbf{F}^\alpha(\mathbf{w})$ are

$$\begin{aligned}
\mathbf{F}^0(\mathbf{w}) &= \Big(\rho W, \rho h W^2 v^j, \rho h W^2 - p - \rho W\Big) && (48)\\
\mathbf{F}^i(\mathbf{w}) &= \Big(\rho W v^i, \rho h W^2 v^j v^i + p\delta^{ij}, \\
&\quad \rho h W^2 v^i - \rho W v^i\Big) && (49)
\end{aligned}$$

The components of $\mathbf{F}^0(\mathbf{w})$

$$D \equiv \rho W \tag{50}$$

$$S^j \equiv \rho h W^2 v^j \tag{51}$$

$$\tau \equiv \rho h W^2 - p - \rho W \tag{52}$$

can be considered, respectively, the coordinate rest-mass density, the relativistic momentum density and the total energy density (substracted the rest-mass density).

An equation of state $p = p(\rho, \varepsilon)$ closes, as usual, the system. A very important quantity derived from the equation of state is the local sound velocity c_s:

$$hc_s^2 = \chi + (p/\rho^2)\kappa \tag{53}$$

with $\chi = \partial p/\partial\rho$ and $\kappa = \partial p/\partial\epsilon$. As it can be verified, for an ideal gas $p = (\Gamma - 1)\rho\epsilon$, the maximum value of the local sound velocity satisfies the following relations:

$$c_s^{max} = \sqrt{\Gamma - 1} = \sqrt{\tilde{\kappa}} \tag{54}$$

$\tilde{\kappa}$ being the quantity $\tilde{\kappa} \equiv \kappa/\rho$.

In the system of equations defined by (122) it is possible to carry out a theoretical analysis of the structure of the characteristic fields – see the next subsection – which will be crucial for numerical applications.

2.5.2 Characteristic fields

Let us introduce into system (122) the Jacobian matrices $\mathcal{A}^\alpha(\mathbf{w})$ associated to the five-vectors $\mathbf{F}^\alpha(\mathbf{w})$

$$\mathcal{A}^\alpha = \frac{\partial \mathbf{F}^\alpha(\mathbf{w})}{\partial \mathbf{w}} \tag{55}$$

then, system (122) can be written as a quasi-linear system of 5 first order partial differential equations for the unknown field $\mathbf{w}$

$$\mathcal{A}^{\mu}(\mathbf{w})\frac{\partial \mathbf{w}}{\partial x^{\mu}} = 0 \tag{56}$$

Finally, we introduce the vectors

$$\mathbf{u} = \mathbf{F}^0(\mathbf{w}) \tag{57}$$

$$\mathbf{f}^i = \mathbf{F}^i \circ (\mathbf{F}^0)^{-1} \tag{58}$$

where $\circ$ means composition of functions and $(.)^{-1}$ stands for the inverse function.

With the above definitions, system (122) reads as a system of conservation laws for the new vector of unknowns $\mathbf{u}$

$$\frac{\partial \mathbf{u}}{\partial x^0} + \frac{\partial \mathbf{f}^i(\mathbf{u})}{\partial x^i} = 0 \tag{59}$$

In the above system (59) we can define three 5×5-Jacobian matrices $\mathcal{B}^i(\mathbf{u})$, the Jacobian matrices associated to the vector $\mathbf{f}^i(\mathbf{u})$, the *flux* in the i-direction of the system (59), as:

$$\mathcal{B}^i = \frac{\partial \mathbf{f}^i(\mathbf{u})}{\partial \mathbf{u}} \tag{60}$$

Following a procedure similar to the one described in Font et al.(1994) we have succeeded in obtaining analytical expressions for the spectral decomposition of the matrices $\mathcal{B}^i(\mathbf{u})$. For the sake of clarity, let us restrict to a 2D case, i.e., to problems involving a dependence on two spatial coordinates (that we will denote with the scripts $i = x,\ y$ instead of $i = 1,2$)

The eigenvalues and the right and left eigenvectors of $\mathcal{B}^x$ (similar for i=y) are going to be displayed explicitly.

The eigenvalues of matrix $\mathcal{B}^x(\mathbf{u})$ are:

$$\lambda_{\pm} = \frac{1}{1 - v^2 c_s^2}\left\{v^x(1 - c_s^2) \pm c_s\sqrt{(1 - \mathrm{v}^2)[1 - v^x v^x - (v^2 - v^x v^x)c_s^2]}\right\} \tag{61}$$

$$\lambda_0 = v^x \quad \text{(double)} \tag{62}$$

Let us make several comments to the above expressions for the eigenvalues:

i) In the case ($v^x = v, v^y = 0$), expression (61) gives the corresponding one-dimensional eigenvalues

$$\lambda_{\pm} = \frac{v \pm c_s}{1 \pm v c_s} \tag{63}$$

ii) In the limit $|v^x| \to 1$, the *genuinely nonlinear* characteristic fields $\lambda_{\pm}$ become *linearly degenerate*.

For the sake of concisness and before showing the complete set of *right* and *left-eigenvectors*, let us define the following quantities:

$$\mathcal{K} = \frac{\tilde{\kappa}}{\tilde{\kappa} - c_s^2} \tag{64}$$

$$\mathcal{A}_{\pm} = \frac{1 - v^x v^x}{1 - v^x \lambda_{\pm}} \tag{65}$$

$$\Delta = h^2 W (\mathcal{K} - 1)(1 - v^x v^x)(\mathcal{A}_+ \lambda_+ - \mathcal{A}_- \lambda_-) \tag{66}$$

being Δ the determinant of the matrix of right-eigenvectors. As it can be proved, $\mathcal{K}$ is always greater than one, and Δ different from zero.

A complete set of *right-eigenvectors* is,

$$\mathbf{r}_{0,1} = \left(\frac{\mathcal{K}}{hW}, v^x, v^y, 1 - \frac{\mathcal{K}}{hW} \right) \tag{67}$$

$$\mathbf{r}_{0,2} = \Big(W v^y, 2hW^2 v^x v^y, h(1 + 2W^2 v^y v^y), 2hW^2 v^y - W v^y \Big) \tag{68}$$

$$\mathbf{r}_{\pm} = (1, hW\mathcal{A}_{\pm}\lambda_{\pm}, hWv^y, hW\mathcal{A}_{\pm} - 1) \tag{69}$$

The corresponding complete set of *left-eigenvectors* is

$$\mathbf{l}_{0,1} = \frac{W}{\mathcal{K} - 1}(h - W, W v^x, W v^y, -W)$$

$$\mathbf{l}_{0,2} = \frac{1}{h(1 - v^x v^x)}(-v^y, v^x v^y, 1 - v^x v^x, -v^y)$$

$$\mathbf{l}_{\mp} = (\pm 1)\frac{h}{\Delta}\begin{bmatrix} hW\mathcal{A}_{\pm}(v^x-\lambda_{\pm}) - v^x - W^2v^yv^y(2\mathcal{K}-1)(v^x-\mathcal{A}_{\pm}\lambda_{\pm}) + \mathcal{K}\mathcal{A}_{\pm}\lambda_{\pm} \\ \\ 1 + W^2v^yv^y(2\mathcal{K}-1)(1-\mathcal{A}_{\pm}) - \mathcal{K}\mathcal{A}_{\pm} \\ \\ W^2v^y(2\mathcal{K}-1)\mathcal{A}_{\pm}(v^x-\lambda_{\pm}) \\ \\ -v^x - W^2v^yv^y(2\mathcal{K}-1)(v^x-\mathcal{A}_{\pm}\lambda_{\pm}) + \mathcal{K}\mathcal{A}_{\pm}\lambda_{\pm} \end{bmatrix}$$

Symmetry relations allow to extend the above spectral decomposition to the other spatial direction y and also to the general 3D case.

As we have emphasized above, in order to apply HRSC methods to solve the equations of relativistic hydrodynamics as written in (59), the knowledge of the spectral decomposition of the Jacobian matrices $\mathcal{B}^i$ is crucial.

2.6 Magnetohidrodinámica Ideal

$\Longrightarrow$ **Escenarios astrofísicos**:

- *Discos de acreción* (campo débil): Binarias de rayos X.
- *Chorros*. En 2D y 3D con MHD y campos toroidales. Será necesaria la RMHD en los AGN.
  Emisión en radio $\rightarrow$ radiación sincrotrón del plasma $\rightarrow$ campos magnéticos.
- *Colapso magnetorotacional*. Mecanismos que generan $10^{14} - 10^{16} G$ (*magnetars, progenitores de erupciones de rayos* γ, ...).

$\Longrightarrow$ **Ecuaciones de la MHD ideal**:

- **Magnetohidrodinámica ideal** $\Longrightarrow$ Despreciamos: corriente de desplazamiento, fuerzas electrostáticas, viscosidad, conducción de calor y efectos de conductividad finita.
- $\vec{\nabla}.\vec{B} = 0 \;\rightarrow$ **Ligadura**
- *Gas ideal*: $p = (\gamma - 1)\rho\epsilon \;\rightarrow\; E = \frac{1}{2}\rho v^2 + \frac{p}{\gamma - 1} + \frac{1}{2}B^2.$

$$\boxed{\begin{aligned}
\frac{\partial \rho}{\partial t} + \vec{\nabla}.(\rho\vec{v}) &= 0 \\
\frac{\partial \vec{v}}{\partial t} + \vec{v}\,.\vec{\nabla}\vec{v} + \frac{1}{\rho}\vec{\nabla}p - \frac{1}{\rho}(\vec{\nabla} \times \vec{B}) \times \vec{B} &= 0 \\
\frac{\partial E}{\partial t} + \vec{\nabla}.\left[\vec{v}\left(E + p - \frac{B^2}{2}\right) + \vec{B} \times (\vec{v} \times \vec{B})\right] &= 0 \\
\frac{\partial \vec{B}}{\partial t} - \vec{\nabla} \times (\vec{v} \times \vec{B}) &= 0
\end{aligned}}$$

2.6.1 Ecuaciones de la MHD ideal en forma conservativa

$$\frac{\partial \vec{u}}{\partial t} + \frac{\partial \vec{F}}{\partial x} = 0$$

$$\begin{aligned}
\vec{u} &= (\rho,\ \rho v_x,\ \rho v_y,\ \rho v_z,\ B_y,\ B_z,\ E)^T \\
\vec{F} &= (\rho v_x,\ \rho v_x^2 + p^* - B_x^2,\ \rho v_x v_y - B_x B_y, \\
&\quad \rho v_x v_z - B_x B_z,\ B_y v_x - B_x v_y,\ B_z v_x - B_x v_z, \\
&\quad (E + p^*) v_x - B_x (B_x v_x + B_y v_y + B_z v_z))^T
\end{aligned}$$

$\Longrightarrow B_x = constante$

$\Longrightarrow p^* = p + \dfrac{1}{2} B^2$

Descomposición espectral

$$\lambda_1 = v_x - c_{mf}\ ,\ \lambda_2 = v_x - c_A\ ,\ \lambda_3 = v_x - c_{ms}\ ,\ \lambda_4 = v_x$$
$$\lambda_5 = v_x + c_{ms}\ ,\ \lambda_6 = v_x + c_A\ ,\ \lambda_7 = v_x + c_{mf}$$

$$c_A = \sqrt{\frac{B_x^2}{\rho}}$$

$$c_{mf} = \left\{ \frac{1}{2} \left[c_s^2 + \frac{B^2}{\rho} + \sqrt{\left(c_s^2 + \frac{B^2}{\rho} \right)^2 - 4 c_s^2 \frac{B_x^2}{\rho}} \right] \right\}^{1/2}$$

$$c_{ms} = \left\{ \frac{1}{2} \left[c_s^2 + \frac{B^2}{\rho} - \sqrt{\left(c_s^2 + \frac{B^2}{\rho} \right)^2 - 4 c_s^2 \frac{B_x^2}{\rho}} \right] \right\}^{1/2}$$

$$c_s = \sqrt{\gamma \frac{p}{\rho}}$$

- c_{mf}, c_A, $y\, c_{ms}$ son las velocidades *rápida*, *de Alfvén* y *lenta*, respectivamente.
- Las λ_i son las velocidades con que se propaga la información localmente: 3 familias de ondas y un modo de entropía (campo λ_4, que se propaga con la velocidad del fluido, y a lo largo del cual la entropía específica se mantiene constante).

- Brio y Wu demuestran la **no convexidad** de la MHD $\Longrightarrow$ *choque+rarefacción.* $\rightarrow$ *renormalización* del conjunto $\vec{r}$
- Ryu y Jones calculan los $\vec{l}$ $\rightarrow$ *mayor eficiencia del código*
- En la MHD puede haber 5 clases de discontinuidades:
  1. choques rápidos.
  2. choques lentos.
  3. discontinuidades tangenciales.
  4. discontinuidades de contacto.
  5. discontinuidades rotacionales.

2.6.2 Ecuaciones de la RMHD en forma conservativa

1. Conservación local del número bariónico:

$$\nabla_\mu J^\mu = 0$$

2. Conservación local de la energía-momento:

$$\nabla_\mu T^{\mu\nu} = 0$$

3. Ecuaciones de Maxwell:

$$\nabla_\mu H^{\mu\nu} = 0$$

$J^\mu = \rho u^\mu$
$T^{\mu\nu} = \rho h^* u^\mu u^\nu + p^* g^{\mu\nu} - \mu b^\mu b^\nu$
$H^{\mu\nu} = u^\mu b^\nu - u^\nu b^\mu$
$u^\mu = W(1, v^x, v^y, v^z)$
$b^\mu = (b^0, b^x, b^y, b^z)$
$h^* = 1 + \varepsilon + p/\rho + \mu \mid b \mid^2 /\rho$
$p^* = p + \mu \mid b \mid^2 /2$
$u^\mu b_\mu = 0$
$b_\mu b^\mu = \mid b \mid^2 \geq 0$
$\sigma^{\mu\nu} = \sigma_0 g^{\mu\nu} \quad \text{con} \quad \sigma_0 \to \infty$
$EOS : p = (\gamma - 1)\rho\epsilon$

$$\boxed{\frac{\partial \vec{U}(\vec{u})}{\partial t} + \frac{\partial \vec{f}(\vec{u})}{\partial x} = \vec{s}(\vec{u})}$$

$$\begin{aligned}
\vec{u} &= (\rho, v^j, \varepsilon, b^j) \\
\vec{U} &= (J^0, T^{oj}, T^{00}, H^{0j}) = \\
&= (\rho W, \rho h^* W^2 v^j, \rho h^* W^2 - p^* - \rho W, W h^j) \\
\vec{f} &= (J^x, T^{xj}, T^{0x}, H^{xj}) = \\
&= (\rho W v^x, \rho h^* W^2 v^j v^x + p^* \delta^{jx} - \mu b^j b^x, \\
&\quad \rho h^* W^2 v^x - \rho W v^x, W(v^j b^x - v^x b^j))
\end{aligned}$$

2.6.3 Caso particular: Campo transversal

$$\boxed{\begin{aligned} u^\mu &= W(1, v^x, 0, v^z) \\ b^\mu &= (0, 0, b, 0) \end{aligned}}$$

Campos característicos:

$$\lambda_0 = v^x \qquad \text{(triple)}$$

$$\lambda_\pm = \frac{v^x(1-\omega^2) \pm \sqrt{(1-v^2)[1-(v^x)^2-(v^2-(v^x)^2)\omega^2]}}{1-v^2\omega^2}$$

$$\omega^2 = c_s^2 + c_A^2 - c_s^2 c_A^2$$

- c_s (*velocidad local del sonido*) : $hc_s^2 = \chi + \dfrac{p}{\rho^2}\kappa$

$$\chi = \left(\frac{\partial p}{\partial \rho}\right)_\varepsilon \qquad , \qquad \kappa = \left(\frac{\partial p}{\partial \varepsilon}\right)_\rho$$

- c_A (*velocidad de Alfvén* relativista): $c_A^2 = \dfrac{\mu |b|^2}{\rho h^*}$

3 Sistemas Hiperbólicos de leyes de conservación

3.1 Introduction

- General Relativity plays a fundamental role when describing astrophysical systems containing compact objects
  - Core collapse supernovae
  - Pulsars
  - X-ray binaries
  - Coalescing neutron stars and/or black holes (BH/BH, BH/NS, NS/NS)
  - Black hole formation
  - Active galactic nuclei
  - Gamma-ray bursts (and superluminal jets)
  - Accretion
- Except from the binary black hole scenario, all astrophysical systems of interest (say, for gravitational wave studies) contain matter fields
- Complete description of fluid flow coupled to geometry only conceivable through accurate numerical simulations
- Many astrophysical scenarios can be described in the 'test fluid' approximation: hydrodynamical computations in predetermined curved (background) spacetimes
- The (GR) hydrodynamic equations constitute a hyperbolic system
- Solid mathematical foundations and accurate numerical methodology at our disposal
- Our preferred choice: **high-resolution shock-capturing** schemes written in **conservation form**

3.2 Linear hyperbolic systems of conservation laws

A, one-dimensional, **linear hyperbolic system** of partial differential equations (PDE) is

$$\frac{\partial \mathbf{u}}{\partial t} + \mathbf{A}\frac{\partial \mathbf{u}}{\partial x} = 0 \tag{70}$$

where $\mathbf{A}$ is a constant $p \times p$ matrix with **real eigenvalues** λ_i $(i = 1 \cdots p)$
By introducing the **characteristic variables**, $\mathbf{w} = \mathbf{R}^{-1}\mathbf{u}$, system (70) can be rewritten

$$\frac{\partial \mathbf{w}}{\partial t} + \mathbf{\Lambda}\frac{\partial \mathbf{w}}{\partial x} = 0 \tag{71}$$

where $\mathbf{\Lambda} = \mathbf{R}^{-1}\mathbf{A}\mathbf{R}$, $\mathbf{\Lambda}$ =diag($\lambda_1 \cdots \lambda_p$) and $\mathbf{R}$ is the matrix of the right-eigenvectors (in columns)
Since $\mathbf{\Lambda}$ is diagonal, system (71) decouples into p independent scalar equations

$$\frac{\partial w_i}{\partial t} + \lambda_i \frac{\partial w_i}{\partial x} = 0 i = 1 \cdots p \tag{72}$$

System (72) consists of **constant coefficient linear advection equations**, whose solution is

$$w_i(x,t) = w_i(x - \lambda_i t, 0) \tag{73}$$

and for the original system (70)

$$\mathbf{u}(x,t) = \mathbf{R}\mathbf{w}(x,t) \tag{74}$$

3.2.1 Numerical schemes

Wide variety of finite difference methods to solve equation “i” in (72) (the scalar advection equation)
Finite difference methods are based on a discretization of the $x - t$ plane defined by the discrete mesh points (x_j, t^n)

$$x_j = (j - 1/2)\Delta x, \quad j = 1, 2, \ldots \tag{75}$$

$$t^n = n\Delta t, \quad n = 0, 1, 2, \ldots \tag{76}$$

where Δx and Δt are, respectively, the cell width and the time step
A finite difference scheme is a time–marching procedure which permits to obtain approximations to the solution in the mesh points, w_j^{n+1}, from the approximations in previous time steps w_j^n

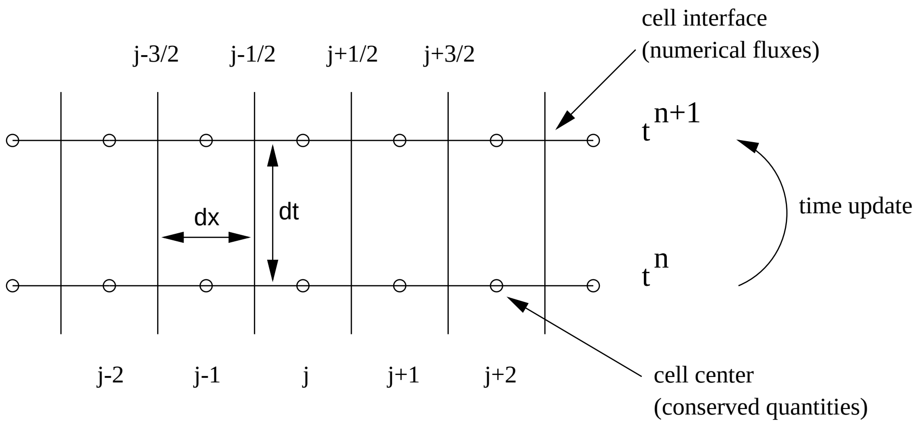

3.2.2 Some examples

Name	Difference equations
Backward Euler	$w_j^{n+1} = w_j^n - \frac{\Delta t}{2\Delta x}\lambda(w_{j+1}^n - w_{j-1}^n)$
One-sided	$w_j^{n+1} = w_j^n - \frac{\Delta t}{\Delta x}\lambda(w_j^n - w_{j-1}^n)$
One-sided	$w_j^{n+1} = w_j^n - \frac{\Delta t}{\Delta x}\lambda(w_{j+1}^n - w_j^n)$
Lax-Friedrichs	$w_j^{n+1} = \frac{1}{2}(w_{j-1}^n + w_{j+1}^n) - \frac{\Delta t}{2\Delta x}\lambda(w_{j+1}^n - w_{j-1}^n)$
Leapfrog	$w_j^{n+1} = w_j^{n-1} - \frac{\Delta t}{2\Delta x}\lambda(w_{j+1}^n - w_{j-1}^n)$
Lax-Wendroff	$w_j^{n+1} = w_j^n - \frac{\Delta t}{2\Delta x}\lambda(w_{j+1}^n - w_{j-1}^n)$
	$+\frac{(\Delta t)^2}{2(\Delta x)^2}\lambda^2(w_{j+1}^n - 2w_j^n + w_{j-1}^n)$
Beam-Warming	$w_j^{n+1} = w_j^n - \frac{\Delta t}{2\Delta x}\lambda(3w_j^n - 4w_{j-1}^n + w_{j-2}^n)$
	$+\frac{(\Delta t)^2}{2(\Delta x)^2}\lambda^2(w_j^n - 2w_{j-1}^n + w_{j-2}^n)$

3.2.3 Definitions

- **Global error**: difference between the true and computed solution
- **Convergence**: a FD scheme is convergent if the global error goes to zero as the mesh is refined
- **Global order of accuracy**: a method has global order p if the global error is $\mathcal{O}(\Delta t^p + \Delta x^p)$ as $\Delta t, \Delta x \to 0$
- **Local truncation error**: measures how well the FD equations model the PDE locally. It is defined by inserting the true solution into the FD equations at a single arbitrary point.

  For smooth functions we can expand in Taylor series to obtain the **local order** of the method

  If the LTE vanishes like $\mathcal{O}(\Delta t^p + \Delta x^p)$ the method is (locally) p'th order accurate

  If the LTE goes to zero as the mesh is refined the method is called **consistent**

- **Explicit and implicit methods**: an **explicit** method is one which yields an explicit expression for each value w_j^{n+1} at time t^{n+1} in terms of nearby values at time t^n

  An **implicit** method couples together values at different grid points at time t^{n+1} and an algebraic system of equations must be solved in each time step to update the solution

  Explicit methods are generally preferable provided they can be used with a reasonable time step (which depends upon grid resolution and smoothness of the solution). In many cases, an explicit method turns out to be **unstable** unless the time step is considerable smaller than what seems reasonable from accuracy considerations

- **The CFL condition**: a numerical method can be convergent only if its numerical domain of dependence contains the true domain of dependence of the PDE, at least in the limit as Δt and Δx go to zero

  For a hyperbolic system with eigenvalues λ the CFL condition would imply $|\lambda \Delta t/\Delta x| \leq 1$ as a necessary condition for stability

3.2.4 Discontinuous initial data

- "Standard" finite difference methods applied to linear systems work generally well for smooth solutions
- What happens when the initial data are discontinuous?

  Example:

$$\frac{\partial u}{\partial t} + a\frac{\partial u}{\partial x} = 0 -\infty < x < \infty t \geq 0 \tag{77}$$

$$u_0(x) = \begin{cases} 1 & \text{if } x < 0 \\ 0 & \text{if } x > 0 \end{cases} \tag{78}$$

The exact solution is $u_0(x - at)$. The numerical method can have difficulties near the discontinuity

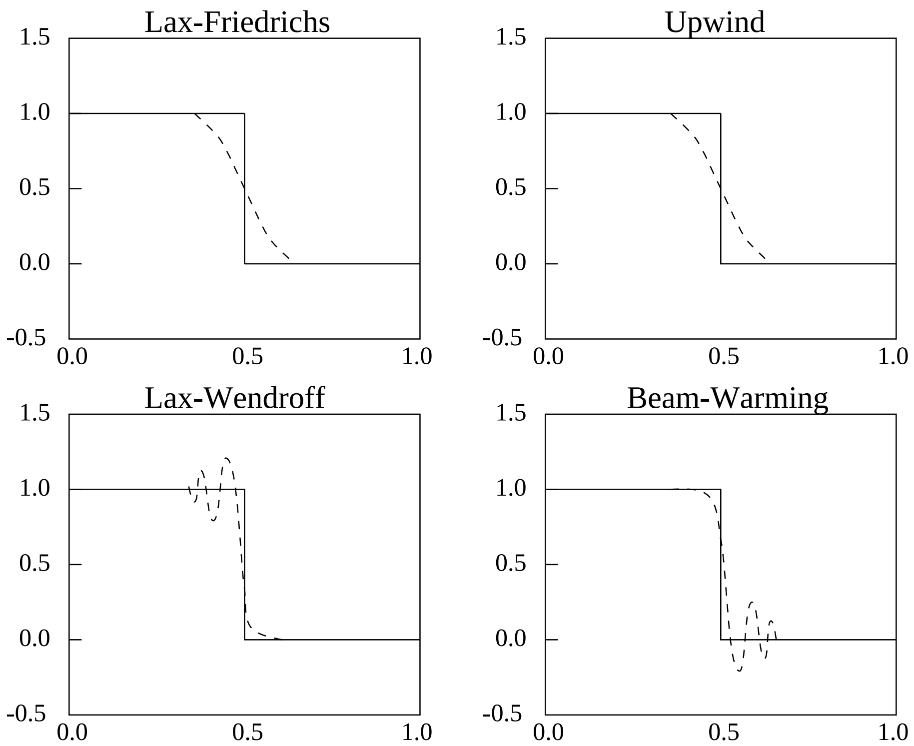

3.2.5 Prelude to nonlinear problems

- For non-linear problems, to be discussed later, the solution can develop discontinuities after a finite time even if the initial data are smooth
- The way to handle properly discontinuous solutions and to converge to the physical solution is to use numerical schemes written in **conservation form**

$$u_j^{n+1} = u_j^n - \frac{\Delta t}{\Delta x}\left(\hat{f}_{j+\frac{1}{2}} - \hat{f}_{j-\frac{1}{2}}\right) \tag{79}$$

Let us consider the Burger's equation with discontinuous initial data

$$\frac{\partial u}{\partial t} + \frac{\partial(\frac{1}{2}u^2)}{\partial x} = 0 \tag{80}$$

It can be discretized by the upwind conservative method

$$u_j^{n+1} = u_j^n - \frac{\Delta t}{\Delta x}\left(\frac{1}{2}(u_j^n)^2 - \frac{1}{2}(u_{j-1}^n)^2\right) \tag{81}$$

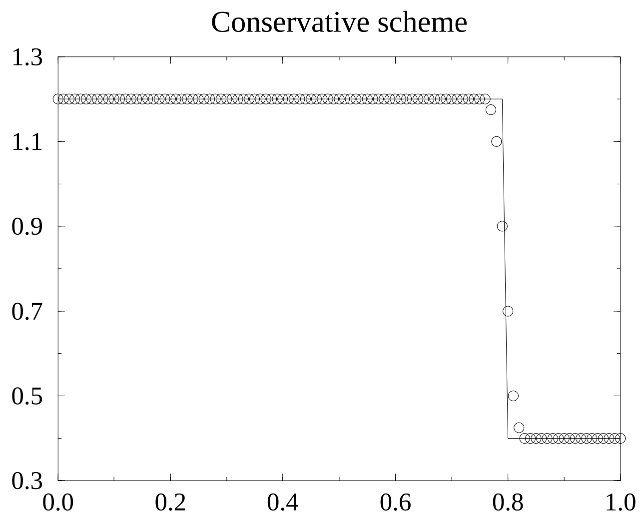

On the other hand, one could discretize the quasilinear form of Burger's equation

$$\frac{\partial u}{\partial t} + u\frac{\partial u}{\partial x} = 0 \tag{82}$$

using the <u>nonconservative</u> upwind method

$$u_j^{n+1} = u_j^n - \frac{\Delta t}{\Delta x} u_j^n \left(u_j^n - u_{j-1}^n \right) \tag{83}$$

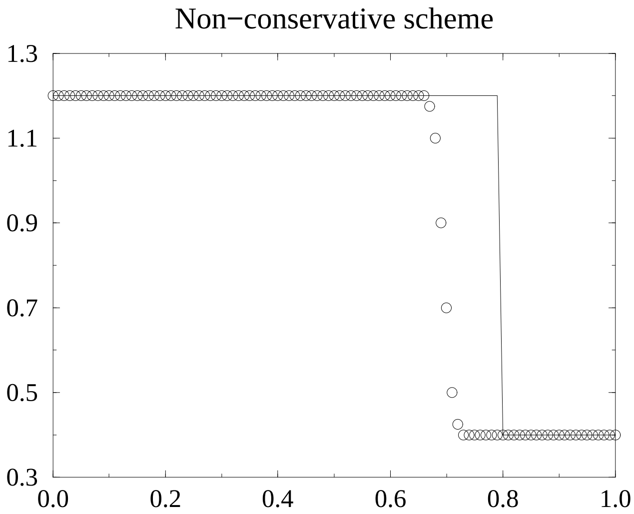

3.3 Non-linear hyperbolic systems of conservation laws

Let us consider the system of p equations of conservation laws

$$\frac{\partial \mathbf{u}}{\partial t} + \sum_{j=1}^{d} \frac{\partial \mathbf{f}_j(\mathbf{u})}{\partial x_j} = 0 \;\; (= \mathbf{s}(\mathbf{u})) \tag{84}$$

with $\mathbf{x} = (x_1, x_2, \ldots, x_d) \in R^d$ and where $\mathbf{u} = (u_1, u_2, \ldots, u_p)^T$ is the vector of unknowns, $\mathbf{u} = \mathbf{u}(\mathbf{x}, t)$ and $\mathbf{f}_j(\mathbf{u}) = (f_{1j}, f_{2j}, \ldots, f_{pj})^T$ is the vector of fluxes.
Formally, system (84) expresses the conservation of the vector $\mathbf{u}$. Let D be an arbitrary domain of R^d and let $\mathbf{n} = (n_1, \ldots, n_d)$ the outward unit normal to the boundary ∂D of D. Then, from (84), it follows that

$$\frac{d}{dt}\int_D \mathbf{u}\, d\mathbf{x} + \sum_{j=1}^{d} \int_{\partial D} \mathbf{f}_j(\mathbf{u}) n_j \, dS = 0. \tag{85}$$

This balance equation establishes that the time variation of $\int_D \mathbf{u}\, d\mathbf{x}$ is equal to the losses through the boundary ∂D.
Now, for all $j = 1, \ldots, d$ let

$$\mathbf{A}_j(\mathbf{u}) = \frac{\partial \mathbf{f}_j(\mathbf{u})}{\partial \mathbf{u}} \tag{86}$$

be the **Jacobian matrix** of $\mathbf{f}_j(\mathbf{u})$.
Definition: The system (84) is called **hyperbolic** if, for any $\mathbf{u}$ and any $\omega = (\omega_1, \ldots, \omega_d) \in R^d$, the matrix

$$\mathbf{A}(\mathbf{u}, \omega) = \sum_{j=1}^{d} \omega_j \mathbf{A}_j(\mathbf{u}) \tag{87}$$

has p real eigenvalues $\lambda_1(\mathbf{u}, \omega) \le \lambda_2(\mathbf{u}, \omega) \le \cdots \le \lambda_p(\mathbf{u}, \omega)$ and p linearly independent (right) eigenvectors $\mathbf{r}_1(\mathbf{u}, \omega)$, $\mathbf{r}_2(\mathbf{u}, \omega)$, ..., $\mathbf{r}_p(\mathbf{u}, \omega)$. If, in addition, the eigenvalues $\lambda_k(\mathbf{u}, \omega)$ are all different, the system (84) is called **strictly hyperbolic**.
In most situations we will consider the so–called **initial value problem** (IVP), i.e., the solution of system (84) with the initial condition

$$\mathbf{u}(\mathbf{x}, 0) = \mathbf{u}_0(\mathbf{x}). \tag{88}$$

A key property of hyperbolic systems is that features in the solution propagate at the **characteristic speeds** given by the eigenvalues of the Jacobian matrices. The characteristic curves associated to system (84) are the integral curves of the differential equations

$$\frac{dx}{dt} = \lambda_k(\mathbf{u}(x, t)), \quad k = 1, \ldots, p, \tag{89}$$

($d = 1$). The so–called <u>**characteristic variables**</u> (a combination of the components of $\mathbf{u}$) are constant along these curves. Essentially, characteristic curves give information about the propagation of the initial data, which formally permits to reconstruct the future solution for the initial value problem (84) with (88) at $t > 0$. Continuous and differentiable solutions that satisfy (84) and (88) pointwise are called <u>**classical solutions**</u>. However, for non-linear systems, classical solutions do not exist in general even when the initial condition $\mathbf{u}_0$ is a smooth function, and discontinuities develop after a finite time.

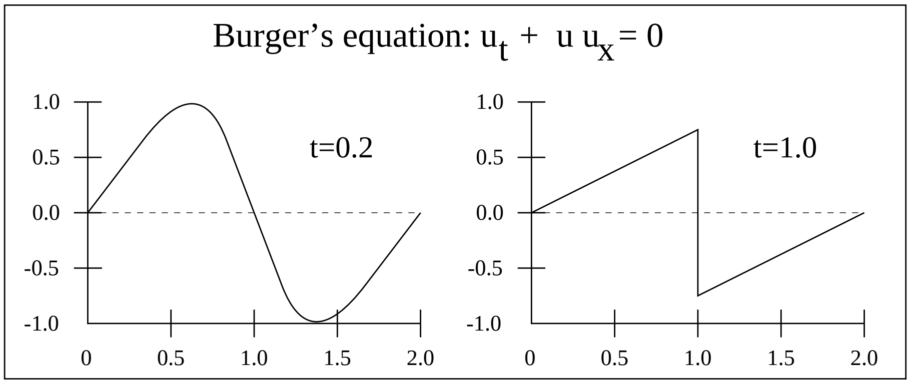

Then we seek <u>generalized solutions</u> that satisfy the integral form of the conservation system (85) which are classical solutions where they are continuous and have a finite number of discontinuities (**weak solutions**)

3.3.1 Weak solutions

Conservation law:

$$\frac{\partial \mathbf{u}}{\partial t} + \frac{\partial \mathbf{f}(\mathbf{u})}{\partial x} = 0 \tag{90}$$

Test function: $\Phi(x,t) \in C_0^1(R \times R)$
C_0^1 is the space of continuously differentiable functions with compact support
Multiplying the conservation law by Φ, integrating over space and time and integrating by parts, we get

$$\int_0^\infty \int_{-\infty}^{+\infty} (\Phi_t \mathbf{u} + \Phi_x \mathbf{f}(\mathbf{u})) dx dt = - \int_{-\infty}^{+\infty} \Phi(x,0)\mathbf{u}(x,0) dx \tag{91}$$

<u>**Definition:**</u> The function $\mathbf{u}(x,t)$ is called a weak solution of the conservation law if the previous integral form holds for all functions $\Phi \in C_0^1(R \times R)$
<u>**Theorem**</u>: Let $\mathbf{u}$ be a piecewise smooth function. Then, $\mathbf{u}$ is a solution of the integral form of the conservation system if and only if the two following conditions are satisfied:

1. $\mathbf{u}$ is a classical solution in the domains where it is continuous.
2. Across a given surface of discontinuity, Σ, it satisfies the jump conditions (Rankine–Hugoniot conditions)

$$(\mathbf{u}_R - \mathbf{u}_L)n_t + \sum_{j=1}^{d} [\mathbf{f}_j(\mathbf{u}_R) - \mathbf{f}_j(\mathbf{u}_L)]\, n_{xj} = 0, \quad (92)$$

   where $\mathbf{u}_L$ and $\mathbf{u}_R$ stand, respectively, for the values of $\mathbf{u}$ on the left and right hand sides of Σ, and $\mathbf{n} = (n_t, n_{x1}, n_{x2}, \ldots, n_{xd})$ denotes a vector normal to Σ.

For 1D systems, the **Rankine–Hugoniot jump condition** (92) reduces to

$$s(\mathbf{u}_R - \mathbf{u}_L) = \mathbf{f}(\mathbf{u}_R) - \mathbf{f}(\mathbf{u}_L) \quad (93)$$

where s is the **propagation velocity of the discontinuity**.
Rankine–Hugoniot conditions follow from the conservation of fluxes across the surfaces of discontinuity.
Shock-tracking techniques: use the RH conditions in combination with standard finite–difference methods for the smooth regions and special procedures for tracking the location of discontinuities → solving the equations in the presence of shocks
In 1D this is often a viable approach.
In multidimensional applications it is more cumbersome: the discontinuities lie along curves (in 2D) or surfaces (in 3D) and in realistic problems there may be many such discontinuities interacting in complicated ways.

3.3.2 Vanishing viscosity approach: an example

Inviscid Burgers' equation: $u_t + uu_x = 0$
Viscous Burgers' equation: $u_t + uu_x = \epsilon u_{xx}$
The correct physical behaviour is determined adopting the vanishing viscosity approach
The inviscid equation is a *model* of the viscous one valid only for small ϵ and smooth u
If the initial data is smooth and ϵ very small the term ϵu_{xx} is negligible before the wave begins to break. The solutions to both PDEs look identical
As the wave begins to break the u_{xx} term grows much faster that the u_x term and the rhs begins to play a role
This term keeps the solution smooth for all time preventing the breakdown of solutions that occurs for the hyperbolic problem

3.3.3 Physical solutions

The class of all weak solutions is too wide in the sense that there is **no uniqueness** for the IVP

The numerical methods should guarantee convergence to the **physically admisible solution**. This is the limit solution, when $\varepsilon \to 0$ of the "viscous version" of system (84)

$$\frac{\partial \mathbf{u}}{\partial t} + \sum_{j=1}^{d} \frac{\partial \mathbf{f}_j(\mathbf{u})}{\partial x_j} = \varepsilon \sum_{j=1}^{d} \frac{\partial^2 \mathbf{u}}{\partial x_j^2} \tag{94}$$

Mathematically, it is characterized by the so–called **entropy condition** (in the language of fluids, the condition that the entropy of any fluid element should increase when running into a discontinuity)

The characterization of the **entropy–satisfying solutions** for scalar equations follows Oleinik (1963), whereas for systems of conservation laws it has been developed by Lax (1972).

Entropy condition (for scalar equations): $u(x,t)$ is the entropy solution if all discontinuities have the property that

$$\frac{f(u) - f(u_l)}{u - u_l} \geq s \geq \frac{f(u) - f(u_r)}{u - u_r} u_l \leq u \leq u_r \tag{95}$$

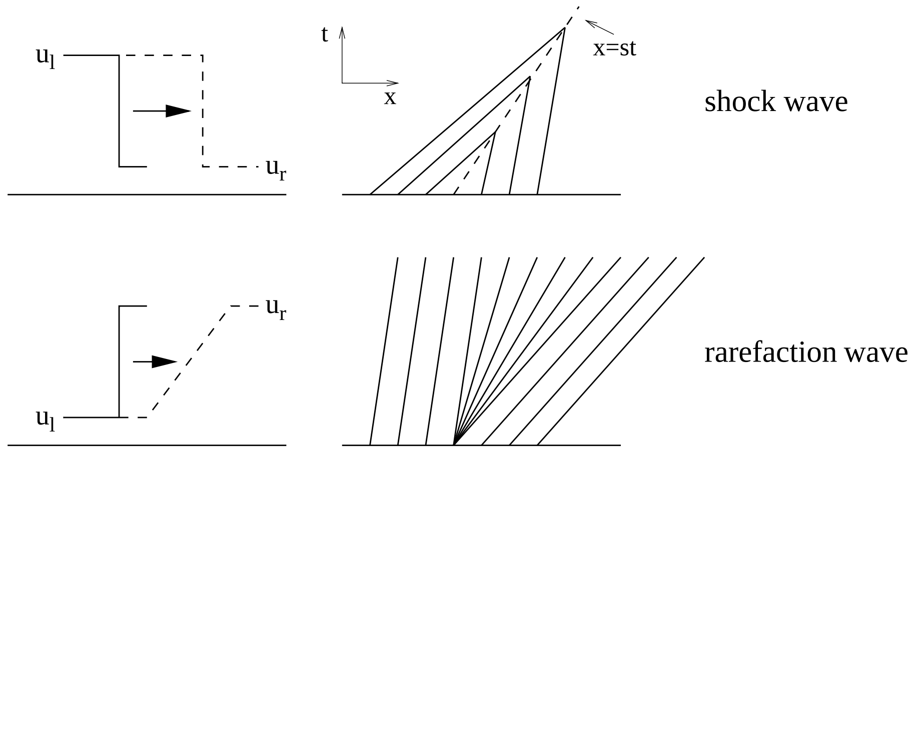

3.3.4 The Riemann problem

Modern conservative methods (HRSC schemes) are based on exact or approximate solutions of Riemann problems between contiguous numerical cells
Consider the hyperbolic system of conservation laws in 1D

$$\frac{\partial \mathbf{u}}{\partial t} + \frac{\partial \mathbf{f}(\mathbf{u})}{\partial x} = 0 \tag{96}$$

with initial data $\mathbf{u}(x,0) = \mathbf{u}_0(x)$
A **Riemann problem** for system (96) is an initial value problem with discontinuous data, i.e.,

$$\mathbf{u}_0 = \begin{cases} \mathbf{u}_L & \text{if } x < 0 \\ \mathbf{u}_R & \text{if } x > 0 \end{cases} \tag{97}$$

The Riemann problem is invariant under similarity transformations $(x,t) \to (ax, at)$, $a > 0$, so that the solution is constant along the straight lines $x/t =$ constant and, hence, self–similar
It consists of constant states separated by **rarefaction waves** (continuous self–similar solutions of the differential system), **shock waves** and **contact discontinuities** (Lax 1972).

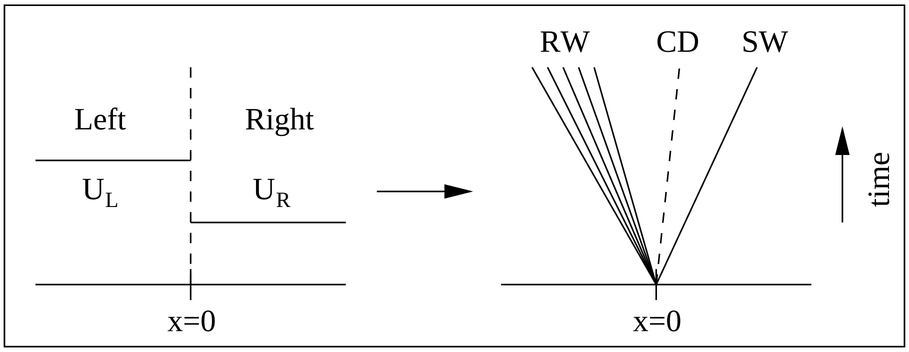

4 Métodos en diferencias finitas en dinámica de fluidos computacional

4.1 High-resolution shock-capturing schemes

High-resolution methods: modified high order methods with the appropriate amount of numerical dissipation in the vicinity of a discontinuity
Let us consider the following (Cauchy) IVP

$$\frac{\partial u}{\partial t} + \frac{\partial f(u)}{\partial x} = 0 \qquad u(x,0) = u_0(x) \tag{98}$$

A finite difference scheme is a time–marching procedure which permits to obtain approximations to the solution in the mesh points, u_j^{n+1}, from the approximations in previous time steps u_j^n
Quantity u_j^n is an approximation to $u(x_j, t^n)$ but, in the case of a conservation law, it is often preferable to view it as an approximation to the average of $u(x,t)$ within the numerical cell $[x_{j-1/2}, x_{j+1/2}]$ $(x_{j\pm 1/2} = (x_j + x_{j\pm 1})/2)$

$$u_j^n \approx \frac{1}{\Delta x} \int_{x_{j-1/2}}^{x_{j+1/2}} u(x, t^n) dx, \tag{99}$$

consistent with the integral form of the conservation law
For hyperbolic systems of conservation laws, schemes written in conservation form guarantee that the convergence (if it exists) is to one of the weak solutions of the original system of equations (**Lax–Wendroff theorem** 1960).
An algorithm written in **conservation form** reads

$$\begin{aligned} u_j^{n+1} &= u_j^n - \frac{\Delta t}{\Delta x} \Big(\hat{f}(u_{j-r}^n, u_{j-r+1}^n, \ldots, u_{j+q}^n) \\ &\qquad - \hat{f}(u_{j-r-1}^n, u_{j-r}^n, \ldots, u_{j+q-1}^n) \Big) \end{aligned} \tag{100}$$

where $\hat{f}$ is a consistent **numerical flux function**

$$\hat{f}(u, u, \ldots, u) = f(u) \tag{101}$$

The Lax–Wendroff theorem does not state whether the method converges.
To guarantee convergence, some form of stability is required, as for linear problems (**Lax equivalence theorem**, see Ritchmyer & Morton 1967)
The notion of **total-variation stability** has proven very successful although powerful results have only been obtained for scalar conservation laws

The **total variation** of a solution at $t = t^n$, $\mathrm{TV}(u^n)$, is defined as

$$\mathrm{TV}(u^n) = \sum_{j=0}^{+\infty} |u^n_{j+1} - u^n_j| \tag{102}$$

and a numerical scheme is said to be TV–stable if $\mathrm{TV}(u^n)$ is bounded for all Δt at any time for each initial data

A convergence theorem for non–linear, scalar, conservation laws (LeVeque 1991): For numerical schemes in conservation form with consistent numerical flux functions, TV–stability is a sufficient condition for convergence

A current line of research focuses on developing high–order, accurate methods in conservation form satisfying the condition of TV–stability

The conservation form is ensured by starting with the integral version of the partial differential equation in conservation form. Integrating the PDE within a space–time computational cell $[x_{j-1/2}, x_{j+1/2}] \times [t^n, t^{n+1}]$, the numerical flux function $\hat{f}_{j+1/2}$ is seen to be an approximation to the time–averaged flux across the interface, i.e.,

$$\hat{f}_{j+1/2} \approx \frac{1}{\Delta t} \int_{t^n}^{t^{n+1}} f(u(x_{j+1/2}, t))dt \tag{103}$$

The flux integral depends on the solution at the numerical interfaces, $u(x_{j+1/2}, t)$, during the time step

Key idea: a possible procedure is to calculate $u(x_{j+1/2}, t)$ by **solving Riemann problems** at every cell interface to obtain

$$u(x_{j+1/2}, t) = u(0; u^n_j, u^n_{j+1}) \tag{104}$$

$u(0; u^n_j, u^n_{j+1})$ denotes the Riemann solution for the (left and right) states u^n_j, u^n_{j+1} along the ray $x/t = 0$

4.1.1 Godunov's method

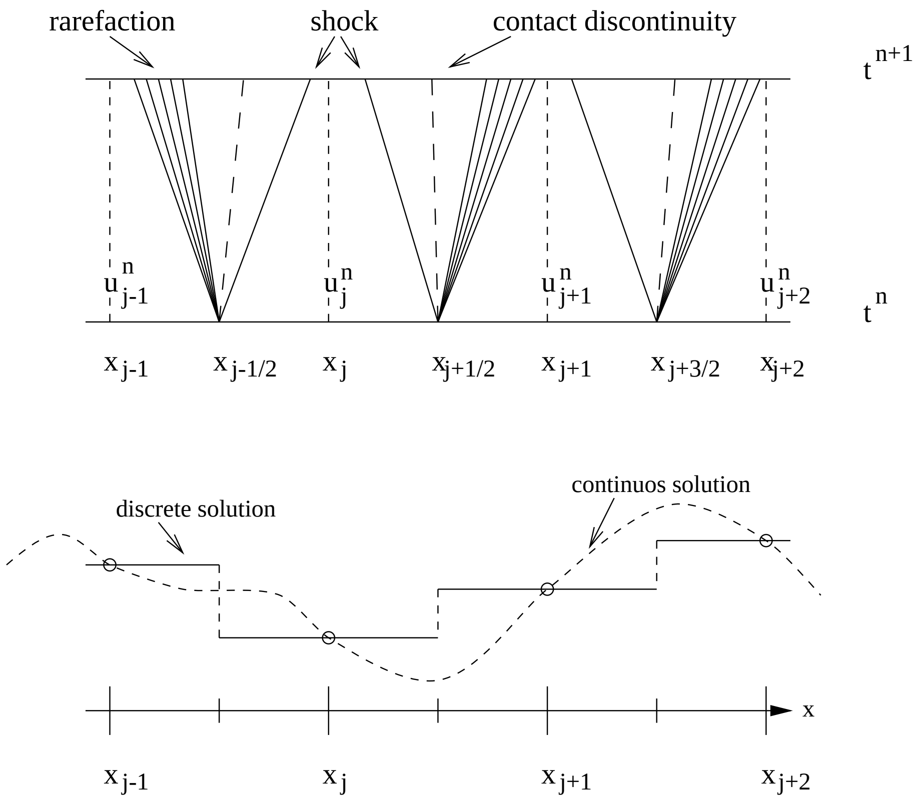

Godunov's scheme: local solutions of Riemann problems

The incorporation of the <u>exact solution</u> of Riemann problems to compute the numerical fluxes is due to Godunov (1959)
Godunov developed his method to solve the Euler equations of classical gas dynamics in the presence of shock waves
<u>**Outline of Godunov's method**</u>:

1. Piecewise constant initial data: $u_j^n \approx \frac{1}{\Delta x}\int_{x_{j-1/2}}^{x_{j+1/2}} u(x,t^n)dx$

2. Solve <u>exactly</u> the conservation law over the time interval $[t^n, t^{n+1}]$ with initial data u_j^n (family of local Riemann problems) $\Rightarrow u(x_{j+1/2}, t)$,
   $t \in [t^n, t^{n+1}]$

The solution to the Riemann problem at $x_{j+1/2}$ is a similarity solution, which is constant along each ray

$$\frac{x - x_{j+1/2}}{t} = const. \tag{105}$$

$u^*(u_l, u_r)$ is the exact solution along the ray $x/t = 0$ with data

$$u(x, 0) = \begin{cases} u_l & \text{if } x < 0 \\ u_r & \text{if } x > 0 \end{cases} \tag{106}$$

then we have $u(x_{j+1/2}, t) \equiv u^*(u_j^n, u_{j+1}^n)$

Δt must be small enough so that waves from the Riemann problems do not travel farther than distance Δx in this time step (CFL condition)

3. Compute the numerical flux function $\hat{f}_{j+1/2} \approx \frac{1}{\Delta t} \int_{t^n}^{t^{n+1}} f(u(x_{j+1/2}, t))dt$

To compute $u^*(u_j^n, u_{j+1}^n)$ we must determine the full wave structure and wave speeds in order to find where it lies in state space $\rightarrow$ computationally expensive procedure

A wide variety of **approximate Riemann solvers** have been proposed $\rightarrow$ much cheaper than the exact solver and equally good results when used in the Godunov or high-resolution methods

4.1.2 Exact solution of a Riemann problem

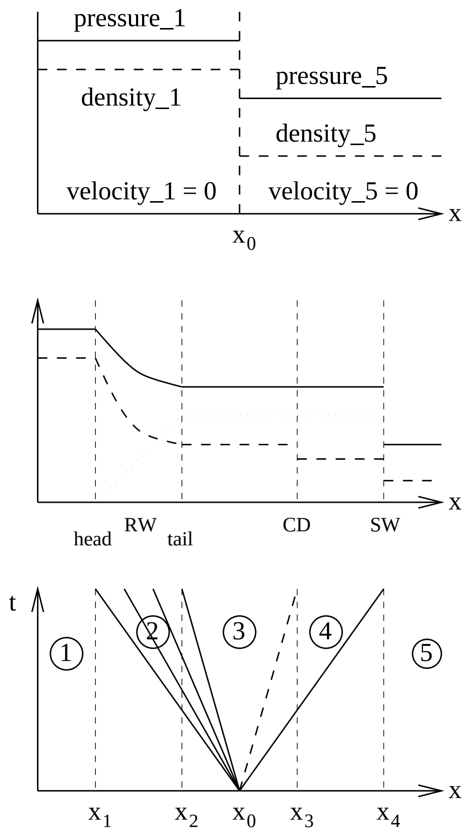

- Self-similar solution: $\xi = \dfrac{x - x_0}{t}$
- 5 regions, 3 elementary waves
- State 1: initial left state (with respect to x_0) $x_1 = x_0 + \xi_1 t$ ($\xi_1 < 0$)
- State 2: rarefaction $v = v_2(\xi), \rho = \rho_2((\xi), p = p_2(\xi)$, $x_2 = x_0 + \xi_2 t$
- States 3 and 4: constant states separated by a contact discontinuity, $x_3 = x_0 + \xi_3 t$
- State 5: initial right state. Its leftmost part is limited by the shock wave moving with speed ξ_4

- Unknowns: $v_3, p_3, \rho_3, v_4, p_4, \rho_4$ (constants), $v_2(\xi), p_2(\xi), \rho_2(\xi)$ (functions) and $\xi_1, \xi_2, \xi_3, \xi_4$ (velocity of points separating the regions)
- Solution procedure:

  First: the RH conditions accross discontinuities provide 6 equations to solve for 6 variables

  Second: the rest of relations are obtained from the condition of self-similar flow accross the rarefaction wave

SRH equations (Cartesian coordinates, planar symmetry):

$$\begin{aligned}
\frac{\partial(\rho W)}{\partial t} + \frac{\partial(\rho W v)}{\partial x} &= 0 \\
\frac{\partial(\rho h W^2 v)}{\partial t} + \frac{\partial(\rho h W^2 v^2 + p)}{\partial x} &= 0 \\
\frac{\partial(\rho h W^2 - p)}{\partial t} + \frac{\partial(\rho h W^2 v)}{\partial x} &= 0
\end{aligned}$$

self-similarity ($\frac{\partial}{\partial x} = \frac{1}{t}\frac{d}{d\xi}, \frac{\partial}{\partial t} = -\frac{\xi}{t}\frac{d}{d\xi}$) and some algebra lead to

$$\begin{aligned}
(v-\xi)\frac{d\rho}{d\xi} + (1-v\xi)\rho W^2 \frac{dv}{d\xi} &= 0 \\
(v-\xi)W^2 \rho h \frac{dv}{d\xi} + (1-v\xi)\frac{dp}{d\xi} &= 0
\end{aligned}$$

A self-similar flow is isentropic: $\frac{dp}{d\xi} = c_s^2 h \frac{d\rho}{d\xi}$

$$\begin{aligned}
(v-\xi)\frac{d\rho}{d\xi} + (1-v\xi)\rho W^2 \frac{dv}{d\xi} &= 0 \qquad (*) \\
(v-\xi)\rho W^2 \frac{dv}{d\xi} + (1-v\xi)c_s^2 \frac{d\rho}{d\xi} &= 0
\end{aligned}$$

whose solution is $\boxed{\xi = \frac{v \mp c_s}{1 \mp v c_s} \qquad (\dagger)}$

$v_1 = 0 \rightarrow \xi_1 = -c_{s_1}$

In Eq. $(*) \rightarrow W^2 dv = -\frac{c_s}{\rho} d\rho$

$$\frac{1}{2}\left[\ln \frac{1+v}{1-v}\right]_{v_1}^{v} = -\int_{\rho_1}^{\rho} \frac{c_s}{\rho} d\rho$$

Adiabatic flow: $p = K\rho^{\gamma}$, $c_s^2 = \dfrac{\gamma(\gamma-1)p}{\rho(\gamma-1)+\gamma p}$

Hence, two arbitrary states are related according to: $\rho = \rho_1 \left[\dfrac{c_s^2(\gamma-1-c_{s_1}^2)}{c_{s_1}^2(\gamma-1-c_s^2)}\right]^{\frac{1}{\gamma-1}}$

$$\rightarrow \frac{1}{2}\left[\ln\frac{1+v}{1-v}\right]_{v_1}^{v} = -\int_{c_{s_1}}^{c_s} \frac{2}{\gamma-1-c_s^2} dc_s \rightarrow \boxed{c_s = f(\gamma, c_{s_1}, v_1, v) \qquad (\ddagger)}$$

Solving Eqs. (†) and (‡) allows to obtain $v(x,t)$ and $c_s(x,t)$ in state 2, and hence ρ and p

Finally, the continuity of the flow guarantees: $v_3 = v(\xi_2), p_3 = p(\xi_2)$ and $\rho_3 = \rho(\xi_2)$

4.1.3 High-resolution shock-capturing schemes

This is the approach followed by an important subset of shock–capturing methods, the so–called **Godunov–type methods** (Harten & Lax 1983, Einfeldt 1988) These methods are written in **conservation form** and use **Riemann solvers** to compute approximations to $u(0; u_j^n, u_{j+1}^n)$
High–order of accuracy is achieved in two different ways:

- Flux-limiter methods
- Slope-limiter methods

A remark: **artificial viscosity methods**

- Idea: take a high order finite difference method (e.g., Lax-Wendroff) and add an "artificial viscosity" term Q to the hyperbolic equation
- damp spurious oscillations
- Q must vanish as Δt, $\Delta x \to 0$
- introduced by von Neumann and Richtmyer (1950) in the context of the classical hydrodynamic equations. Q is a term accompanying the pressure of the form

$$Q = \begin{cases} -\alpha \frac{\partial v}{\partial x} & \text{if } \frac{\partial v}{\partial x} < 0 \qquad \frac{\partial \rho}{\partial t} > 0 \\ 0 & \text{otherwise} \end{cases} \tag{107}$$

  with $\alpha = \rho (k \Delta x)^2 \frac{\partial v}{\partial x}$

- Advantages:
  - easy to implement
  - efficient
- Disadvantages:
  - problem dependent
  - problematic for ultrarelativistic flows

Flux limiter methods:
The numerical flux is obtained from a high order flux (e.g., the Lax-Wendroff flux) in the smooth regions and from a low order flux (e.g., the flux from some monotone method) near discontinuities

$$\hat{f} = \hat{f}_h - (1 - \Phi)(\hat{f}_h - \hat{f}_l) \tag{108}$$

with the limiter $\Phi \in [0, 1]$
Example: the flux–corrected–transport algorithm (Boris and Book 1973), one of the earliest high resolution methods
Slope limiter methods:
Use of conservative polynomial functions to interpolate the approximate solutions within the numerical cells
The idea is to produce more accurate left and right states for the Riemann problems by substituting the mean values u_j^n (that give only first–order accuracy) for better approximations of the true flux near the interfaces, $u^{\mathrm{L}}_{j+1/2}$, $u^{\mathrm{R}}_{j+1/2}$
The interpolation algorithms have to preserve the TV–stability of the scheme and this is usually achieved by using monotonic functions which lead to a decrease in the total variation (**total–variation–diminishing schemes**, TVD, Harten 1984)
If R is an interpolant function for the approximate solution u^n and $\tilde{u}(x, t^n)$ is the interpolated function within the cells, i.e., $\tilde{u}(x, t^n) = \mathrm{R}(u^n; x)$, satisfying $\mathrm{TV}(\tilde{u}(\cdot, t^n)) \leq \mathrm{TV}(u^n)$ then it can be proven that the whole scheme verifies $\mathrm{TV}(u^{n+1}) \leq \mathrm{TV}(u^n)$.
High–order TVD schemes were first constructed by van Leer (1979) who obtained second–order accuracy by using monotonic **piecewise linear** slopes for cell reconstruction

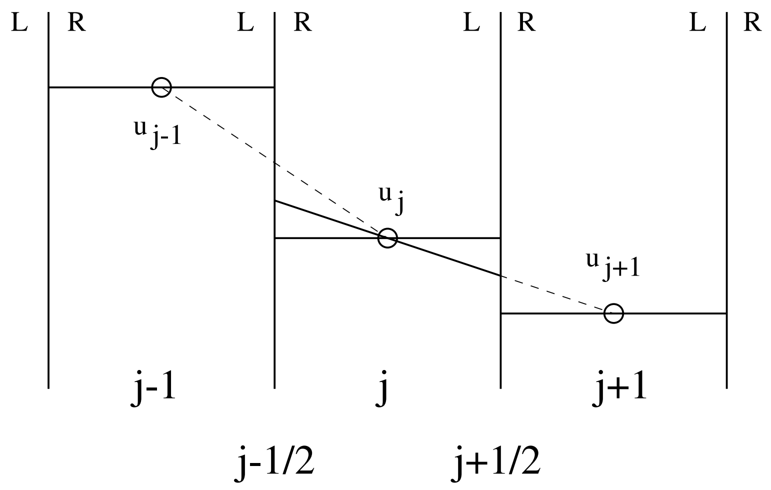

$$\mathbf{u}_j^{L,R} = \mathbf{u}_j + s_j(x_{j\pm\frac{1}{2}} - x_j) \qquad\qquad x_j = \frac{1}{2}(x_{j+\frac{1}{2}} - x_{j-\frac{1}{2}})$$

$$s_j = \begin{cases} \min(\Delta Q^{j+\frac{1}{2}}, \Delta Q^{j-\frac{1}{2}}) \times sgn(\Delta Q^{j+\frac{1}{2}}) & \text{if } sgn(\Delta Q^{j+\frac{1}{2}}) = sgn(\Delta Q^{j-\frac{1}{2}}) \\ 0 & \text{otherwise} \end{cases}$$

$$\Delta Q^{j+\frac{1}{2}} = \frac{\mathbf{u}_{j+1} - \mathbf{u}_j}{x_{j+1} - x_j}$$

The **piecewise parabolic method** (PPM) of Colella and Woodward (1984) provides third-order accuracy
The TVD property implies TV-stability but can be too restrictive. In fact, TVD methods degenerate to first order accuracy at extreme points (Osher & Chakravarthy 1984)
Other reconstruction alternatives have been developed in which some growth of the total variation is allowed:

- **total–variation–bounded** (TVB) schemes (Shu 1987)
- **essentially nonoscillatory** (ENO) schemes (Harten, Engquist, Osher & Chakravarthy 1987)
- **piecewise–hyperbolic method** (PHM) (Marquina 1994)

4.2 Riemann solvers

4.2.1 Exact Riemann solvers in relativistic hydrodynamics

Analysis of the breakup of an initial discontinuity separating two constant states L (left) and R (right) of an ideal gas (with adiabatic exponent Γ) in arbitrary (1D) conditions, in the absence of any gravitational field

In relativistic hydrodynamics this problem was first considered by Martí & Müller (1994) who derived an **exact solution**

The discontinuity between the two constant initial states $\mathbf{V}_L$ and $\mathbf{V}_R$ ($\mathbf{V} = (p, \rho, v)$) breaks up into two elementary nonlinear waves (**shocks** or **rarefactions**), one moving towards the initial left state and the other towards the initial right state

Between the waves two new states appear, $\mathbf{V}_{L*}$ and $\mathbf{V}_{R*}$, separated from each other through a **contact discontinuity** moving along with the fluid. Across the contact discontinuity, pressure and velocity are continuous, while density exhibits a jump.

As in classical hydrodynamics (see, e.g., Courant and Friedrichs 1976) the self-similar character of the flow through rarefaction waves and the Rankine-Hugoniot conditions across shocks provide the conditions for linking the intermediate states $\mathbf{V}_{S*}$ ($S = L, R$) with their corresponding initial state $\mathbf{V}_S$

- Martí & Müller (1996) constructed an exact Riemann solver to be implemented in a one-dimensional relativistic extension of the PPM method (Colella & Woodward 1984)

- Another exact solver was also implemented by Wen, Panaitescu & Laguna (1997) in their relativistic (1D) version of Glimm's random choice method (Glimm 1965). Besides being conservative on the average, Glimm's method produces completely sharp shocks and contact discontinuities and it is free of difussion and dispersion

4.2.2 Approximate Riemann solvers

The facts that:

1. in Godunov-type methods the structure of the Riemann solution is "lost" in the cell averaging process
2. the exact solution of a Riemann problem is computationally expensive, particularly in multidimensions
3. Multidimensional problems: coupling of all flow velocity components through the Lorentz factor

   $\rightarrow$ shocks: increase in the number of algebraic jump conditions

   $\rightarrow$ rarefactions: solving a system of ODEs

motivated the proposal of approximate (linearized) Riemann solvers

- Linearized Riemann solvers are based in the exact solution of Riemann problems corresponding to a new system of equations obtained by a suitable linearization of the original one
- The local linearization of the Jacobian matrices of the original system and its subsequent spectral decomposition is on the basis of all these solvers

Standard solvers for classical fluid dynamics:

- **Roe** solver (JCP **43**, 357-372, 1981)
- **Osher** solver (Math. Comp. **38**, 339-374, 1982)
- **HLLE** solver (Harten, Lax, van Leer & Einfeldt) (SIAM Review **25**, 35-61, 1983; SIAM J. Num. Anal. **25**, 294-318, 1988)
- **Marquina** solver (JCP **125**, 42-58, 1996)

4.2.3 The Roe solver

- Idea: determine the approximate solution by solving a constant coefficient linear system instead of the original nonlinear system
- $\rightarrow$ solve a modified conservation law with flux $\mathbf{f} = \hat{\mathbf{A}}\mathbf{u}$
- The linear problem reads:

$$\frac{\partial \mathbf{u}}{\partial t} + \hat{\mathbf{A}}(\mathbf{u}_l, \mathbf{u}_r)\frac{\partial \mathbf{u}}{\partial x} = 0 \tag{109}$$

- to determine $\hat{\mathbf{A}}$ Roe suggested the following conditions:
  1. $\hat{\mathbf{A}}(\mathbf{u}_l, \mathbf{u}_r)(\mathbf{u}_r - \mathbf{u}_l) = \mathbf{f}(\mathbf{u}_r) - \mathbf{f}(\mathbf{u}_l)$
  2. $\hat{\mathbf{A}}(\mathbf{u}_l, \mathbf{u}_r)$ is diagonalizable with real eigenvalues
  3. $\hat{\mathbf{A}}(\mathbf{u}_l, \mathbf{u}_r) \rightarrow \mathbf{f}^{'}(\bar{\mathbf{u}})$ smoothly as $\mathbf{u}_l, \mathbf{u}_r \rightarrow \bar{\mathbf{u}}$
- Condition 1 (provided 2 is fulfilled) ensures that if a single discontinuity is located at the interface, then the solution of the linearized problem gives the exact solution to the Riemann problem
- Condition 3 is necessary to recover the linearized algorithm from the nonlinear one smoothly
- Once the Roe matrix is obtained for every numerical interface, the numerical fluxes are computed by solving the locally linear system
- **Roe's numerical flux** is as follows

$$\hat{\mathbf{f}}^{\mathrm{ROE}} = \frac{1}{2}\left[\mathbf{f}(\mathbf{u}_{\mathrm{l}}) + \mathbf{f}(\mathbf{u}_{\mathrm{r}}) - \sum_p |\widetilde{\lambda}^{(p)}|\widetilde{\alpha}^{(p)}\widetilde{\mathbf{r}}^{(p)}\right] \tag{110}$$

$$\widetilde{\alpha}^{(p)} = \widetilde{\mathbf{l}}^{(p)}(\mathbf{u}_{\mathrm{r}} - \mathbf{u}_{\mathrm{l}}) \tag{111}$$

$\widetilde{\lambda}^{(p)}$, $\widetilde{\mathbf{r}}^{(p)}$, $\widetilde{\mathbf{l}}^{(p)}$ being the eigenvalues and right and left eigenvectors of $\hat{\mathbf{A}}$, respectively (p extends from 1 to the number of equations of the system)

4.2.4 The Marquina solver

References: Donat and Marquina, JCP, **125**, 42 (1996)
Donat, Font, Ibáñez and Marquina, JCP, **146**, 58 (1998)

- No "artificial" averaged states at cell interfaces
- **Marquina's numerical flux** is as follows

$$\hat{\mathbf{f}}^M(\mathbf{u}_l, \mathbf{u}_r) = \sum_p \left(\phi_+^p \mathbf{r}^p(\mathbf{u}_l) + \phi_-^p \mathbf{r}^p(\mathbf{u}_r)\right) \tag{112}$$

where $\mathbf{r}^p(\mathbf{u}_l)$, $\mathbf{r}^p(\mathbf{u}_r)$, are the right (normalized) eigenvectors of the Jacobian matrices $\mathbf{A}(\mathbf{u}_l)$,$\mathbf{A}(\mathbf{u}_r)$

- The *sided* local characteristic variables and fluxes:

$$\omega_l^p = \mathbf{l}^p(\mathbf{u}_l) \cdot \mathbf{u}_l \qquad \phi_l^p = \mathbf{l}^p(\mathbf{u}_l) \cdot \mathbf{f}(\mathbf{u}_l) \tag{113}$$
$$\omega_r^p = \mathbf{l}^p(\mathbf{u}_r) \cdot \mathbf{u}_r \qquad \phi_r^p = \mathbf{l}^p(\mathbf{u}_r) \cdot \mathbf{f}(\mathbf{u}_r) \tag{114}$$

where $\mathbf{l}^p(\mathbf{u}_l)$, $\mathbf{l}^p(\mathbf{u}_r)$, are the (normalized) left eigenvectors

- If eigenvalue $\lambda_k(\mathbf{u})$ does not change sign in $[\mathbf{u}_l, \mathbf{u}_r]$, then (upwind)

If $\lambda_k(\mathbf{u}_l) > 0$ then
$\phi_+^k = \phi_l^k$
$\phi_-^k = 0$
else
$\phi_+^k = 0$
$\phi_-^k = \phi_r^k$
endif

else (entropy-satisfying local-Lax-Friedrichs)

$$\alpha_k = \max_{\mathbf{u}\in\Gamma(\mathbf{u}_l,\mathbf{u}_r)} |\lambda_k(\mathbf{u})| \qquad \phi_\pm^k = .5(\phi_{l,r}^k \pm \alpha_k \omega_{l,r}^k)$$

endif

where $\Gamma(\mathbf{u}_l, \mathbf{u}_r)$ is a curve in phase space connecting $\mathbf{u}_l$ and $\mathbf{u}_r$

- For any hyperbolic system where the fields are either genuinely nonlinear or linearly degenerate, we can test the possible sign changes of $\lambda_k(\mathbf{u})$ by checking the sign of $\lambda_k(\mathbf{u}_l) \cdot \lambda_k(\mathbf{u}_r)$
- α_k can also be determined as

$$\alpha_k = \max\{|\lambda_k(\mathbf{u}_l)|, |\lambda_k(\mathbf{u}_r)|\}.$$

- Interesting properties:

  1. Designed for general hyperbolic systems of conservation laws
  2. When applied to constant-coefficient one-dimensional systems yields the exact solution to the Riemann problem
  3. Able to handle ultrarelativistic flows with great accuracy
  4. The dissipation of the scheme eliminates undesired numerical "pathologies":
     - overheating in shock reflections
     - long wavelength noise behind slowly moving shocks
     - "carbuncle" formation in hypersonic flow past blunt bodies

- Extended to relativistic hydrodynamics in Donat, Font, Ibáñez and Marquina, JCP, **146**, 58 (1998)

4.2.5 Extensions of classical solvers to relativistic fluid dynamics

- Eulderink solver (A&ASS **110**, 587-623, 1995):
  - Eulderink and Mellema extended the Roe solver to compute numerical approximations of the general relativistic hydrodynamic equations
  - They look for a local linearization of the Jacobian matrices of the system which fulfills the properties demanded by Roe's matrix
  - It is done in terms of the average state

$$\widetilde{\mathbf{w}} = \frac{\mathbf{w}_{\mathrm{L}} + \mathbf{w}_{\mathrm{R}}}{k_{\mathrm{L}} + k_{\mathrm{R}}}, \tag{115}$$

$$\mathbf{w} = (ku^0, ku^1, ku^2, ku^3, k\frac{p}{\rho h}), \tag{116}$$

$$k^2 = \sqrt{-g}\rho h. \tag{117}$$

  - The role played by ρ in the non relativistic Roe solver as weight for averaging, is now played by k, which apart from geometrical factors, tends to ρ in the non relativistic limit

    Relaxing Condition 1 in Roe's linearization, the Roe/Eulderink solver is no longer exact for shocks but still produces accurate solutions. The advantage is that the reduced set of conditions is fulfilled by a large number of averages, a typical choice being the arithmetic mean

- Falle & Komissarov (MNRAS **278**, 586, 1996)
  - proposed several approximate special relativistic Riemann solvers relying on a *primitive–variable formulation* of the relativistic hydrodynamic equations in quasilinear form:

$$\frac{\partial \mathbf{V}}{\partial t} + \mathbf{B}\frac{\partial \mathbf{V}}{\partial x} = 0, \tag{118}$$

    with $\mathbf{B} = \mathbf{B}(\mathbf{V})$ and $\mathbf{V}$ being any set of primitive variables, e.g., (ρ, v_x, v_y, v_z, p)

  - A local linearization of the system above allows to obtain the solution of the Riemann problem

- Schneider et al (JCP **105**, 92, 1993)
  - proposed the use of the method of Harten, Lax and van Leer (1983) to integrate the equations of special relativistic fluid dynamics
  - This method avoids the explicit calculation of the eigenvectors of the Jacobian matrices
  - The numerical flux function is given by

$$\widehat{\mathbf{f}}^{\rm HLL} = \frac{a_{\rm R}^{+}\mathbf{f}(\mathbf{u}_{\rm L}) - a_{\rm L}^{-}\mathbf{f}(\mathbf{u}_{\rm R}) + a_{\rm R}^{+}a_{\rm L}^{-}(\mathbf{u}_{\rm R} - \mathbf{u}_{\rm L})}{a_{\rm R}^{+} - a_{\rm L}^{-}} \tag{119}$$

    where

$$a_{\rm L}^{-} = \min\{0, a_{\rm L}\}, \quad a_{\rm R}^{+} = \max\{0, a_{\rm R}\}. \tag{120}$$

    and $a_{\rm L}$ and $a_{\rm R}$ are lower and upper bounds for the smallest and largest signals velocities
  - Einfeldt proposed calculating them based on the smallest and largest eigenvalues of the system

- All-shock approximation (Colella, SIAM J. Sci. Stat. Comput. **3**, 76, 1982)
  - extended to relativistic hydrodynamics by
    1. Balsara (JCP **114**, 284, 1994)
    2. Dai & Woodward (SIAM J. Sci. Stat. Comput. **18**, 982, 1997)
  - simplification to the Riemann solver: ignore the possibility of rarefaction waves, finding Riemann solutions in which each pair of states is connected along the Hugoniot locus
  - the solution cosnsists only of discontinuities satisfying the algebraic Rankine-Hugoniot conditions

4.3 A standard implementation of a HRSC scheme

$$\frac{\partial \mathbf{u}}{\partial t} + \frac{\partial \mathbf{f}(\mathbf{u})}{\partial x} = 0 \qquad \mathbf{f} = \mathbf{f}(\mathbf{u})$$

1. Numerical grid:

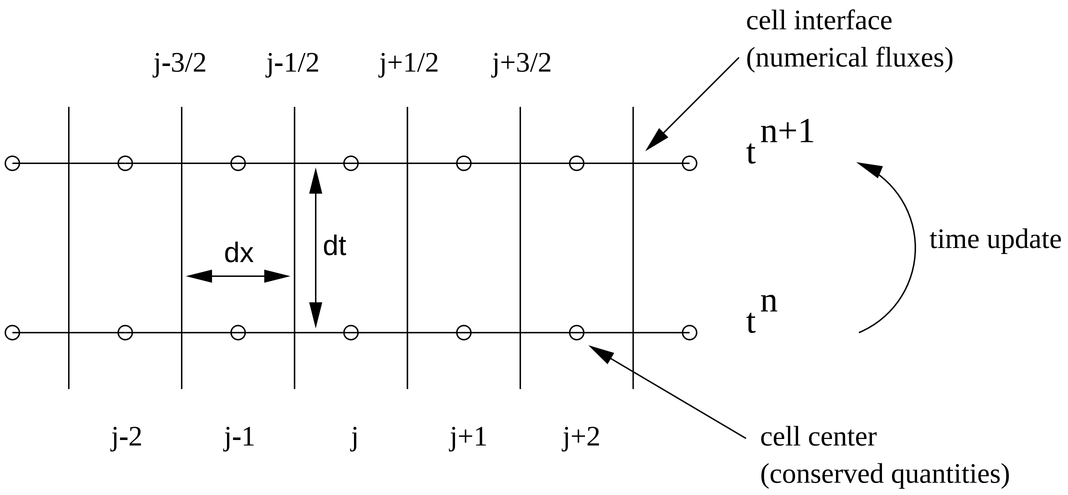

2. Time update: $\rightarrow$ **Conservation form algorithm**

$$\mathbf{u}_j^{n+1} = \mathbf{u}_j^n - \frac{\Delta t}{\Delta x}\left(\hat{\mathbf{f}}_{j+\frac{1}{2}} - \hat{\mathbf{f}}_{j-\frac{1}{2}}\right)$$

In practice: 2nd or 3rd order time accurate conservative Runge-Kutta schemes (Shu and Osher 1989)

$$t^n \rightarrow t^* \rightarrow t^{**} \rightarrow \cdots \rightarrow t^{n+1}$$

$$L \equiv -\frac{\hat{\mathbf{f}}_{j+\frac{1}{2}} - \hat{\mathbf{f}}_{j-\frac{1}{2}}}{\Delta x}$$

$$\mathbf{u}^{(1)} = \mathbf{u}^n + \Delta t L(\mathbf{u}^n)$$

$$\mathbf{u}^{(2)} = \mathbf{u}^n + \frac{1}{4}\Delta t L(\mathbf{u}^n) + \frac{1}{4}\Delta t L(\mathbf{u}^{(1)})$$

$$\mathbf{u}^{n+1} = \mathbf{u}^n + \frac{1}{6}\Delta t L(\mathbf{u}^n) + \frac{1}{6}\Delta t L(\mathbf{u}^{(1)}) + \frac{2}{3}\Delta t L(\mathbf{u}^{(2)})$$

3. Numerical fluxes:
Approximate Riemann solvers: Roe, HLLE, Marquina
Explicit use of the characteristic information of the system
Flux Formula

$$\widehat{\mathbf{f}}_{j\pm\frac{1}{2}} = \frac{1}{2} \left(\mathbf{f}(\mathbf{u}^L_{j\pm\frac{1}{2}}) + \mathbf{f}(\mathbf{u}^R_{j\pm\frac{1}{2}}) - \underbrace{\sum_{\alpha=1}^{p} \mid \widetilde{\lambda}_\alpha \mid \Delta\widetilde{\omega}_\alpha \widetilde{r}_\alpha}_{\uparrow} \right)$$

"numerical viscosity"

$\mathbf{u}^L$, $\mathbf{u}^R$: left and right "reconstructed" variables
λ: eigenvalues
$\Delta\omega$: jump of characteristic variables
r: right-eigenvectors

4. Cell reconstruction:
Piecewise constant (Godunov) or linear ("MUSCL" scheme, van Leer) interpolation procedures of $\mathbf{u}$ from cell centers to cell interfaces. Higher-order procedures also available: parabolic (PPM, Colella and Woodward) or hyperbolic (PHM, Marquina)

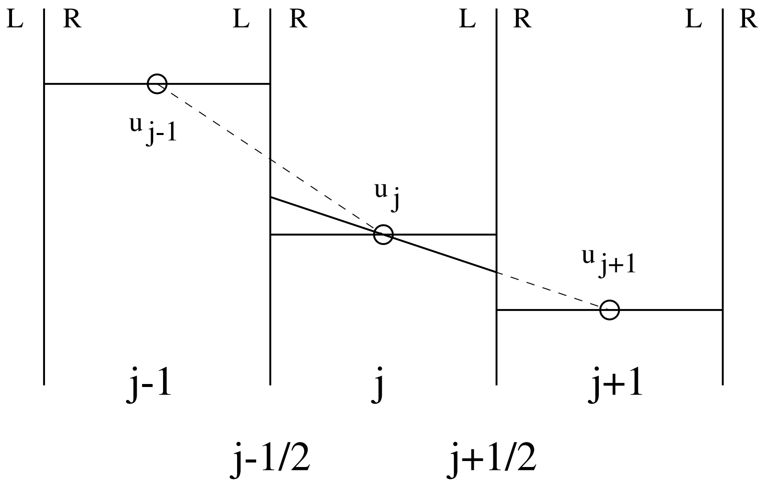

$$\mathbf{u}^{L,R}_j = \mathbf{u}_j + s_j(x_{j\pm\frac{1}{2}} - x_j) \qquad\qquad x_j = \frac{1}{2}(x_{j+\frac{1}{2}} - x_{j-\frac{1}{2}})$$

with

$$s_j = \begin{cases} \min(\Delta Q^{j+\frac{1}{2}}, \Delta Q^{j-\frac{1}{2}}) \times sgn(\Delta Q^{j+\frac{1}{2}}) & \text{if } sgn(\Delta Q^{j+\frac{1}{2}}) = sgn(\Delta Q^{j-\frac{1}{2}}) \\ 0 & \text{otherwise} \end{cases}$$

with

$$\Delta Q^{j+\frac{1}{2}} = \frac{\mathbf{u}_{j+1} - \mathbf{u}_j}{x_{j+1} - x_j}$$

4.4 Source terms

Most "conservation laws" include source terms (ex: relativistic hydrodynamic equations)

$$\frac{\partial \mathbf{u}}{\partial t} + \frac{\partial \mathbf{f}}{\partial x} = \mathbf{s} \qquad \mathbf{f} = \mathbf{f}(\mathbf{u}),\ \mathbf{s} = \mathbf{s}(\mathbf{u}) \tag{121}$$

Two basic ways of handling source terms:

1. Unsplit methods: a single finite difference formula advances the full equation over one time step

$$\mathbf{u}_j^{n+1} = \mathbf{u}_j^n - \frac{\Delta t}{\Delta x}\left(\hat{\mathbf{f}}_{j+\frac{1}{2}} - \hat{\mathbf{f}}_{j-\frac{1}{2}}\right) + \Delta t\ \mathbf{s}$$

   This algorithm can be improved by introducing succesive sub-steps to perform the time update (ex: predictor-corrector, Shu & Osher's conservative high order Runge-Kutta schemes)

2. Fractional step or splitting methods: split the equation into different pieces (transport + sources) and apply appropriate methods for each piece independently
   $\mathbf{u}^{n+1} = \mathcal{L}_s^{\Delta t}\mathcal{L}_f^{\Delta t}\mathbf{u}^n$ (Godunov splitting, first order)

   (a) First step (PDE), $\mathcal{L}_f^{\Delta t}$: $\quad \dfrac{\partial \mathbf{u}}{\partial t} + \dfrac{\partial \mathbf{f}(\mathbf{u})}{\partial x} = 0 \quad \rightarrow \quad \mathbf{u}^*$

   (b) Second step (ODE), $\mathcal{L}_s^{\Delta t}$: $\quad \dfrac{\partial \mathbf{u}^*}{\partial t} = \mathbf{s}(\mathbf{u}^*) \quad \rightarrow \quad \mathbf{u}^{n+1}$

   to get second order accuracy (assuming each independent method is second order) $\rightarrow$ Strang splitting: $\mathbf{u}^{n+1} = \mathcal{L}_s^{\Delta t/2}\mathcal{L}_f^{\Delta t}\mathcal{L}_s^{\Delta t/2}\mathbf{u}^n$

$$\mathbf{u}^n \;\underset{\substack{\Delta t/2\\ \text{source}}}{\longrightarrow}\; \mathbf{u}^* \;\underset{\substack{\Delta t\\ \text{transport}}}{\longrightarrow}\; \mathbf{u}^{**} \;\underset{\substack{\Delta t/2\\ \text{source}}}{\longrightarrow}\; \mathbf{u}^{n+1}$$

Stiff source terms: model phenomena which

1. occur on much faster time scales than Δt
2. act over much smaller spatial scales than Δx

$\rightarrow$ lead to numerical difficulties

- Example: **combustion**

  the chemical reactions (or nuclear reactions in stars) occur on much faster time scales than the gas flow $\rightarrow$ waves may propagate at nonphysical speeds

  Model problem: two chemical species, "unburnt gas" and "burnt gas"

  unburnt gas $\underset{k(T)}{\longrightarrow}$ burnt gas $k(T)$: reaction rate

$$k(T) = \begin{cases} 1/\tau & T \geq T_0 \\ 0 & T < T_0 \end{cases}$$

  T_0: ignition temperature

  τ: time scale of the chemical reaction

  Equations:

$$\begin{aligned} (\rho)_t + (\rho u)_x &= 0 \\ (\rho u)_t + (\rho u^2 + p)_x &= 0 \\ (E)_t + (u(E+p))_x &= 0 \\ (\rho Z)_t + (\rho u Z)_x &= -k(T)\rho Z \end{aligned}$$

  $E = \frac{1}{2}\rho u^2 + \frac{p}{\gamma - 1} + q_0 \rho Z$

  Z: mass fraction of the unburnt gas

  γ: adiabatic exponent

  q_0: heat release

4.5 Multidimensional problems

$$\frac{\partial \mathbf{u}}{\partial t} + \frac{\partial \mathbf{f}(\mathbf{u})}{\partial x} + \frac{\partial \mathbf{g}(\mathbf{u})}{\partial y} + \frac{\partial \mathbf{h}(\mathbf{u})}{\partial z} = \mathbf{s}(\mathbf{u})$$

- **Dimensional splitting**

$$\mathbf{u}_{i,j,k}^{n+1} = \mathcal{L}_s^{\Delta t/2} \mathcal{L}_h^{\Delta t} \mathcal{L}_g^{\Delta t} \mathcal{L}_f^{\Delta t} \mathcal{L}_s^{\Delta t/2} \mathbf{u}_{i,j,k}^{n}$$

where $\mathcal{L}_f$, $\mathcal{L}_g$ and $\mathcal{L}_h$ stand for the operators associated, respectively, to the 1D systems (PDEs)

$$\frac{\partial \mathbf{u}}{\partial t} + \frac{\partial \mathbf{f}(\mathbf{u})}{\partial x} = 0 \qquad \frac{\partial \mathbf{u}}{\partial t} + \frac{\partial \mathbf{g}(\mathbf{u})}{\partial y} = 0 \qquad \frac{\partial \mathbf{u}}{\partial t} + \frac{\partial \mathbf{h}(\mathbf{u})}{\partial z} = 0$$

$\mathcal{L}_s$ is the one that solves a system of ordinary differential equations (ODEs) of the form

$$\frac{\partial \mathbf{u}}{\partial t} = \mathbf{s}(\mathbf{u})$$

- **Method of lines**

$$\begin{aligned}\frac{d\mathbf{u}_{i,j,k}(t)}{dt} = & -\frac{\hat{\mathbf{f}}_{i+\frac{1}{2},j,k} - \hat{\mathbf{f}}_{i-\frac{1}{2},j,k}}{\Delta x} - \\ & -\frac{\hat{\mathbf{g}}_{i,j+\frac{1}{2},k} - \hat{\mathbf{g}}_{i,j-\frac{1}{2},k}}{\Delta y} - \\ & -\frac{\hat{\mathbf{h}}_{i,j,k+\frac{1}{2}} - \hat{\mathbf{h}}_{i,j,k-\frac{1}{2}}}{\Delta z} + \hat{\mathbf{s}}_{i,j,k}\end{aligned}$$

where the numerical fluxes are given by

$$\hat{\mathbf{f}}_{i+\frac{1}{2},j,k} = \mathbf{f}(\mathbf{u}_{i-p,j,k}, \mathbf{u}_{i-p+1,j,k}, ..., \mathbf{u}_{i+p,j,k})$$

$$\hat{\mathbf{g}}_{i,j+\frac{1}{2},k} = \mathbf{g}(\mathbf{u}_{i,j-p,k}, \mathbf{u}_{i,j-p+1,k}, ..., \mathbf{u}_{i,j+p,k})$$

$$\hat{\mathbf{h}}_{i,j,k+\frac{1}{2}} = \mathbf{h}(\mathbf{u}_{i,j,k-p}, \mathbf{u}_{i,j,k-p+1}, ..., \mathbf{u}_{i,j,k+p})$$

4.6 General Relativistic Hydrodynamic Equations

References: Banyuls, Font, Ibáñez, Martí and Miralles, ApJ, **476** 221 (1997)
Font, Miller, Suen and Tobias, Phys. Rev. D (1999) in press
gr-qc/9811015

- **Equations of motion**:
local conservation laws $J^{\mu}_{;\mu} = 0$ and $T^{\mu\nu}{}_{;\nu} = 0$ where the current J^{μ} and the energy-momentum tensor $T^{\mu\nu}$ are

$$J^{\mu} = \rho u^{\mu}$$

$$T_{\mu\nu} = \rho h u_{\mu} u_{\nu} + p g_{\mu\nu}$$

ρ is the rest-mass density, p is the pressure, h is the specific enthalpy, $h = 1 + \epsilon + p/\rho$, ϵ is the specific internal energy and $g_{\mu\nu}$ denotes the space-time metric.

- **Equation of state**:
$p = p(\rho, \epsilon)$ and the local sound velocity c_s:

$$h c_s^2 = \chi + (p/\rho^2)\kappa$$

with $\chi = \partial p/\partial \rho$ and $\kappa = \partial p/\partial \epsilon$.

- **$\{3 + 1\}$ formalism**:
the metric is split into the objects α (*lapse*), β^i (*shift*) and γ_{ij}.

$$ds^2 = -(\alpha^2 - \beta_i \beta^i) dt^2 + 2\beta_i dx^i dt + \gamma_{ij} dx^i dx^j$$

- **Conserved Variables**:
rest-mass density (D), momentum density in the j-direction (S_j) and total energy density (E). In terms of the *primitive variables* $\mathbf{w} = (\rho, v_i, \varepsilon)$

$$\begin{aligned} D &= \rho W \\ S_j &= \rho h W^2 v_j \\ E &= \rho h W^2 - p \end{aligned}$$

where $v_i = \frac{\mathbf{u} \cdot \partial_i}{-(\mathbf{u} \cdot \mathbf{n})}$, $v^i = \frac{u^i}{\alpha u^t} + \frac{\beta^i}{\alpha}$ and $W \equiv -(\mathbf{u} \cdot \mathbf{n}) = \alpha u^t$ (Lorentz factor) $W = (1 - v^2)^{-1/2}$ with $v^2 = \gamma_{ij} v^i v^j$.

- **Fundamental System (Hyperbolic)**:

$$\frac{1}{\sqrt{-g}}\left(\frac{\partial\sqrt{\gamma}\mathbf{F}^0(\mathbf{w})}{\partial x^0}+\frac{\partial\sqrt{-g}\mathbf{F}^i(\mathbf{w})}{\partial x^i}\right)=\mathbf{s}(\mathbf{w})$$

$$\begin{aligned}
\mathbf{F}^0(\mathbf{w}) &= (D, S_j, \tau)^T \\
\mathbf{F}^i(\mathbf{w}) &= \left(D\left(v^i-\frac{\beta^i}{\alpha}\right), S_j\left(v^i-\frac{\beta^i}{\alpha}\right)+p\delta^i_j, \tau\left(v^i-\frac{\beta^i}{\alpha}\right)+pv^i\right)^T \\
\mathbf{s}(\mathbf{w}) &= \left(0, T^{\mu\nu}\left(\frac{\partial g_{\nu j}}{\partial x^\mu}-\Gamma^\delta_{\nu\mu}g_{\delta j}\right), \alpha\left(T^{\mu 0}\frac{\partial \ln\alpha}{\partial x^\mu}-T^{\mu\nu}\Gamma^0_{\nu\mu}\right)\right)^T
\end{aligned}$$

where $\tau \equiv E - D$, $g \equiv \det(g_{\mu\nu})$, $\sqrt{-g}=\alpha\sqrt{\gamma}$, $\gamma \equiv \det(\gamma_{ij})$.

- **Numerical Integration**:

$$\int_\Omega \frac{1}{\sqrt{-g}}\frac{\partial\sqrt{\gamma}\mathbf{F}^0}{\partial x^0}d\Omega+\int_\Omega \frac{1}{\sqrt{-g}}\frac{\partial\sqrt{-g}\mathbf{F}^i}{\partial x^i}d\Omega=\int_\Omega \mathbf{s}d\Omega$$

$$\begin{aligned}
& (\overline{\mathbf{F}}^0\Delta V)_{t+\Delta t}-(\overline{\mathbf{F}}^0\Delta V)_t = \\
- & \left(\int_{\Sigma_{x^1+\Delta x^1}}\sqrt{-g}\hat{\mathbf{F}}^1 dx^0dx^2dx^3-\int_{\Sigma_{x^1}}\sqrt{-g}\hat{\mathbf{F}}^1 dx^0dx^2dx^3\right) \\
- & \left(\int_{\Sigma_{x^2+\Delta x^2}}\sqrt{-g}\hat{\mathbf{F}}^2 dx^0dx^1dx^3-\int_{\Sigma_{x^2}}\sqrt{-g}\hat{\mathbf{F}}^2 dx^0dx^1dx^3\right) \\
- & \left(\int_{\Sigma_{x^3+\Delta x^3}}\sqrt{-g}\hat{\mathbf{F}}^3 dx^0dx^1dx^2-\int_{\Sigma_{x^3}}\sqrt{-g}\hat{\mathbf{F}}^3 dx^0dx^1dx^2\right) \\
+ & \int_\Omega \mathbf{s}d\Omega
\end{aligned}$$

$$\overline{\mathbf{F}}^0=\frac{1}{\Delta V}\int_{\Delta V}\sqrt{\gamma}\mathbf{F}^0dx^1dx^2dx^3$$

$$\Delta V=\int_{x^1}^{x^1+\Delta x^1}\int_{x^2}^{x^2+\Delta x^2}\int_{x^3}^{x^3+\Delta x^3}\sqrt{\gamma}dx^1dx^2dx^3$$

- **Characteristic fields** (x direction)

  Eigenvalues:

$$
\begin{aligned}
\lambda_0 &= \alpha v^x - \beta^x \quad \text{(triple)} \\
\lambda_\pm &= \frac{\alpha}{1 - v^2 c_s^2}\left\{ v^x(1-c_s^2) \pm c_s \sqrt{(1-v^2)[\gamma^{xx}(1-v^2c_s^2) - v^x v^x (1-c_s^2)]} \right\} - \beta^x
\end{aligned}
$$

Right-eigenvectors:

$$
\mathbf{r}_\pm = \begin{bmatrix} 1 \\ hW\left(v_x - \dfrac{v^x - \Lambda_\pm^x}{\gamma^{xx} - v^x\Lambda_\pm^x}\right) \\ hWv_y \\ hWv_z \\ \dfrac{hW(\gamma^{xx} - v^x v^x)}{\gamma^{xx} - v^x\Lambda_\pm^x} - 1 \end{bmatrix}, \quad \mathbf{r_{0,1}} = \begin{bmatrix} \dfrac{\mathcal{K}}{hW} \\ v_x \\ v_y \\ v_z \\ 1 - \dfrac{\mathcal{K}}{hW} \end{bmatrix}
$$

$$
\mathbf{r_{0,2}} = \begin{bmatrix} Wv_y \\ h\left(\gamma_{xy} + 2W^2 v_x v_y\right) \\ h\left(\gamma_{yy} + 2W^2 v_y v_y\right) \\ h\left(\gamma_{zy} + 2W^2 v_z v_y\right) \\ Wv_y(2hW - 1) \end{bmatrix}, \quad \mathbf{r_{0,3}} = \begin{bmatrix} Wv_z \\ h\left(\gamma_{xz} + 2W^2 v_x v_z\right) \\ h\left(\gamma_{yz} + 2W^2 v_y v_z\right) \\ h\left(\gamma_{zz} + 2W^2 v_z v_z\right) \\ Wv_z(2hW - 1) \end{bmatrix}
$$

with $\tilde{\kappa} \equiv \kappa/\rho$, $\Lambda_\pm^i \equiv \tilde{\lambda}_\pm + \tilde{\beta}^i$, $\tilde{\lambda} \equiv \lambda/\alpha$ and $\tilde{\beta}^i \equiv \beta^i/\alpha$

In numerical relativity the GRH equations must be solved in conjunction with the gravitational field equations (Einstein equations)

ADM formulation (γ_{ij}, K_{ij})

- spacetime foliated into a set of non-intersecting spacelike hypersurfaces
- two kinematic variables describe the evolution between these surfaces: the lapse function α, describing the rate of advance of time along a timelike unit vector n^μ normal to a surface, and the spacelike shift vector β^i describing the motion of coordinates
- Metric:

$$ds^2 = -(\alpha^2 - \beta_i\beta^i)dt^2 + 2\beta_i dx^i dt + \gamma_{ij}dx^i dx^j$$

- Evolution equations:

$$\begin{aligned}
\partial_t \gamma_{ij} &= -2\alpha K_{ij} + \nabla_i \beta_j + \nabla_j \beta_i, \\
\partial_t K_{ij} &= \alpha \left[R_{ij} + K\ K_{ij} - 2K_{im}K_j^m - 8\pi(S_{ij} - \frac{1}{2}\gamma_{ij}S) - 4\pi\rho_{\mathtt{ADM}}\gamma_{ij} \right] \\
&\quad + \beta^m \nabla_m K_{ij} + K_{im}\nabla_j \beta^m + K_{mj}\nabla_i \beta^m - \nabla_i \nabla_j \alpha
\end{aligned}$$

  where ∇_i denotes a covariant derivative with respect to the 3-metric γ_{ij} and R_{ij} is the Ricci curvature of the 3-metric

- Constraint equations:

$$\begin{aligned}
{}^{(3)}R + K^2 - K_{ij}K^{ij} &= 16\pi\rho_{\mathtt{ADM}} \\
\nabla_j K^{ij} - \gamma^{ij}\nabla_j K &= 8\pi j^i
\end{aligned}$$

  with

$$\begin{aligned}
\rho_{\mathtt{ADM}} &= \rho h W^2 - P \\
j^i &= \rho h W^2 v^i \\
S_{ij} &= \rho h W^2 v_i v_j + \gamma_{ij} P \\
S &= \rho h W^2 v_i v^i + 3P
\end{aligned}$$

4.7 One-dimensional numerical tests

4.7.1 Relativistic shock tube

<u>Initial configuration ($t = 0$):</u>

Left State	Right state
Hot gas, high pressure	Cold gas, low pressure
pressure = 13.3	pressure = 0
density = 10	density = 1
velocity = 0	velocity = 0

membrane

<u>Final configuration ($t = 0.4$):</u>

- First-order scheme, perfect fluid EOS ($\gamma = 5/3$), $\Delta x = 1/200$

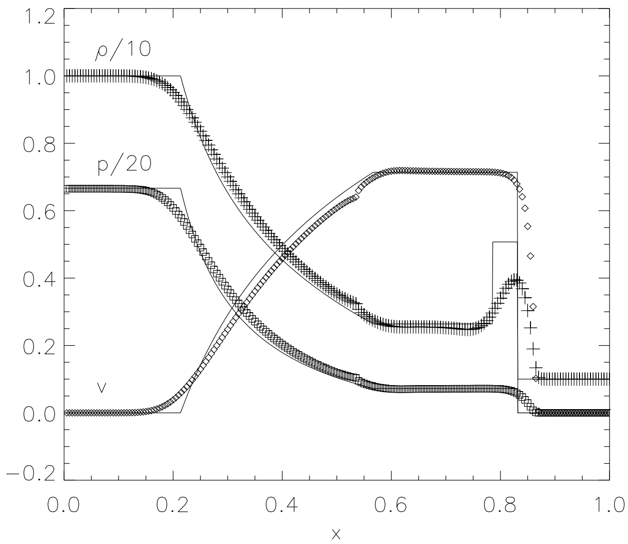

- Second-order scheme, perfect fluid EOS ($\gamma = 5/3$), $\Delta x = 1/200$

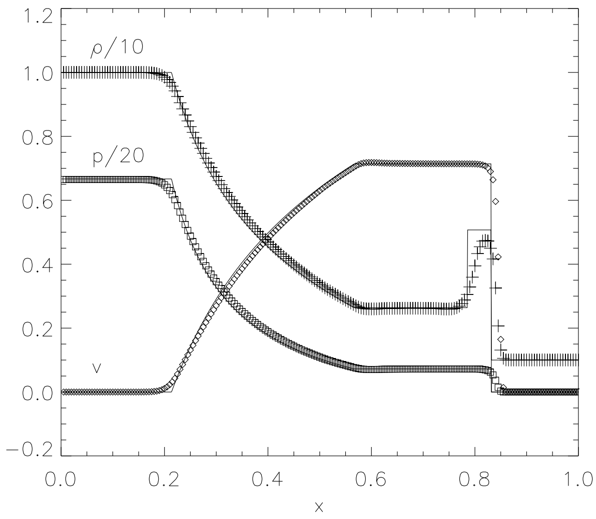

- Third-order scheme, perfect fluid EOS ($\gamma = 5/3$), $\Delta x = 1/200$

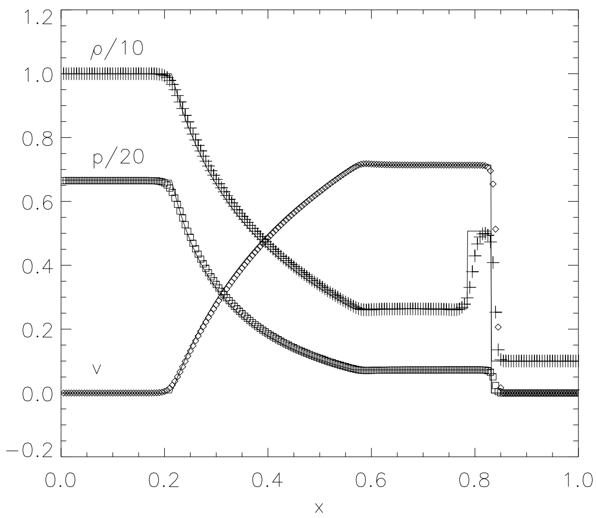

4.7.2 Relativistic blast wave

Initial configuration ($t = 0$):

Left State	Right state
Hot gas, high pressure	Cold gas, low pressure
pressure = 10^3	pressure = 10^{-2}
density = 1	density = 1
velocity = 0	velocity = 0

membrane

Final configuration ($t = 0.35$):

- First-order scheme, perfect fluid EOS ($\gamma = 5/3$), $\Delta x = 1/400$

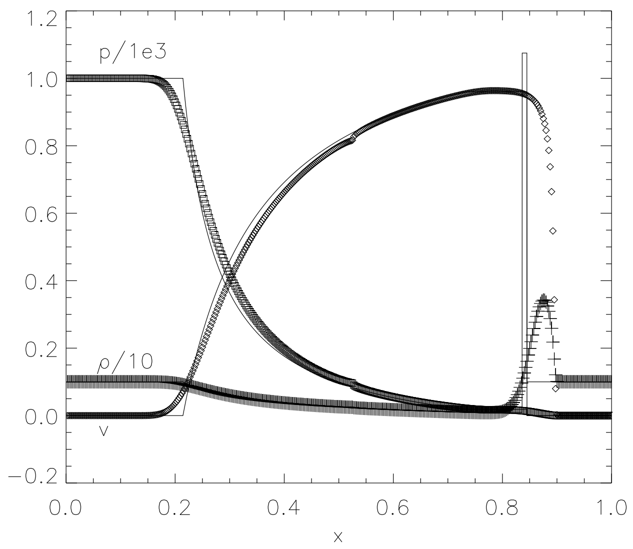

- Second-order scheme, perfect fluid EOS ($\gamma = 5/3$), $\Delta x = 1/400$

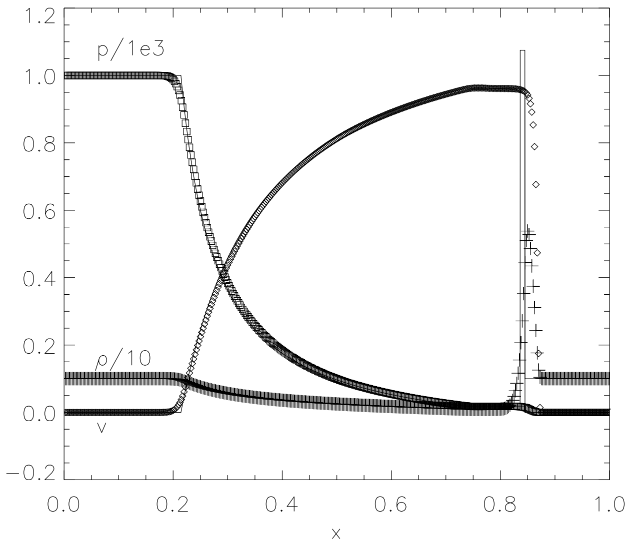

- Third-order scheme, perfect fluid EOS ($\gamma = 5/3$), $\Delta x = 1/400$

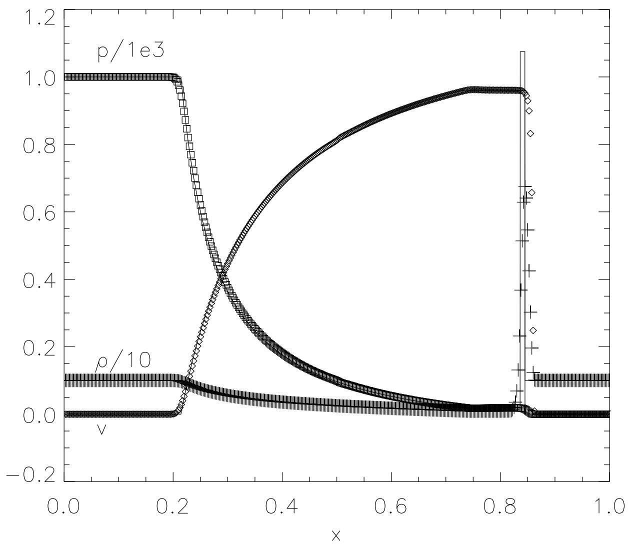

4.7.3 Relativistic shock reflection

Problem setup:

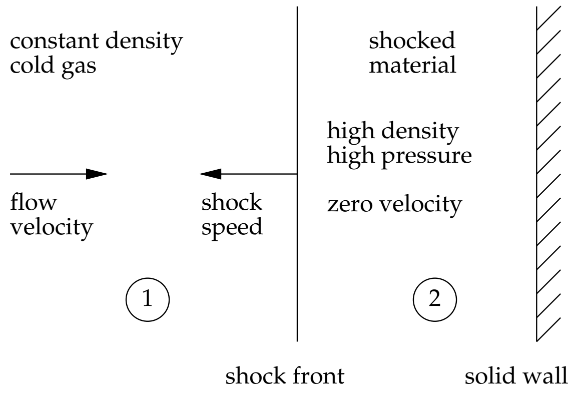

$$\frac{\rho_2}{\rho_1} = \frac{\gamma+1}{\gamma-1} + \frac{\gamma}{\gamma-1}\varepsilon_2 \qquad\qquad \varepsilon_2 = W_1 - 1$$

- Third-order scheme, perfect fluid EOS ($\gamma = 5/3$), $\Delta x = 1/400$, $v_1 = 0.99999c$ ($W_1 = 224$)

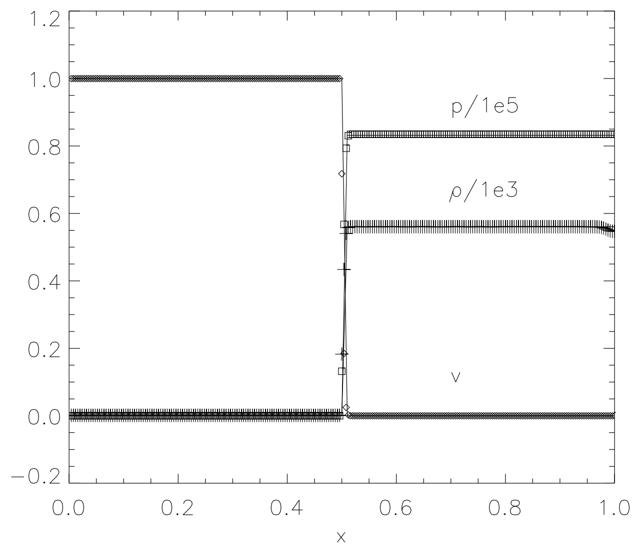

4.7.4 Spherical (Bondi) accretion onto a black hole

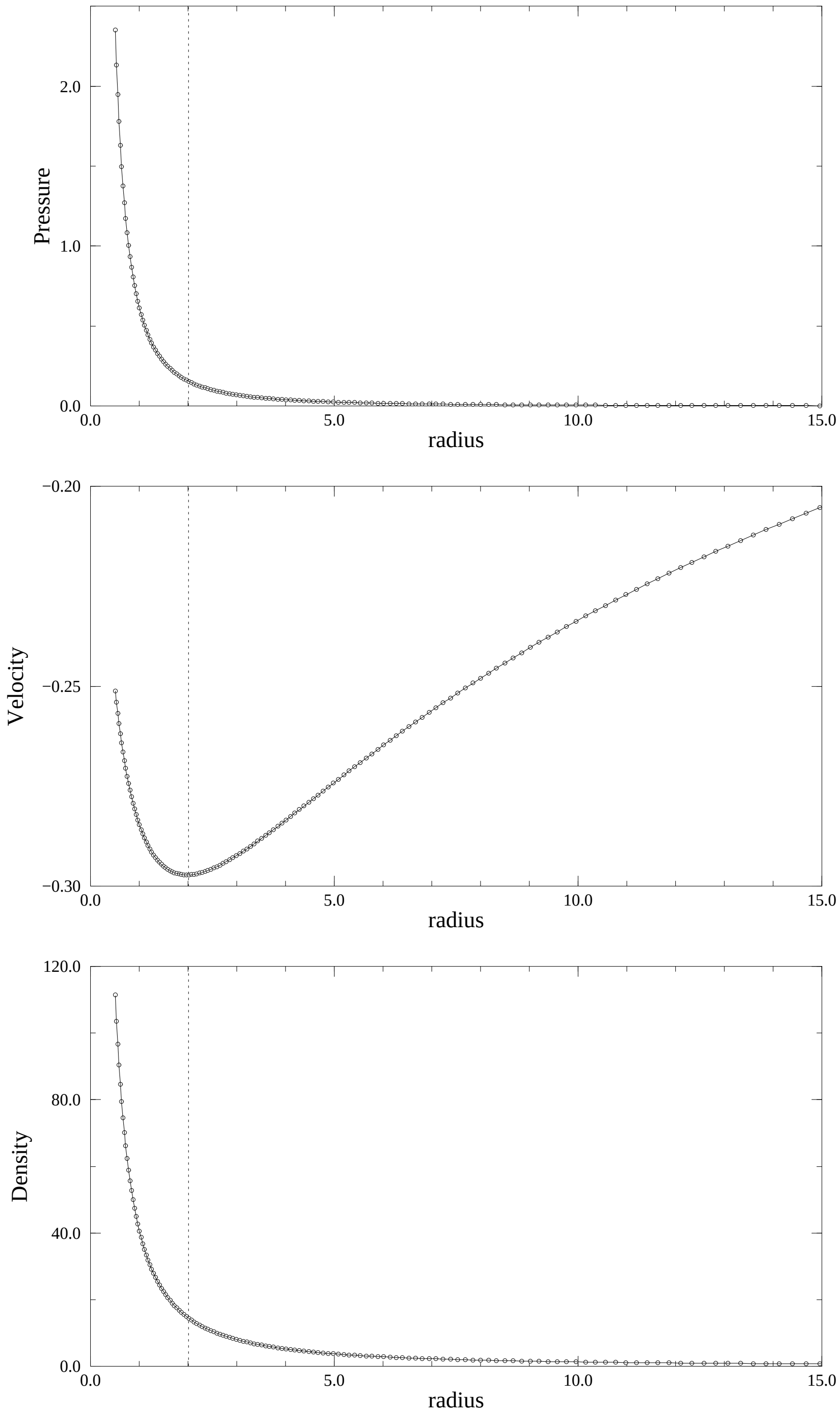

4.8 Two-dimensional numerical tests

Wind tunnel with a flat-faced step

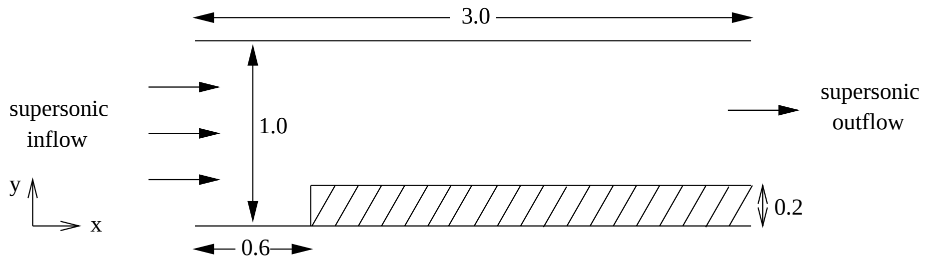

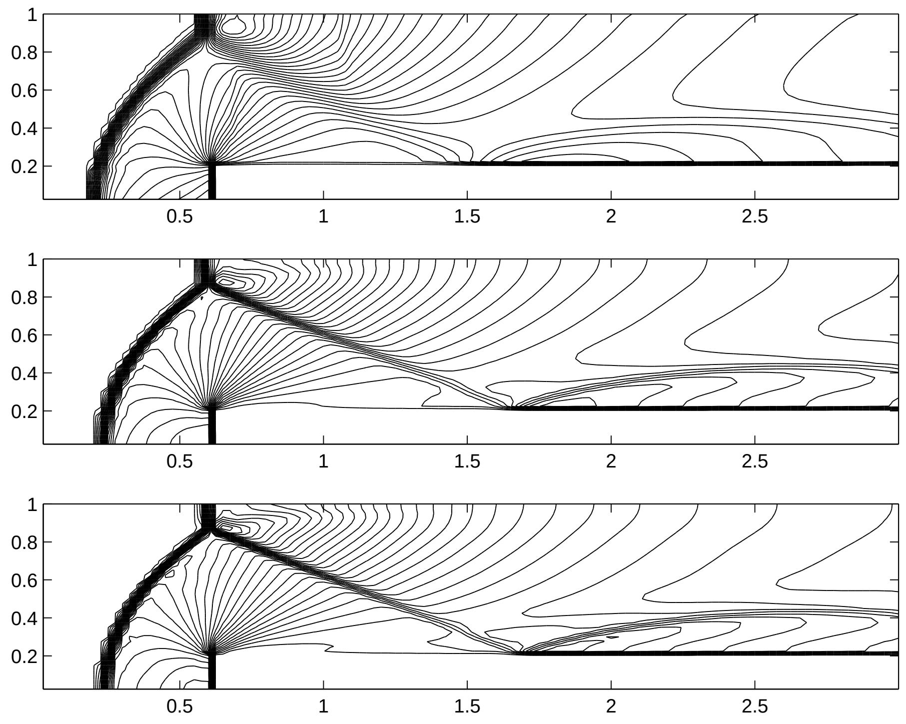

5 Aplicaciones astrofísicas

5.1 Dinámica de nebulosas planetarias

- Introducción : http://www.astro.washington.edu/balick/WFPC2/index.html
- Simulaciones : http://www.strw.leidenuniv.nl/ icke/html/VincentPNO.html
- The formation of bipolar planetary nebulae.
  Mellema, G.
  Astronomy and Astrophysics, v.321, p.L29-L32 (1997)
- Ram Pressure Stripping in Planetary Nebulae.
  Villaver, Eva; García-Segura, Guillermo; Manchado, Arturo
  Astrophysical Journal, Volume 585, Issue 1, pp. L49-L53 (2003)
- Three-dimensional Magnetohydrodynamic Modeling of Planetary Nebulae. II. The Formation of Bipolar and Elliptical Nebulae with Point-symmetric Structures and Collimated Outflows.
  García-Segura, G.; López, J. A.
  Astrophysical Journal, Volume 544, Issue 1, pp. 336-346 (2000)
- Three-dimensional Magnetohydrodynamical Modeling of Planetary Nebulae: The Formation of Jets, Ansae, and Point-symmetric Nebulae via Magnetic Collimation.
  Garcia-Segura, Guillermo
  Astrophysical Journal Letters v.489, p.L189 (1997)
- The Morphology of Planetary Nebulae: Simulations with Time-evolving Winds.
  Dwarkadas, Vikram V.; Balick, Bruce
  Astrophysical Journal v.497, p.267-275 (1998)

5.2 Supernovae

- Introducción y simulaciones:

  http://jupiter.as.arizona.edu/ burrows/scidac/scidac.html

  http://www.phy.ornl.gov/tsi (visitar Background, Requirements & Challenges, y Simulations)

  http://www.mpa-garching.mpg.de/ ewald/SNII/snii.html

- Non-spherical core collapse supernovae.
  Kifonidis, K.; Plewa, T.; Hanka, H.-Th.; Müller, E.
  Astronomy and Astrophysics, v.408, p.621-649 (2003)

5.3 Stellar Core Collapse

- A New Spherically Symmetric General Relativistic Hydrodynamical code.
  Romero, J.V.; Ibáñez, J.Ma.; Martí, J.Ma.; Miralles, J.A.
  Astrophysical Journal, Volume 462, pp. 839-854 (1996).

- Relativistic simulations of rotational core collapse I. Methods, initial models, and code tests.
  Dimmelmeier, H.; Font, J. A.; Müller, E.
  Astronomy and Astrophysics, v.388, p.917-935 (2002).

- Relativistic simulations of rotational core collapse II. Collapse dynamics and gravitational radiation.
  Dimmelmeier, H.; Font, J. A.; Müller, E.
  Astronomy and Astrophysics, v.393, p.523-542 (2002).

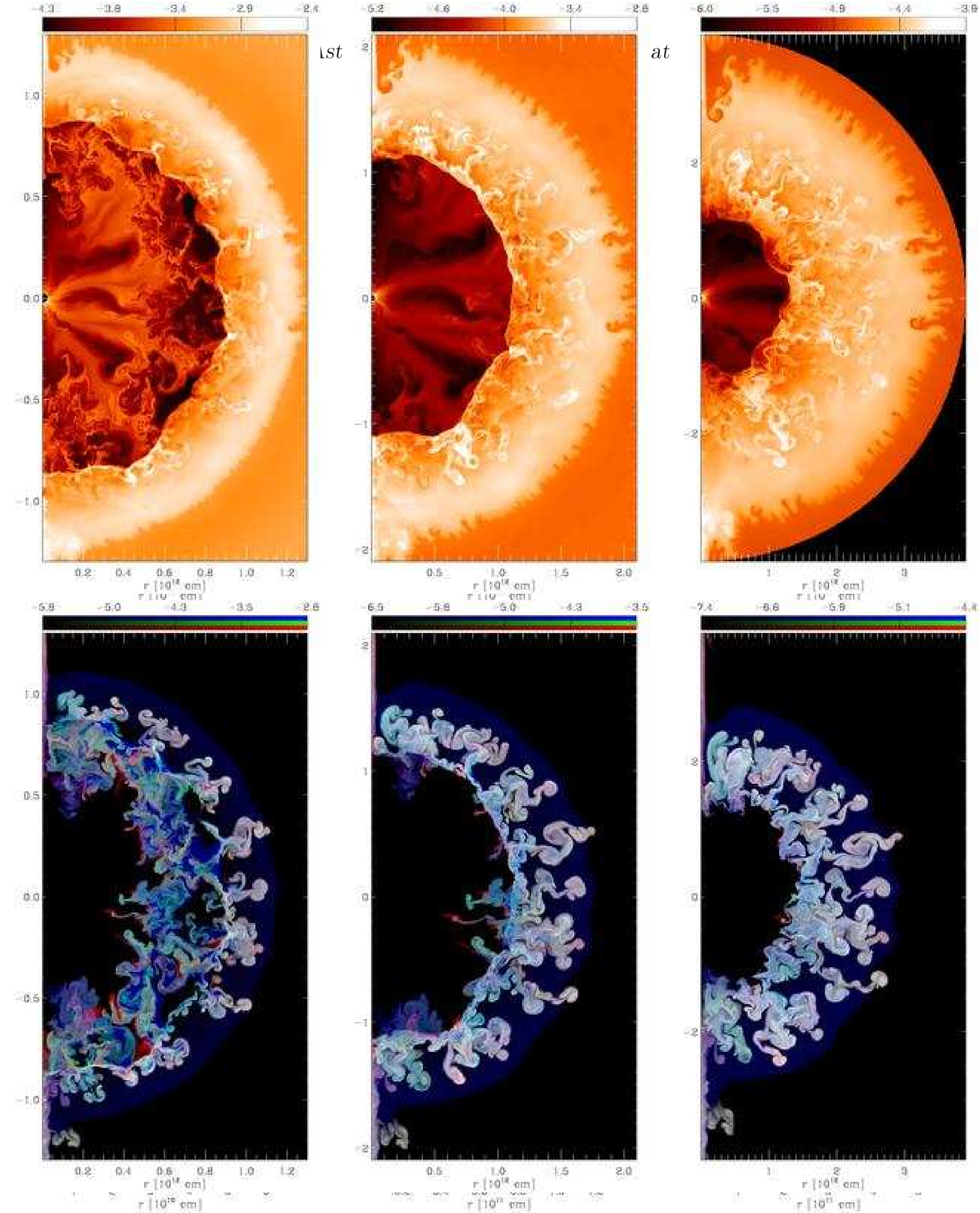

Fig. 14. Same as Fig. 12. a) t = 5000 s (left), b) t = 10 000 s (middle), c) t = 20 000 s (right). Note the change of the radial scale. The circular orange/black boundary in the upper right panel corresponds to the outer edge of the computational domain, which the supernova shock has crossed long before.

Fig. 12. Snapshots of the density (left), and the partial densities of ^{16}O (red), ^{28}Si (green), and ^{56}Ni (blue) in Model T310a at selected early epochs. Data values are coded according to the color bars given for each frame. In case of the partial densities, colors other than red, green and blue (resulting from the superposition of these color channels) indicate mixing of the composition. From left to right a) t = 4 s, b) t = 10 s, c) t = 20 s. Note the change of the radial scale. The supernova shock is visible as the outermost circular discontinuity in the density plots.

Fig. 13. Same as Fig. 12. a) t = 100 s (left), b) t = 300 s (middle), c) t = 1500 s (right).

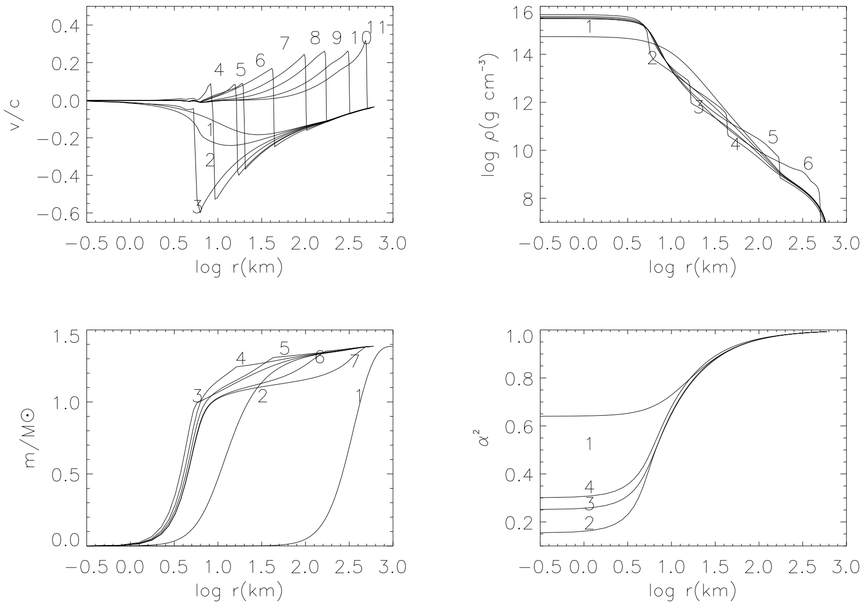

A2B4G1 model.

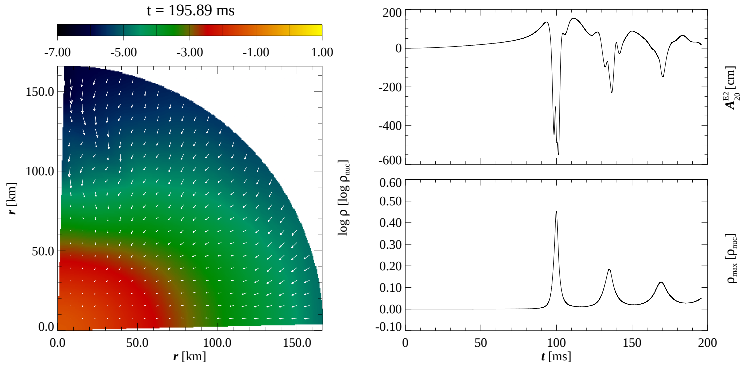

A3B2G4 model.

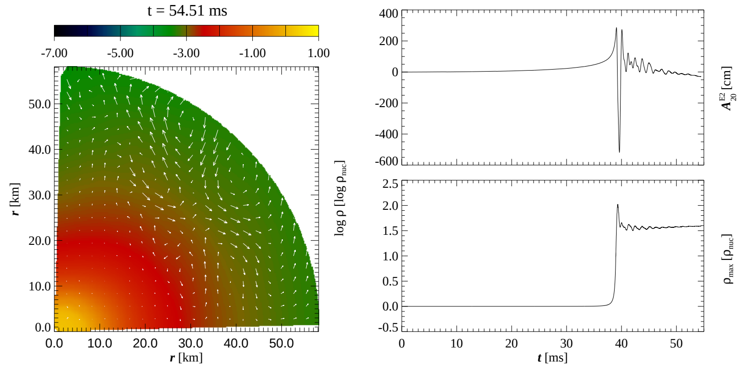

A4B5G5 model.

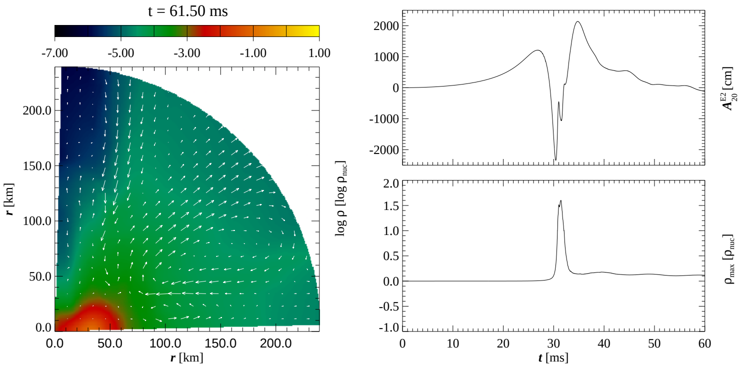

5.4 Interaction of SNe with their Surroundings

- Interaction of Type IA Supernovae with Their Surroundings: The Exponential Profile in Two Dimensions
  Dwarkadas, Vikram V.
  Astrophysical Journal, Volume 541, Issue 1, pp. 418-427 (2000)

- Type IA Supernova Explosions in Binary Systems: The Impact on the Secondary Star and Its Consequences
  Marietta, E.; Burrows, Adam; Fryxell, Bruce
  Astrophysical Journal Supplement Series, Volume 128, Issue 2, pp. 615-650 (2000).
  (Postscript images, MPEG movies, and a selection of figures presented in this paper are posted at http://www.astrophysics.arizona.edu and are available via FTP at www.astrophysics.arizona.edu , in directory pub/marietta.)

5.5 Chorros astrofísicos

- Introducción: http://www.livingreviews.org/Articles/Volume2/1999-3marti/index.html (Sección 7.1)

- [movie] (créditos: L. Scheck, J.-M. Martí, M.-A. Aloy, E. Müller)

- Kelvin-Helmholtz Instability in a Slab Relativistic Jet (symmetric and antisymmetric modes).
  Manuel Perucho.
  [movie]

- Imágenes de chorros extragalácticos: http://www.cv.nrao.edu/ abridle/images.htm

- Simulaciones: http://www.astro.lsa.umich.edu/users/hughes/icon_dir/relproj.html

5.6 Gamma ray burst

- Introducción: http://www.livingreviews.org/Articles/Volume2/1999-3marti/index.html (Sección 7.2)

- Introducción y simulaciones:

  http://science.nasa.gov/newhome/headlines/ast02nov99_1.htm

  http://www.mpa-garching.mpg.de/HIGHLIGHT/2000/highlight0003_e.html

5.7 Jets from Collapsars

- Relativistic Jets from Collapsars.
  Aloy, M. A.; Müller, E.; Ibáñez, J. M.; Martí, J. M.; MacFadyen, A.
  Astrophysical Journal, Volume 531, Issue 2, pp. L119-L122. (2000).

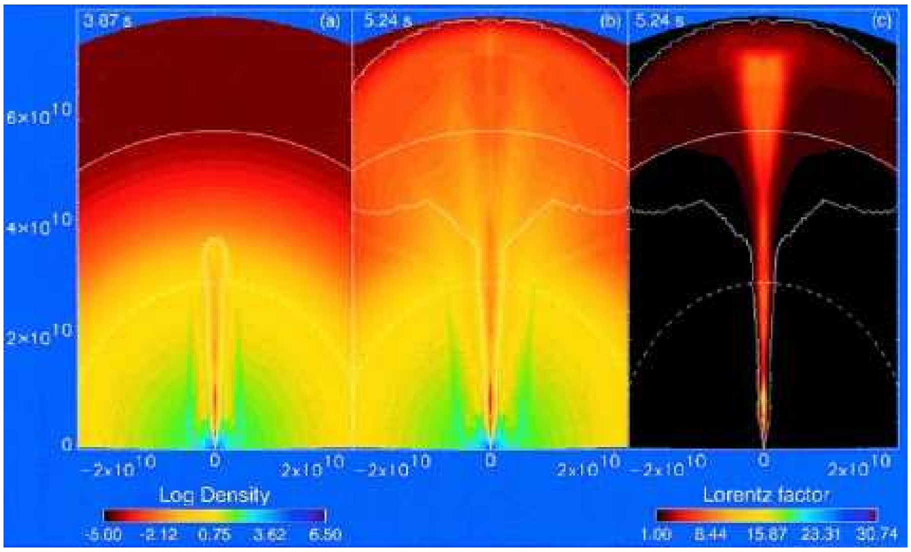

5.8 Jets in AGNs

- High-Resolution Three-dimensional Simulations of Relativistic Jets.
  Aloy, M. A.; Ibáñez, J. M. [a].; Martí, J. M. [a].; Gómez, J.-L.; Müller, E.
  Astrophysical Journal, Volume 523, Issue 2, pp. L125-L128 (1999).

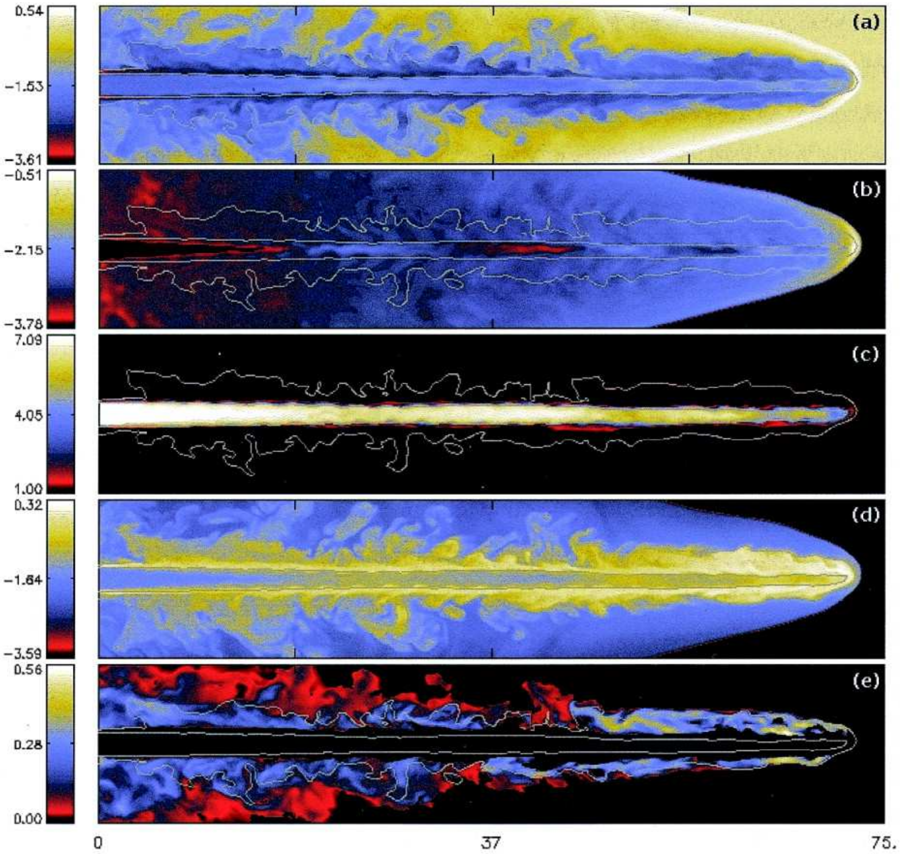

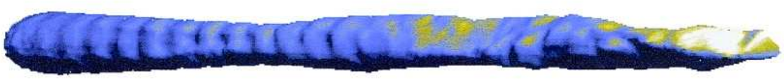

- Morphology and Dynamics of Relativistic Jets.
  Martí, J. M.[a]; Müller, E.; Font, J. A.; Ibáñez, J. M.[a]; Marquina, A.
  Astrophysical Journal v.479, p.151 (1997).

5.9 Dinámica galáctica e interacción de galaxias

- Introducción y simulaciones: http://www.ifa.hawaii.edu/faculty/barnes/saas-fee/chapter-outline.html

5.10 Multidimensional General-Relativistic Hydrodynamics

- http://www.livingreviews.org/Articles/Volume3/2000-2font/index.html (Sección 4)

- Numerical 3+1 General Relativistic Hydrodynamics: A Local Characteristic Approach.
  Banyuls, Francesc; Font, José A.; Ibáñez, Jose M. A.; Martí, Jose M. A.; Miralles, Juan A.
  Astrophysical Journal v.476, p.221 (1997).

- Three-dimensional numerical general relativistic hydrodynamics. II. Long-term dynamics of single relativistic stars.
  Font, José A.; Goodale, Tom; Iyer, Sai; Miller, Mark; Rezzolla, Luciano; Seidel, Edward; Stergioulas, Nikolaos; Suen, Wai-Mo; Tobias, Malcolm
  Physical Review D, vol. 65, id. 084024 (2002).

5.11 Medio Interestelar

- Hydrodynamic Interaction of Strong Shocks with Inhomogeneous Media. I. Adiabatic Case.
  Poludnenko, A. Y.; Frank, A.; Blackman, E. G
  Astrophysical Journal, Volume 576, Issue 2, pp. 832-848 (2002)

5.12 Young Stellar Objects

- Hydrodynamical Models of Outflow Collimation in Young Stellar Objects.
  Frank, Adam; Mellema, Garrelt
  Astrophysical Journal v.472, p.684 (1996)

- Outflow collimation in young stellar objects.
  Mellema, Garrelt; Frank, Adam
  Royal Astronomical Society, Monthly Notices, vol. 292, p. 795 (1997)

5.13 Accretion onto Compact Objects

- Non-axisymmetric relativistic Bondi-Hoyle accretion on to a Kerr black hole.
  Font, José A.; Ibáñez, José Maria; Papadopoulos, Philippos
  Monthly Notices of the Royal Astronomical Society, Volume 305, pp.920-936 (1999).

- Quasi-periodic accretion and gravitational waves from oscillating 'toroidal neutron stars' around a Schwarzschild black hole.
  Zanotti, Olindo; Rezzolla, Luciano; Font, José A.
  Monthly Notice of the Royal Astronomical Society, Volume 341, pp. 832-848 (2003).

5.14 Computational Cosmology

- Introducción y simulaciones: http://www.MPA-Garching.MPG.DE/NumCos/

- Gone with the Wind: The Origin of S0 Galaxies in Clusters.
  Quilis, Vicent; Moore, Ben; Bower, Richard
  Science, Volume 288, Issue 5471, pp. 1617-1620 (2000).

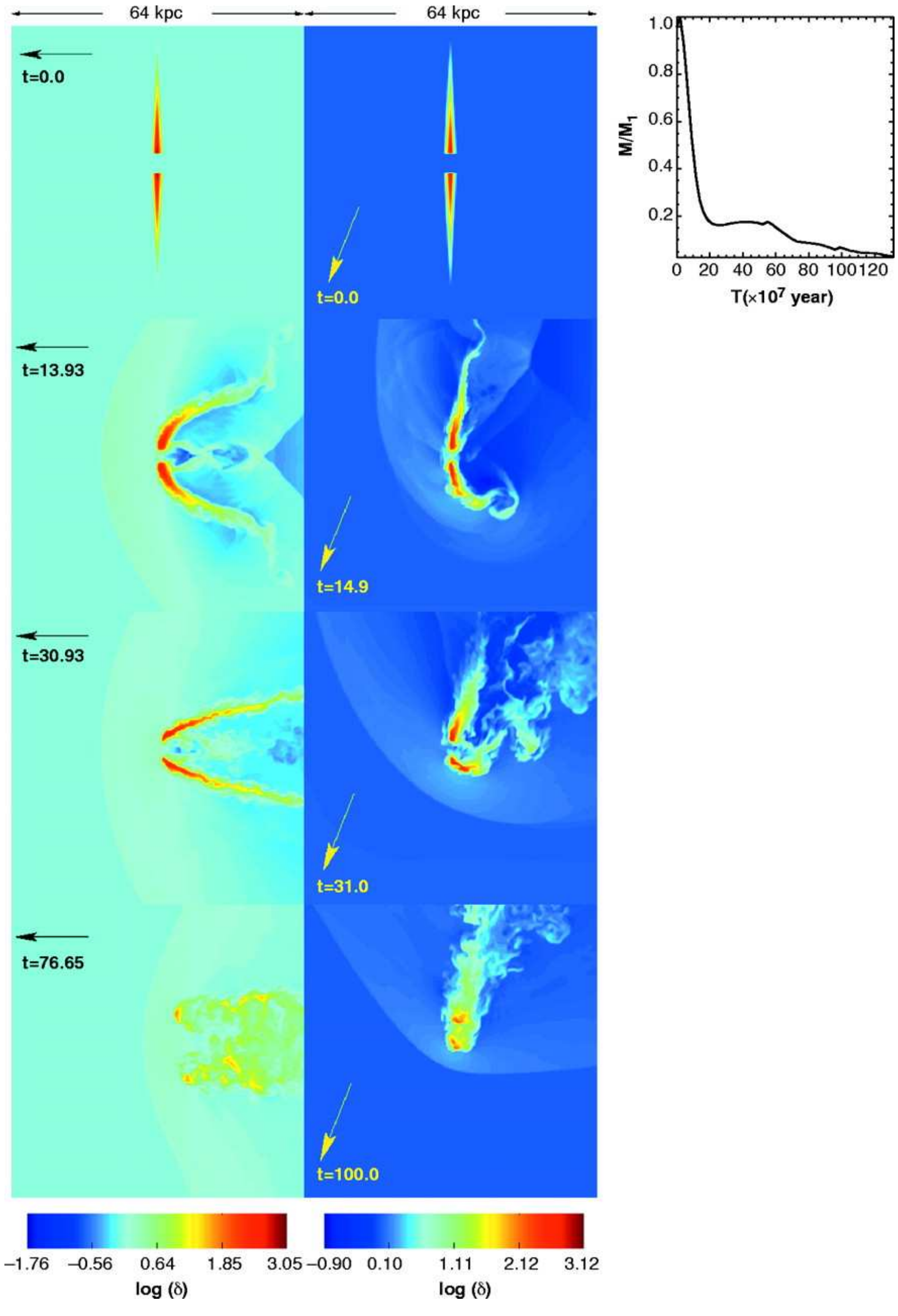
64 kpc
64 kpc
t=0.0
t=13.93
t=30.93
t=76.65
t=0.0
t=14.9
t=31.0
t=100.0
–1.76 –0.56 0.64 1.85 3.05
log (δ)
–0.90 0.10 1.11 2.12 3.12
log (δ)
M/M1
1.0
0.8
0.6
0.4
0.2
0 20 40 60 80 100 120
T(×10^7 year)

- On the Role of Shock Waves in Galaxy Cluster Evolution.
  Quilis, Vicent; Ibanez, Jose M. A.; Saez, Diego
  Astrophysical Journal v.502, p.518 (1998).

5.15 AMR-Cosmology

- A New Multidimensional AMR Hydro+Gravity Cosmological Code.
  Quilis, Vicent
  MNRAS, in press (2004).

6 Prácticas

Las prácticas que se detallan a continuación se basan en programas FORTRAN. Puedes encontrar un Manual de Referencia de FORTRAN77 Standard en http://www.fortran.com/fortran/F77_std/rjcnf0001.html .

Práctica 1:Resolución exacta del Problema de Riemann para las ecuaciones de Euler

Introducción

- El Problema de Riemann es un problema de valores iniciales discontinuos de la forma:

$$\frac{\partial \mathbf{u}}{\partial t} + \frac{\partial \mathbf{F}(\mathbf{u})}{\partial x} = 0, \quad \mathbf{u} = \begin{bmatrix} \rho \\ \rho u \\ E \end{bmatrix}, \quad \mathbf{F} = \begin{bmatrix} \rho u \\ \rho u^2 + p \\ u(E+p) \end{bmatrix}$$

  con

$$\mathbf{u}(x,0) = u_0(x) = \begin{cases} \mathbf{u}_{\mathrm{L}} & \text{si } x < x_0 \\ \mathbf{u}_{\mathrm{R}} & \text{si } x > x_0 \end{cases}$$

- El dato inicial no tiene escala espacial definida, por lo que su solución es autosemejante: $\mathbf{u}(x,t) = \mathbf{u}(x/t)$. La solución consiste en dos estados constantes (L_*, R_*) separados de los estados iniciales por ondas de choque ($\mathcal{S}$) y/o rarefacciones ($\mathcal{R}$) con una discontinuidad de contacto ($\mathcal{C}$) entre ellos:

$$I \;\rightarrow\; L\, \mathcal{W}_{\leftarrow}\, L_*\, \mathcal{C}\, R_*\, \mathcal{W}_{\rightarrow}\, R \tag{122}$$

  ($\mathcal{W} = \mathcal{S}, \mathcal{R}$; las flechas ($\leftarrow$ / $\rightarrow$) indican la dirección desde la que los elementos de fluido atraviesan la correspondiente onda).

- Ondas de choque: Soluciones discontinuas de las ecuaciones de Euler con flujo de masa a través de la discontinuidad. Los estados a izquierda y derecha de la onda de choque y su velocidad están relacionados mediante las condiciones de Rankine-Hugoniot. Las ondas de choque son compresivas (las partículas de fluido aumentan su presión al atravesarlas).

- Discontinuidades de contacto: Soluciones discontinuas de las ecuaciones de Euler. A diferencia de las ondas de choque, a través de la discontinuidades de contacto no hay flujo de masa. La presión y la velocidad del fluido son iguales a ambos lados de la discontinuidad de contacto.

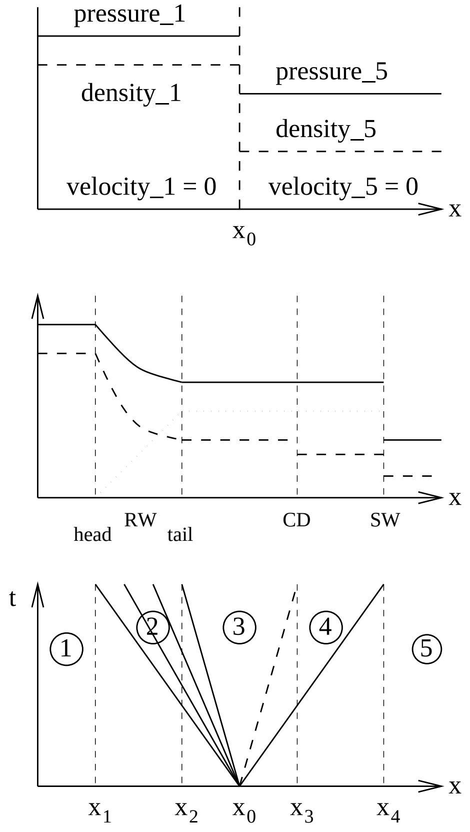

- Ondas de rarefacción: Soluciones continuas autosemejantes de las ecuaciones de Euler que conectan estados constantes. Las partículas de fluido reducen su presión al atravesarlas.

- La solución para la presión en los estados intermedios, p_*, de un problema de Riemann con una ecuación de estado de gas ideal viene dada por la raíz de la ecuación algebraica

$$f(p; \mathbf{u}_{\rm L}, \mathbf{u}_{\rm R}) = f_{\rm L}(p; \mathbf{u}_{\rm L}) + f_{\rm R}(p; \mathbf{u}_{\rm R}) + u_{\rm R} - u_{\rm L} = 0, \qquad (123)$$

  donde la función $f_{\rm I}$ $(I = L, R)$ viene dada por:

$$f_{\rm I}(p; \mathbf{u}_{\rm I}) = \begin{cases} (p - p_{\rm I}) \left[\frac{A_{\rm I}}{p + B_{\rm I}}\right]^{1/2} & \text{si } p > p_{\rm I} \text{ (onda de choque)} \\ \frac{2a}{(\gamma-1)} \left[\left(\frac{p}{p_{\rm I}}\right)^{(\gamma-1)/2\gamma} - 1\right] & \text{si } p < p_{\rm I} \text{ (onda de rarefacción)} \end{cases}$$

  donde γ es el cociente de calores específicos del gas ideal, a la velocidad del sonido y las constantes $A_{\rm I}$ y $B_{\rm I}$ están dadas por

$$A_{\rm I} = \frac{2}{(\gamma+1)\rho_{\rm I}}, \;\; B_{\rm I} = \frac{(\gamma-1)}{(\gamma+1)} p_{\rm I} \tag{124}$$

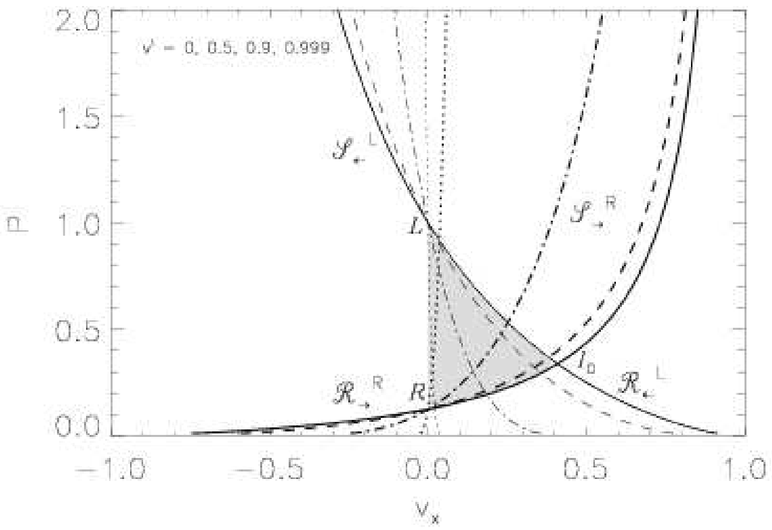

- La solución para la velocidad del fluido en el estado intermedio, u_*, viene dada por

$$u_* = \frac{1}{2}(u_{\rm L} + u_{\rm R}) + \frac{1}{2}\left[f_{\rm R}(p_*) - f_{\rm L}(p_*)\right] \tag{125}$$

- Una vez obtenidas p_*, u_*, se pueden obtener los valores del resto de variables en los estados intermedios y las velocidades de propagación de las ondas de choque, los extremos de las rarefacciones y la discontinuidad de contacto, que separan los diferentes estados constantes. Por último se pueden obtener los valores de las variables en la rarefacción.

- Referencias:

E.F. Toro, *Riemann solvers and Numerical Methods for Fluid Dynamics*, Springer, 1997. Capítulo 4

R. Courant, K.O. Friedrichs, *Supersonic Flow and Shock Waves*, Springer, 1976. Epígrafes 80 y 81

L.D. Landau, E.M. Lifshitz, *Fluid Mechanics*, Springer, 1987. Epígrafe 100

Desarrollo de la práctica

- Usando el programa `e1rpex.f`, obtén la solución, en el dominio espacial $[0, 1]$, de los problemas de Riemann que aparecen en la siguiente tabla:

Test	ρ_L	u_L	p_L	ρ_R	u_R	p_R
1	1.0	0.75	1.0	0.125	0.0	0.1
2	1.0	-2.0	0.4	1.0	2.0	0.4
3	1.0	0.0	1000.0	1.0	0.0	0.01
4	6.0	20.	400.0	6.0	-6.0	40.0

- Para cada uno de los problemas anteriores, **1)** identifica las ondas de choque, discontinuidades de contacto y rarefacciones que aparecen separando los diferentes estados constantes, y **2)** calcula los flujos de masa, momento y energía por unidad de superficie en $x = 0.5$.

Resumen del programa `e1rpex.f`

`program e1rpex`: resuelve el problema de Riemann exacto para las ecuaciones de Euler unidimensionales, dependientes del tiempo, de un gas ideal.

`subroutine starpu`: calcula, a partir de los datos iniciales del problema de Riemann, la presión y velocidad del fluido en el estado intermedio, p_*, u_*, resolviendo mediante un Newton-Raphson, una ecuación algebraica para la presión.

`subroutine guessp`: proporciona el valor inicial de la presión para el Newton-Raphson.

`subroutine prefun`: evalúa las funciones de la presión f_L y f_R y sus primeras derivadas.

`subroutine sample`: a partir de los valores de p_* y u_*, proporciona la solución completa (densidad, velocidad, presión) en todos los puntos de la malla numérica en un cierto instante.

Representación gráfica

- Puedes representar gráficamente las variables hidrodinámicas usando el paquete `gnuplot`, suministrado con diversas distribuciones de *Linux*.

- Para representar una figura sencilla usa `plot` "*fichero*" `using` (\$*col*):(\$*col*), donde *fichero* es el nombre del fichero en el que están almacenados los datos, *col* es el número de la columna que contiene los datos a representar (abcisas la primera, ordenadas la segunda).
- Usa el comando `replot` para representar otra función sobre la misma figura.
- Para guardar las figuras en un fichero, selecciona primero `set terminal postscript` y luego `set output` "*fichero*", donde *fichero* es el nombre del fichero en el que se van a guardar las figuras (extensión *.ps*).
- Usa `help` para acceder a un menú de ayuda.

Material

- Programas:
  Código fuente: e1rpex.f
  Datos iniciales: e1rpex.ini

Práctica 2: Aspectos básicos de los métodos en diferencias finitas aplicados a los sistemas hiperbólicos de leyes de conservación. Métodos en diferencias finitas estándar

Introducción

- Consideremos la ley de conservación escalar en una dimensión espacial dada por

$$\frac{\partial u}{\partial t} + \frac{\partial f(u)}{\partial x} = 0 \tag{126}$$

  con la condición inicial $u(x, t = 0) = u_0(x)$.

  Si la ecuación es no lineal (i.e., $\partial f/\partial u \neq 0$), pueden generarse soluciones discontinuas en un tiempo finito a partir de un dato inicial continuo.

- Discretización espacio-temporal: En códigos hidrodinámicos basados en diferencias o volúmenes finitos, la ecuación (126) se resuelve sobre una malla numérica discreta (x_j, t^n) con

$$x_j = (j - 1/2)\Delta x, \quad j = 1, 2, \dots , \tag{127}$$

  y

$$t^n = n\Delta t, \quad n = 0, 1, 2, \dots , \tag{128}$$

  donde Δt and Δx representan el paso de tiempo y el tamaño de la celda numérica, respectivamente.

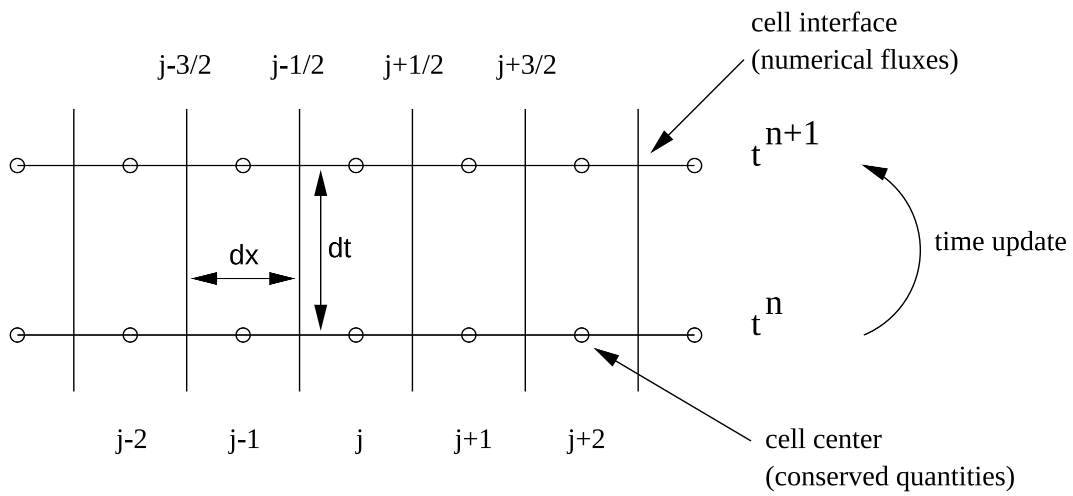

- Un esquema en diferencias finitas es un procedimiento por el que se obtiene una aproximación a la solución en un tiempo posterior, u_j^{n+1}, a partir de aproximaciones en instantes anteriores.

- La cantidad u_j^n es una aproximación a $u(x_j, t^n)$. En el caso de leyes de conservación es preferible considerarla como una aproximación al valor medio de $u(x,t)$ en la celda $[x_{j-1/2}, x_{j+1/2}]$, donde $x_{j\pm 1/2} = (x_j + x_{j\pm 1})/2$:

$$\bar{u}_j^n = \frac{1}{\Delta x}\int_{x_{j-1/2}}^{x_{j+1/2}} u(x,t^n)dx. \tag{129}$$

- La convergencia de la solución numérica a la analítica al refinar la malla numérica implica que el error global, $||E_{\Delta x}||$, definido según

$$||E_{\Delta x}|| = \Delta x \sum_j |\bar{u}_j^n - u_j^n|, \tag{130}$$

  tienda a cero conforme $\Delta x \to 0$.

  En general, en un método es de orden p, $||E_{\Delta x}|| \propto \Delta x^p$.

- Métodos en forma conservativa: garantizan la convergencia (en caso de que ésta exista) a una de las soluciones discontinuas admisibles del sistema original de ecuaciones (teorema de Lax-Wendroff). Forma conservativa significa que el algoritmo puede escribirse en la forma

$$u_j^{n+1} = u_j^n - \frac{\Delta t}{\Delta x}\left(\hat{f}(u_{j-r}^n, u_{j-r+1}^n, \ldots, u_{j+q}^n) - \hat{f}(u_{j-r-1}^n, u_{j-r}^n, \ldots, u_{j+q-1}^n)\right) \tag{131}$$

  donde q y r son enteros positivos, y $\hat{f}$ es una función flujo numérico consistente (i.e., $\hat{f}(u,u,\ldots,u) = f(u)$).

- Ejemplos de métodos en diferencias finitas conservativos:

Nombre	Algoritmo	Orden
Lax-Friedrichs	$u_j^{n+1} = \frac{1}{2}(u_{j-1}^n + u_{j+1}^n) - \frac{\Delta t}{2\Delta x}(f(u_{j+1}^n) - f(u_{j-1}^n))$	1
Godunov	$u_j^{n+1} = u_j^n - \frac{\Delta t}{\Delta x}(f(u(0; u_j^n, u_{j+1}^n)) - f(u(0; u_{j-1}^n, u_j^n)))$	1
Two-step Lax-Wendroff	$u_{j+1/2}^{n+1/2} = \frac{1}{2}(u_j^n + u_{j+1}^n) - \frac{\Delta t}{2\Delta x}(f(u_{j+1}^n) - f(u_j^n))$	
	$u_j^{n+1} = u_j^n - \frac{\Delta t}{\Delta x}(f(u_{j+1/2}^{n+1/2}) - f(u_{j-1/2}^{n+1/2}))$	2
MacCormack	$u_j^* = u_j^n - \frac{\Delta t}{\Delta x}(f(u_{j+1}^n) - f(u_j^n))$	
	$u_j^{n+1} = \frac{1}{2}(u_j^n + u_j^*) - \frac{\Delta t}{2\Delta x}(f(u_j^*) - f(u_{j-1}^*))$	2

Los métodos de primer orden son estables (suponiendo que se satisface la condición de Courant: $\left|\frac{df}{du}\right| \frac{\Delta t}{\Delta x} (\equiv \text{CFL}) \leq 1$) y, por tanto convergentes, aunque excesivamente difusivos.

Los métodos de segundo orden son menos disipativos pero oscilatorios en las proximidades de discontinuidades (y, por tanto, no convergentes).

- Referencias:

R.J. LeVeque, *Numerical Methods for Conservation Laws*, Birkhäuser, 1992. Parte II

Desarrollo de la práctica

- Conéctate a la página web http://grape.c.u-tokyo.ac.jp/ hachisu/java.shtml
- Seleccionando las opciones correspondientes, resuelve la ecuación de Burgers sin viscosidad
$$\frac{\partial u}{\partial t} + \frac{\partial u^2/2}{\partial x} = 0$$
con dato inicial $u(t = 0, x) = \sin(2\pi x)$ con los métodos de la tabla anterior.
- Para cada uno de los métodos rellena la siguiente tabla:

  Método:

CFL	0.1	0.5	0.9	1.0	1.1	1.5	2.0
t_{dif}							
t_{inst}							

donde $t_{\rm dif}$ es el instante de tiempo (aproximado) en el que se alcanza un estado homogéneo, y $t_{\rm inst}$, el instante (también aproximado) en el que se hacen visibles las primeras oscilaciones numéricas.

¿Cómo evoluciona el estado inicial sinusoidal?

¿Qué diferencias observas entre los métodos de primer orden y los de segundo?

¿Qué métodos son más difusivos?

¿Qué métodos son más inestables?

¿Cómo cambia la difusión con la CFL en los métodos de primer orden?

¿Qué pasa con todos los métodos cuando se usa una CFL superior a la unidad?

- Repite todos los puntos anteriores pero resolviendo ahora las ecuaciones de Euler para un fluido perfecto con un dato inicial discontinuo (problema del *tubo de Sod*).

Material

- Links:
  Hachisu I. 1997, 1D Numerical Simulation by Java:
  http://grape.c.u-tokyo.ac.jp/ hachisu/java.shtml

Práctica 3: Aspectos básicos de los métodos en diferencias finitas aplicados a los sistemas de leyes de conservación. Métodos de alta resolución de captura de choques

Introducción

- Los métodos de alta resolución de captura de choques tienen forma conservativa.

- Son algoritmos de alto orden que tienen variación total estable. La variación total de una solución en $t = t^n$, $\mathrm{TV}(u^n)$, se define como

$$\mathrm{TV}(u^n) = \sum_{j=0}^{+\infty} |u^n_{j+1} - u^n_j| \,. \tag{132}$$

  Un esquema numérico se dice que es TV-estable si $\mathrm{TV}(u^n)$ está acotada para cualquier Δt en cualquier instante y para cualquier dato inicial. El interés en los métodos TV-estables radica en el hecho de que para esquemas numéricos en forma conservativa con flujos numéricos consistentes, la estabilidad TV es una condición suficiente de convergencia.

  El alto orden se consigue mediante funciones polinómicas monótonas conservativas que interpolan las soluciones aproximadas o los flujos numéricos en las celdas numéricas. Algoritmos de reconstrucción bien conocidos son el MINMOD (segundo orden), PPM (tercer orden) o los métodos ENO (que mantienen la variación total acotada).

  Reconstrucción MINMOD: en cada celda numérica se efectúa una interpolación lineal con la menor de las pendientes con las celdas contiguas.

- La disipación numérica necesaria en las proximidades de los choques se consigue mediante la resolución de problemas de Riemann exactos o aproximados entre las celdas numéricas contiguas (métodos tipo Godunov) o mediante la adición de términos disipativos conservativos a métodos en diferencias finitas estándar.

- La precisión de alto orden en el tiempo se consigue mediante métodos semidiscretos tipo Runge-Kutta, que permiten preservar la propiedad TVD del esquema completo de forma natural.

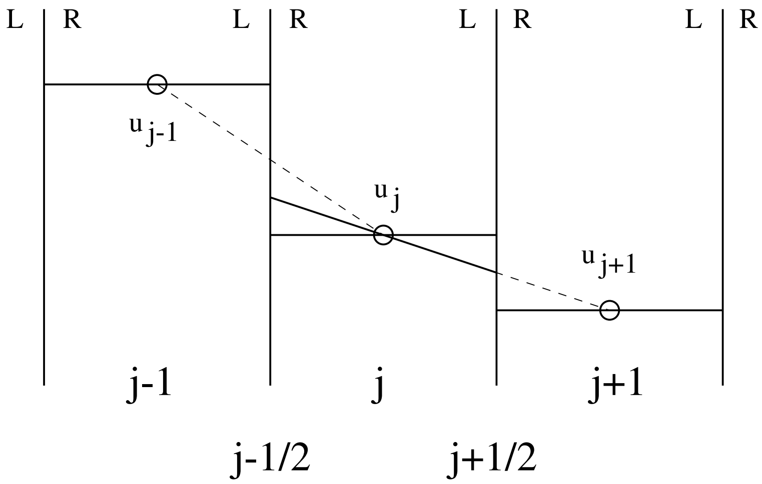

- Referencias:

  R.J. LeVeque, *Numerical Methods for Conservation Laws*, Birkhäuser, 1992. Parte II

  E.F. Toro, *Riemann solvers and Numerical Methods for Fluid Dynamics*, Springer, 1997. Capítulo 4

  C.-W. Shu, S. Osher, *Efficient Implementation of Essentially Non-Oscillatory Shock-Capturing Schemes*, JCP, **77**, 439 (1988)

Desarrollo de la práctica

Considera el programa `bugod.f` que integra la ecuación de Burgers (ver práctica 2) usando el método de Godunov (primer orden).

1. Haz un diagrama de flujo del programa

2. Algoritmo de segundo orden espacial. Programa una subrutina que

   - Calcule las pendientes entre los valores de `U` de celdas contiguas.

     ```
     DO I = 0, CELLS+2
        S(I) = (U(I) - U(I-1))/DX
     END DO
     ```

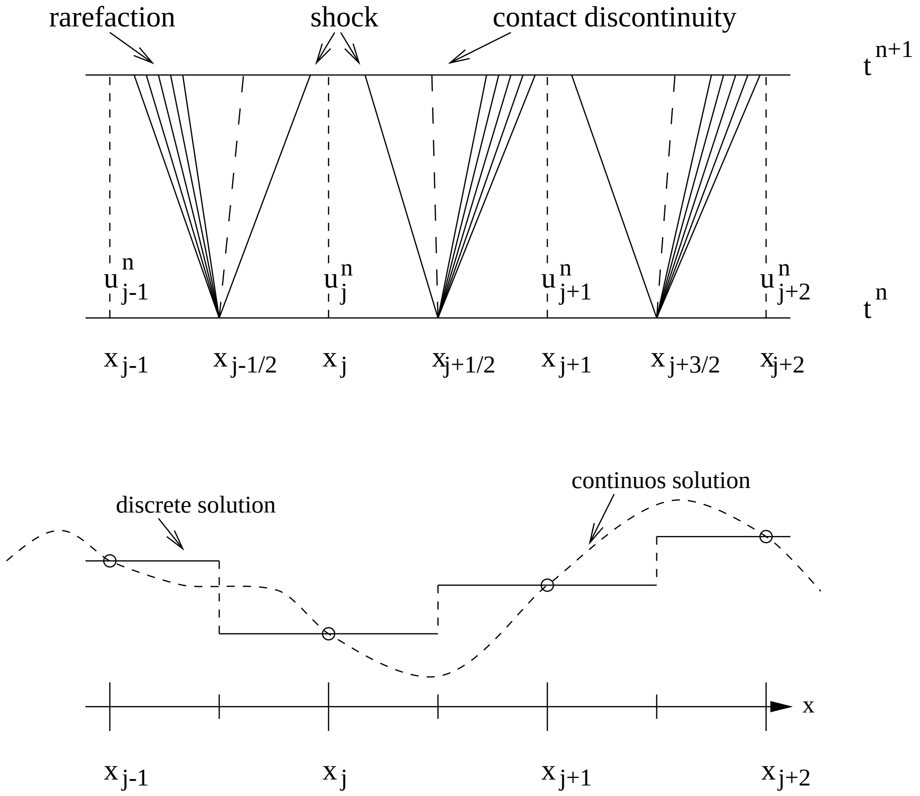

Godunov's scheme: local solutions of Riemann problems

- Construya valores de `U` a ambos extremos de cada celda numérica, `UM`, `UP`, usando las pendientes anteriores convenientemente monotonizadas para preservar la condición TVD.

  Limitador de pendiente MINMOD:

```
      DO I = 0, CELLS+1
         IF ((S(I).EQ.0.0).OR.(S(I+1).EQ.0.0)) THEN
            SL(I) = 0.0
         ELSE
            SL(I) = 0.5*(S(I)/ABS(S(I)) + S(I+1)/ABS(S(I+1)))
     &                *AMIN1(ABS(S(I)),ABS(S(I+1)))
         END IF
         UM(I) = U(I) - SL(I)*DX/2.0
         UP(I) = U(I) + SL(I)*DX/2.0
      END DO
```

Limitador de pendiente SUPERBEE:

```
      DO I = 0, CELLS+1
         IF ((S(I).EQ.0.0).OR.(S(I+1).EQ.0.0)) THEN
            SL(I) = 0.0
          ELSE IF (ABS(S(I)).GE.ABS(S(I+1))) THEN
            SL(I) =  0.5*(S(I)/ABS(S(I)) + S(I+1)/ABS(S(I+1)))
     &                    *AMIN1(ABS(S(I)),ABS(2*S(I+1)))
         ELSE
            SL(I) =  0.5*(S(I)/ABS(S(I)) + S(I+1)/ABS(S(I+1)))
                          *AMIN1(ABS(2*S(I)),ABS(S(I+1)))
         END IF
         UM(I) = U(I) - SL(I)*DX/2.0
         UP(I) = U(I) + SL(I)*DX/2.0
      END DO
```

Limitador de pendiente VANLEER:

```
      DO I = 0, CELLS+1
         IF ((S(I).EQ.0.0).AND.(S(I+1).EQ.0.0)) THEN
            SL(I) = 0.0
         ELSE
            SL(I) = 2.D0*S(I)*S(I+1)/(S(I) + S(I+1))
         END IF
         UM(I) = U(I) - SL(I)*DX/2.D0
         UP(I) = U(I) + SL(I)*DX/2.D0
      END DO
```

- Inserta la subrutina que acabas de programar (`minmod.f`, `superbee.f`, `vanleer.f`) en `bugod.f`, junto con las declaraciones de variables, actualizaciones de los bloques `COMMON`, redefiniciones de dimensiones y modificaciones de las condiciones de contorno necesarias.

- Modifica la subrutina `fluxes.f` para usar los valores de `U` reconstruidos (`UM`, `UP`) en la definición de los problemas de Riemann locales:

```
      DO 10 I = 0, CELLS
         UL = UP(I)
         UR = UM(I+1)
         ...
 10   CONTINUE
```

3. Algoritmo de segundo orden temporal. El algoritmo básico del avance temporal es el del esquema explícito conservativo de primer orden (ver práctica 2)

$$u_j^{n+1} = u_j^n - \frac{\Delta t}{\Delta x}(\hat{f}_{j+1/2} - \hat{f}_{j-1/2}) \quad (\equiv u_j^n + \Delta t L(u^n)).$$

   Implementa el siguiente algoritmo de Runge-Kutta en el avance temporal de `bugod.f` para conseguir segundo orden de precisión temporal:

$$\begin{aligned} u_j^{n+1/2} &= u_j^n + \Delta t L(u^n) \\ u_j^{n+1} &= \frac{1}{2}u_j^n + \frac{1}{2}u_j^{n+1/2} + \frac{1}{2}\Delta t L(u^{n+1/2}) \end{aligned}$$

4. Utiliza el programa para integrar la ecuación de Burgers con dato inicial $u_0(x) = \sin(2\pi x)$ en el intervalo $[0, 1]$. Puedes usar `gnuplot` (ver práctica 1) para visualizar los resultados.

Resumen del programa `bugod.f`

`program bugod`: Resuelve la ecuación de Burgers sin viscosidad usando el esquema de Godunov de primer orden, explícito, con el resolvedor de Riemann exacto.

`subroutine reader`: lee los parámetros iniciales del fichero `bugod.ini`.

`subroutine initia`: especifica el dato inicial.

`subroutine bconci`: establece las condiciones de contorno.

`subroutine cflcon`: calcula el paso de tiempo de la siguiente iteración temporal de acuerdo con la condición de Courant.

`subroutine fluxes`: calcula los flujos numéricos a partir de la solución exacta de los problemas de Riemann en cada interfase.

`subroutine riemann`: resuelve el problema de Riemann para la ecuación de Burgers de forma exacta.

`subroutine update`: obtiene la solución al final del paso temporal usando el algoritmo conservativo explícito de primer orden.

`subroutine output`: guarda la solución en el fichero `bugod.out`.

Material

- Programa:
  Cdigo fuente: bugod.f
  Datos iniciales: bugod.ini

Práctica 4: Simulaciones hidrodinámicas uni y multidimensionales mediante técnicas de alta resolución de captura de choques. Piecewise-Parabolic Method (PPM)

Introducción

- El método PPM es una extensión a alto orden del método de Godunov, de uso muy extendido en Astrofísica Computacional.
- Características fundamentales:
  - Reconstrucción de las funciones en las celdas numéricas mediante parábolas monótonas, lo que permite una representación muy precisa de los gradientes espaciales suaves y las discontinuidades, especialmente las discontinuidades de contacto. El algoritmo tiene una precisión de tercer orden (o incluso superior) en el caso de flujos suaves.
  - Construcción de los estados efectivos a izquierda y derecha de cada interfase numérica mediante promedios en los correspondientes *dominios de dependencia* de las interfases, para cada variable característica. Con este procedimiento se consigue una precisión de segundo orden en un único paso temporal.
  - Cálculo de los flujos numéricos en las distintas interfases numéricas a partir de la solución exacta de problemas de Riemann.
- Referencias:

Colella, P., and Woodward, P.R., *The Piecewise Parabolic Method (PPM) for Gas-Dynamical Simulations*, JCP, **54**, 174 (1984)

Martí, J.M., and Müller, E., *Extension of the Piecewise Parabolic Method to One-Dimensional Relativistic Hydrodynamics*, JCP, **123**, 1 (1996)

Martí, J.M., and Müller, E., *The Analytical Solution of the Riemann Problem in Relativistic Hydrodynamics*, J. Fluid Mech., **258**, 317 (1994)

Primera parte de la práctica: Simulaciones unidimensionales

- Considera el programa `rppm.f` que integra las ecuaciones de la hidrodinámica relativista en una dimensión espacial usando el método PPM.
- Haz un diagrama de flujo del programa.

- Efectúa alguno de los tests propuestos en el programa.
- Modifica los datos iniciales y las condiciones de contorno para simular diferentes escenarios: interacción de vientos en una nebulosa protoplanetaria, ruptura de la onda de choque al alcanzar la superficie estelar en una explosión de supernova, onda de detonación en una explosión de GRB, ...

Segunda parte de la práctica: Simulaciones multidimensionales

- Considera el código `vhone.f` (que previamente hemos descargado de la página web `http://wonka.physics.ncsu.edu/pub/VH-1/VH-1_Code.tar.Z`). VH-1 resuelve las ecuaciones de la dinámica de fluidos compresibles en una y dos dimensiones espaciales según el método PPM. Ha sido desarrollado por J. Blondin (North Carolina State University) y cols.
- Familiarízate con el código consultando la guía del usuario `http://wonka.physics.ncsu.edu/pub/VH-1/VH-1_guide.html`
- Copia los ficheros .tar de los directorios `VHONE/` y `TESTS/` en directorios similares previamente creados en tu cuenta y extrae su contenido
- Sitúate en el directorio `VHONE/` y compila el código tecleando `make`
- Ejecuta el código tecleando `vhone`. El programa ejecutará el *tubo de Sod* en 1D. El resultado final quedará almacenado en el fichero `sod1d.1001`, en formato `ASCII`. Puedes usar `gnuplot` (ver práctica 1) para visualizar los resultados.
- Intenta resolver ahora algún problema más complicado (tienes una lista de tests en la guía del usuario y también la página web `http://wonka.physics.ncsu.edu/pub/VH-1/testpage/`):
  - Sitúate en el directorio `TESTS/`.
  - El fichero correspondiente a cada test se identifica mediante la primera letra de su nombre (se incluyen también subrutinas originales para restaurar la versión original del código)

    `a_`: Strong shock
    `b_`: Supersonic flow past a ball or a cylinder
    `h_`: Hawley-Zabusky shock tube
    `m_`: Supersonic flow past a step (Mach step)

`o_`: Oblique wall shock
`s_`: Sod shock tube in 1, 2 or 3 dimensions

- Copia las subrutinas relevantes (al menos `init.f` e `indat`) en el directorio `VHONE/` (ejemplo: `cp TESTS/a_init.f VHONE/init.f`)
- Modifica las dimensiones de las matrices en `zone.h` y `sweepsize.h` de acuerdo con los requerimientos del problema.
- Compila y ejecuta el código como explicamos antes

- Visualización de resultados multidimensionales:
  - Puedes usar el programa `plot2d.pro` de `IDL` que se encuentra en el directorio `VHONE/` y en el que tendrás que introducir el nombre del fichero que contiene los datos y adaptar las dimensiones de las variables.
  - Películas: Puedes seguir el siguiente procedimiento:
    1. Ejecuta el programa de `IDL` `movie.pro` (del directorio `VHONE/`) una vez modificados adecuadamente la raíz del nombre de los ficheros de datos (`root`) y el número de ficheros (`n`).
    2. El programa anterior genera una serie de ficheros `.png` que puedes visualizar directamente con `animate` (`animate *.png`).

- Ahora puedes preparar tu propia simulación modificando adecuadamente los parámetros del programa, los datos iniciales y las condiciones de contorno. Prueba, por ejemplo, con un chorro extragaláctico.

Material

- Programa:
  - Primera parte: Simulaciones en una dimensión espacial
    Código fuente: rppm.f (incluye fichero size)
    Datos iniciales: inpt.dat
    Gráficos: plot1d.pro
  - Segunda parte: Simulaciones multidimensionales
    Código fuente: en el directorio VHONE/
    Datos iniciales: en el directorio TESTS/
    (lista de tests en http://wonka.physics.ncsu.edu/pub/VH-1/testpage/)

Manual el usuario: http://wonka.physics.ncsu.edu/pub/VH-1/VH-1_guide.html
Imágenes: plot2d.pro
Películas: movie.pro